THE UNIVERSITY OF CHICAGO

PATTERNS OF MORPHOLOGICAL AND FUNCTIONAL EVOLUTION IN THE FEEDING SYSTEM OF WATERFOWL (ANSERIFORMES): INSIGHTS FROM DIET, BEAK SHAPE, AND CRANIAL MECHANICS

A DISSERTATION SUBMITTED TO
THE FACULTY OF THE DIVISION OF THE BIOLOGICAL SCIENCES
AND THE PRITZKER SCHOOL OF MEDICINE
IN CANDIDACY FOR THE DEGREE OF
DOCTOR OF PHILOSOPHY

DEPARTMENT OF ORGANISMAL BIOLOGY AND ANATOMY

BY

AARON MICHAEL OLSEN

CHICAGO, ILLINOIS

AUGUST 2016

Just enough work had already been done
on everything—moths, say, or meteorites—
to get you started and interested,
but not so much there was nothing left to do.

—Annie Dillard, *An American Childhood*

TABLE OF CONTENTS

LIST OF TABLES

LIST OF FIGURES

ACKNOWLEDGEMENTS

Of all the things I have learned in graduate school, one of the most important has been the value of community. Science lives up to its highest ideals when scientists can depend on the encouragement, support, and critical feedback of those both within the traditional scientific community – mentors and colleagues – and those part of one's larger community of family and friends. After years of painstaking work, scientists can often only deliver vague ideas, esoteric knowledge, or the potential for future utility. In a society eager to give everything, even endangered species, an economic value, a scientist frequently contends with doubts as to the significance of their contributions. In facing these struggles I consider myself immensely fortunate to have had the continual support of a wonderful community of colleagues, friends, and family.

I thank my undergraduate advisor at the University of Kansas, Rob Ward, who deserves much, if not all, of the credit for my decision to go to graduate school rather than medical school. The ability for me to pursue my own independent research in his lab awakened in me a love for the creativity of science. And the chance to attend the annual *Drosophila* research conference opened my eyes to the potential of a career in research. The further afield I get from developmental biology the more enjoyable it is to reveal that my love for science had its origins in the extension of fruit fly leg imaginal discs during pupariation. One time I was in the lab with Rob. He had received a request from another lab for an antibody that Rob had purchased and used in a previous experiment. He was packaging up the antibody to share with this colleague. Knowing how expensive antibodies are, I was a bit surprised. I asked him why he was freely sharing the antibody with a colleague, perhaps even a competing lab. "That is what we do in science," he replied. It was a formative moment in developing my philosophy toward scientific

collaboration. Every day in my interactions with colleagues I strive to uphold collaboration in the advancement of science over personal gain.

The blame for my switch from developmental biology to biomechanics cannot be cast at Rob but rather falls squarely on the shoulders of my graduate advisor, Mark Westneat. I entered the graduate program at the University of Chicago with the intention of doing a PhD in evo-devo but once here I took an interest in the neuromechanics research and the potential to integrate computer programming into my research (this is the risk of admitting students to a program encompassing such a broad scope of research). My first year I was taking evo-devo courses while rotating in neuromechanics labs. Needless to say, some within the department were concerned about a lack of direction in choosing a lab and thesis topic. I first had a sense that I would like Mark as an advisor when I showed him a hobby programming project I had been working on, having little to do with my thesis work. He showed nothing but enthusiasm and encouragement. Before the end of my first year I had made the choice to work with Mark and have never looked back. My time in grad school spanned a significant transition for the lab as Mark moved from being a curator of fishes at the Field Museum of Natural History to a professor at the University of Chicago. This coincided with a budget crisis at the museum, an administrative overhaul, and a culture of great uncertainty about the future of science at the museum. I cannot imagine the stress that this placed on Mark. Yet through it all Mark worked around the clock to ensure that we as graduate students could continue our thesis work unaffected. I am immensely grateful to Mark for giving me the freedom to pursue my own projects and ideas (even when they were less than successful...), for his confidence in my potential, for encouraging me to establish outside collaborations, for allowing me to TA human anatomy as many times as I did, for buying a round of tequila shots at SICB Austin 2014, for

bringing me in on a grant proposal and then allowing me to draft my own so that I could get more grant writing experience, for his guidance in not losing sight of the larger picture, and for being my first Twitter follower.

I am grateful to my fantastic thesis committee members: Melina Hale, John Bates, and Callum Ross. They have been incredibly flexible as I have shifted gears on various projects to incorporate more interesting (read more tractable) research trajectories. Melina has been an invaluable source of great career, postdoc, and grant writing advice. And I am grateful to her and Mark for so graciously opening their home to the Westneat-Hale lab members every Halloween with food and drinks, for treating us to dinner every year at SICB, and for making me feel like an honorary Hale lab member. It has been so great to have John as a committee member, particularly notable as the only committee member who actually studies birds! During the budget crisis at the museum it was incredibly assuring to us as students to see John so engaged in what was happening and so vocal in his support for grad student research at the museum. I owe much of what I have learned about the value of collections-based research to John and his passion for natural history. I remember when the submission of my first, sole-authored thesis chapter was rejected after review. The rejection caused me to question the value of the article. Was I overestimating the impact? Or was I just not effectively communicating the true impact? John encouraged me to believe in my own work and even to appeal the editorial decision. Although I ended up not appealing the decision and submitted elsewhere (partly for time considerations), John's belief in my work meant so much to me. I want to thank John for making me feel like an integral member of the museum and AOU community.

I owe many thanks to Callum Ross for his mentorship and friendship. Being a TA for his human anatomy course has been a great privilege and the most meaningful and valuable teaching

experience I have had as a graduate student. The human anatomy course forged a unique and memorable camaraderie. Some of my favorite days in grad school were the days of practical exams, starting with pinning in the early morning and unwinding over drinks in the evening. Another of my favorite memories of grad school was the chance to work with Callum (and Mark) in drafting a grant proposal on rhythmicity in the feeding apparatus of waterfowl. I am inspired by Callum's ability to simultaneously maintain a clinical research program on swallowing neuromechanics and a complementary basic research program on rhythmicity in motor systems. The chance to work with him in designing a research project that was inspired by his basic research but applied to my study system was the most enjoyable intellectual experience I had in graduate school. I also want to thank Callum for connecting with grad students as a peer and colleague. This was manifest not only in his willingness to socialize with us late into the night at SICB (if 2am pancakes at Denny's isn't commitment I don't know what is; SICB Austin 2014 resurfaces...) but also in the way he spoke and listened to us. To echo the refrain of a colleague who is known for his love of somewhat annoying but yet somehow endearing aphorisms, Callum is both a gentleman and a scholar. And someone whom I am deeply grateful to call a colleague and friend.

There are several other University of Chicago faculty members I would like to thank. I wish to thank Trevor Price who graciously adopted the role of an honorary committee member. I actually first met Trevor before I even started graduate school, when I visited the University of Chicago in the summer of 2008. Early in my second year I had asked Trevor whether he would like to be on my committee as I was planning my thesis work. He told me 'yes' but in my ignorance of how one went about assembling a committee I had interpreted this more as a "sure I'd be willing" rather than a more binding commitment. As time went on I finalized my

committee (without Trevor) and scheduled my proposal hearing for early June (Trevor had left for fieldwork in May). Later that fall at EvMorph Thai dinner someone congratulated me on passing my proposal hearing. Trevor was there and immediately asked, "Wait, wasn't I on your committee?" I was mortified with embarrassment at my miscommunication and that I had not included him. I apologized and asked him if he would still like to join my committee; he graciously offered to advise in a more informal capacity. Over the years he has been an invaluable source of critical feedback on my work. He has engaged more in reading and critically evaluating my writing than any other colleague, returning copious comments on a manuscript in just a couple of days. His feedback has made me a better scholar and has led me to take more pride in my work. I am also thankful to him and Tina for opening up their home to students on many occasions, including NAOC Chicago 2013 and during prospective student visits. I have never felt more at peace in Chicago than the time spent at their home in the Dunes Park in the company of friends.

Many thanks to Mike Coates, an intellectual powerhouse with insights, or at least witty banter, on nearly any topic. I have greatly enjoyed our many and wide-ranging conversations on walks at EvMorph dinner, taking two of his courses, and TAing his Chordates class. His invitation for me to participate on a project simulating a fossil shark skull as a linkage mechanism was a key inspiration in making the linkR R package fully generalizable to bird and fish cranial mechanisms. To this day, I can still remember his question to me at my proposal hearing (paraphrased): If the motion of the quadrates coupled with elasticity at the mandibular symphysis can cause the bird mandible to expand (bow), could this be a mechanism for elastic recoil during jaw closing? I do not have a definitive answer to this question yet but hopefully

someday I will! I am grateful to Mike for the insights and questions that linger in the back of the mind and urge further study.

Many thanks to Urs Schmidt-Ott who worked very patiently with me on my first GRFP application and was a great mentor to me during my first year when I was finding my bearings and setting the course I would ultimately take through grad school. Thank you to Sliman Bensmaia who took the time to advise me in basic programming when I rotated in his lab, who gave me the great opportunity of TAing his computational neuroscience course, and who is by far my funkiest friend. Thank you to Mike LaBarbera for providing essential direction during my first few years of grad school in choosing a lab and research project. My first year, everyone in my cohort (who was applicable) was extremely fortunate to receive the GRFP, except me. Given the low chances of receiving a GRFP no one should ever feel depressed if they are not selected. However being the only one of my cohort who had not received it was devastating. His words of encouragement at that moment were the main motivation for me to continue on and strive to do better - for that I am immensely grateful. Thank you to Vicky Prince for her responsiveness to concerns and feedback about the graduate program. Thank you to Robert Ho for his support of my work and for maintaining the health of the department. Thank you to both Vicky and Robert for opening their home to the department every year during the prospective visits. Thanks to Stephanie Palmer for providing great and immediate advice on high-speed videography, for offering her dogs as stress therapy to the department, and for being an all around amazing person. Many thanks to Dave Jablonski and Sue Kidwell - I have enjoyed our many great conversations at EvMorph dinner and your dance party is a highlight of my year. A huge thanks to Jim O'Reilly, who was the first person to make sure I understood just how competitive the academic job market is and how important it was that I regularly publish and present at

conferences. For whatever reason this is a matter that is rarely raised in clear terms. I am thankful for Jim's sincerity, wit, and friendship.

I want to thank the BSD, OBA, E&E, and CEB administrators for making sure everything keeps running smoothly, for throwing an amazing holiday party every year, and for offering their help whenever I needed it: Alison Anastasio, Audrey Aronowsky, Josh Berg, Annetha Bartley, Jeff Wisniewski, Connie Brown, Norma Del Real, Connie Homan, Mary Johnson, Cindy King, Stephanie Manick, Ian Miller, Melissa Lindberg and Diane Hall. A special thanks to Audrey, whose refreshingly honest and hilariously snarky take on academia has helped me keep a healthy perspective on life. I am so glad that I had a chance to spend so many years working with her, from her former position at BioSync to her current position as OBA graduate manager, and benefitting from her advice.

I have also benefitted from the advice and feedback of several colleagues at institutions other than the University of Chicago, particularly in the SICB community. This includes Jim Cooper, Sharlene Santana, Paul Gignac, Anthony Herrel, Betsy Dumont, Chris Marshall, Dominique Adriaens, Peter Wainwright, Robert Druzinsky, Ty Hedrick, Nicolai Konow, Tom Roberts, and Beth Brainerd. I am especially grateful to Beth who last year invited me to participate in a fantastic collaboration with her and Ariel Camp and who gave generously of her time in helping me to draft a post-doctoral fellowship proposal. On the first day I met with Beth and Ariel in May 2015 to plan our collaborative project fitting linkage models to Ariel's *in vivo* operculum data she had me walk through each step of the linkage simulation program that I had written. As we proceeded she took notes and continuously asked questions to make sure that she understood the entire process. No one had ever taken so much time to sit down with me and fully

understand my code; it meant so much to me for someone to show so much respect for my work. I am ecstatic to work with her as a post-doc.

The Darwinian cluster has become something akin to an extended family for me over the years. These friendships have sustained me through the rough times, kept me sane, and kept me social. First of all thank you to my many roommates over the years: Tom Stewart, Ben Rubin, Colin Kyle, Joel Smith, Amy Henry, Hilary Katz, Max Witynski (a rare summer migrant!), and Mark Bitter. I could not have asked for a more awesome and chill group of people to live with. Many thanks to my cohort: Tom Stewart, Ben Rubin, Colin Kyle, Kristen Jenkins, Ben Winger, Laura Merwin, Alice MacQueen, Chris Schell, Justin Lemberg, Carrie Albertin, Talia Karasov, and Mike Werner. You are all amazing and I am so proud to call you my friends. Thank you for all the grad school memories and support over the years. And Lunch Club for life! I owe many thanks to our many (relatively) senior graduate students - those who set a precedent to which our cohort could only hope to live up to. Thank you to Dave Reed, Erin Reed, Nate Smith, Dave K, Dave T, Dave T's mom, Kacy Gordon, Emma Grieg, Andy Dossman, Katie Brooks, Brandon Kilbourne, Liz Scordato, Sophie McCoy, Nate Upham, Deren Eaton, Daniel Matute, Yen-Chyi Liu, Heather King, Charlie McCord, and Joanna Mandecki. Thanks to Nate Smith for letting me crash on his sofa in DC while I was collecting data the Smithsonian! And thanks to Dave Reed for letting me barge into your desk space any time and pester you with questions. I owe many thanks to the amazing post-docs that have come through the University of Chicago over the years: Pepe Iriarte-Díaz, Laura Porro, Erica Westerman, Anjan Bhullar, Ali Nabavizadeh, Nick Gidmark, and Julia Schultz. Thank you for your much needed reminders that there is indeed a life beyond the PhD! Thank you to Rick Madden, easily the most interesting man in the world;

thank you for sharing your love of life and for introducing us to your wonderful *media naranja*, Regan.

I would like to thank the many up and coming stars within the Darwinian cluster (and affiliates) who have let me crash their party (in no particular order): Kate Criswell, Justin Garber (honorary member), Haley Stinnett, Courtney Orsbon, Dallas Krentzel, Timothy Sosa, Rey Ayon, Christina Masco, Jon Mitchell, Jackie Lungmus, Courtney Stepien, Robert Arthur, Robert Burroughs, Robert Lockhart (honorary member), Roberto Marquez, Max Winston, Simon Lax, Daniela Palmer, Daniel Hooper, Laura Southcott, Katharine Henderson, Julie Szymaszek, Andrew Gehrke, Adam Hardy, Arvind Pillai, Marcos Vieira, Heather Skeen, Peter Smits, Peter Tierney, Joyce Pieretti, Mo Siddiq, Nicole Bitler, Liz Sander, Kyler Brown, Natalia Piland, Dave Grossnickle, Kathleen Beilsmith, Benjamin Blanchard, Giselle Garcia, Sara Jackrel, Carlos Cardenas, Darcy Ross, and Michael Alcorn. I am so thankful to each and every one of you for all the barbeques on the Point, dinners, science conversations, plots to save the world and epic parties.

In particular I owe thanks to Brett Aiello. Before starting grad school I had this impression that grad students spent most of their time working together in the lab on large projects, constantly collaborating, exchanging ideas, dreaming up new schemes together. In reality, and somewhat unfortunately, grad school turned out to be largely an individual effort with each student working on their own thing, getting feedback from peers time to time. For the first few years this left me rather dispirited. Then along came Brett. We joked for a while about various projects we could do together. Then we realized, “Wait, why don’t we just do it?” Planning and carrying out collaborative projects with Brett has been one of my favorite intellectual experiences of grad school. Both of us bring our own skills to the table and we make

a great team; it has been a privilege to work with him. I also want to thank Andrew George. I am so glad I have gotten the chance to know Andrew over the past year as he has shifted to being a full time Westneat lab member. I had always wanted an afternoon coffee buddy – I just had to wait seven years until one came along. I wish that I were staying so we could work together longer. I would like to thank two members of the University of Chicago community who passed away during my time as a graduate student. Thank you to Phil Ulinski for letting me audit his introductory neurobiology course; Phil's lectures were phenomenal. He cared so much for his students and for the material. Also thank you to John Adams – you were such an amazingly unique, talented, intelligent, and kind friend.

I would like to thank the spectacular scientific community at the Field Museum, including Peggy Macnamara, Tom Gnoske, Akiko Shinya, John Bates, Dave Willard, Steve Goodman, Jason Weckstein, Mary Hennen, Ben Marks, Bruce Patterson, Corrie Moreau, Rick Ree, Leo Smith, Jim Boone, Mary Anne Rogers, Janet Voight, Doug Stotz, Peter Lowther, Josh Engel, Sushma Reddy, Susan Mochel, Kevin Swagel, FuiLian Tan, Anna Ferraroni, Kevin Feldheim, Erica Zahnle, Amanda Zeigler, Shannon Hackett, Heather Skeen, and Holly Lutz. Even in the midst of the budget crisis you all maintained a dedication to the museum's scientific mission and deep care for the well-being of colleagues. You all made the Field Museum a magical and unforgettable place to work. I want to extend a special thanks to Dave Willard who made me feel especially welcome at the museum. Dave is one of the most selfless, kind, and passionate people I have ever met. Not to mention his unparalleled scientific achievements: he has coordinated what is arguably the most comprehensive, longitudinal sampling of birds in the world. I am inspired both by his scientific achievements and his kindness as a friend. Every year since I began working at the Field Museum Dave has invited me to participate in a count circle

he organizes in South Central Wisconsin for the Audubon's Christmas Bird Count. I am not a particularly good birder. Especially in comparison to the rest of the crew, people who are lifelong birders, people who have literally written books on ornithology. Yet Dave still invites me, he pays for our hotel room, he is never angry at our performance. These counts are the most fun you could have during mid-December in South Central Wisconsin – and then some! It has been an incredible honor to participate in these counts, a ritual focused entirely around a most beautiful philosophy: collect data now to benefit the future. I would also like to extend a special thanks to the late Bill Stanley. You were always so kind to me and obliging of my requests for specimens to decimate. I once asked him for a specimen to dissect in Mark's comparative vertebrate anatomy class. He said, "Let me check and I'll get back to you." Well, he got back to me with a frozen beaver. "It didn't have any data so it's yours," he said. The comparative vertebrate anatomy class of 2012 has Bill Stanley to thank for their possibly once in a lifetime experience dissecting a beaver.

Many thanks to the amazingly supportive members of the Westneat and Hale labs: Jillian Henss, Joanna Mandecki, Michael Alcorn, Charlie McCord, Josh Drew, Meg Malone, Andrew George, Lyda Harris, Marianne Seneczko, Theresa Tatum-Naecker, Hannah Weller, Trevor Thompson, Matt Green, Heather King, Yen-Chyi Liu, Richard Williams IV, Hilary Katz, Brett Aiello, Adam Hardy, Katie Henderson, and Chery Cherian. You all brightened my days, gave me great advice, helped me work through problems, built up my confidence, and made SICB meetings an event to look forward to all year. Heather, Yen-Chyi, and Matt: SICB is not the same without you all. With everything that has changed over the years in the Westneat lab, Charlie has been one of the few constants for me. Thanks for giving me advice and being there whenever I needed someone to talk to. Thank you to Hannah Weller, whom I have had the great

privilege of working with in the Westneat lab and who has given me many great ideas on how to improve StereoMorph. Hannah is an exceptionally talented, enthusiastic, and dedicated scientist; I look forward to seeing all of the amazing things she accomplishes in the future.

I would like to thank my German host family: Adalbert Kirchgaessner, Beate Grossman, and their five children, especially my good friend since high school, Otmar Kirchgaessner. I applied to and was accepted into the University of Chicago graduate program while living with them in 2009; it was also while staying with them that I had the time to develop many of my early programming projects and skills. They have been like family to me and I am forever grateful to them for making me feel like a full member of their family. I would like to thank my extended family and siblings. I am so incredibly fortunate to have such a loving and fun family. You all remind me that our relationships with friends and family are the most important thing in our lives.

And more than anyone else I am grateful to my mom and dad. You are the constant in my life, my foundation, the ones I know I can always turn to when I need help, advice, or someone to talk to. As I have gotten older I have loved how our relationship has developed and deepened. Completing a PhD often delays the typical stages of "adulthood". This can be quite frustrating for the student as they feel as though they are "failing" to develop on time (the "perpetual student"). Yet, you have never pushed me to go faster than I needed or wanted and you have gone out of your way to show your pride in my accomplishments. Thank you for always loving me and believing in me.

Specimen access

I would like to thank the following people for their assistance with accessing specimens: Dave Willard (FMNH), Ben Marks (FMNH), Mary Hennan (FMNH), Rauri Bowie (MVZ), Carla Cicero (MVZ), Chris Milensky (NMNH), Christina Gebhard (NMNH), Mark Florence (NMNH), and Helen James (NMNH).

Funding

This work was supported by an NSF Graduate Research Fellowship (DGE-1144082), an NSF Integrative Graduate Education and Research Traineeship grant (DGE-0903637), an NSF IOS grant (IOS-1425049), the University of Chicago Hinds Fund, the University of Chicago Biological Sciences Division Travel Fund, the University of Chicago GRAD Travel Fund, the Charlotte Mangum Fund, the Carol Schneider Fund, and travel funds from the Department of Organismal Biology and Anatomy.

ABSTRACT

The avian order Anseriformes (waterfowl) is an ecologically diverse and globally distributed clade of approximately 150 species. Owing to their ecological and economic importance there is an extensive literature documenting the feeding behaviors and diet of waterfowl, making this an ideal clade in which to study the morphological and functional evolution of feeding systems. The central objective of this dissertation is to integrate dietary and morphological data using shape analysis, evolutionary modeling, and biomechanical simulation to identify processes underlying the evolution of functional systems. The dietary dataset, compiled from the literature for 99 waterfowl species, represents the most comprehensive compilation of avian diet data to date applied to phylogenetic comparative analyses. These data are used to test the hypothesis that the evolution of herbivory is associated with an increase in body mass due to a potential advantage in the digestion of low-quality diets (chapter 2). The results reveal at least five independent transitions toward increased herbivory in waterfowl and that increased herbivory is not associated with increased body mass when phylogeny is taken into account. The morphometric dataset, collected from over 130 museum specimens and representing 50 waterfowl species, is one of the first surveys of bird skull shape to incorporate both three-dimensional beak curvature and the geometry of the cranial linkage mechanism, the bones underlying cranial kinesis. To evaluate the force transmission properties of the cranial linkage a new biomechanical simulation platform is developed, with the capacity to simulate cranial kinesis in birds and fishes (chapter 3). Diet and beak shape data are combined to test the correlation between beak shape and diet in waterfowl and examine how the major axes of beak shape variation relate to a performance trade-off in waterfowl between filter-feeding and grazing (chapter 4). Beak shape and diet in waterfowl are strongly correlated, with the first major axis of

variation in beak shape corresponding to different positions along a performance trade-off gradient between filter-feeding and grazing. The morphometric dataset of waterfowl skull shapes is then used to test the hypothesis that the avian cranial linkage geometry evolves in association with beak feeding behaviors (chapter 5). The beak and linkage of waterfowl skulls exhibit strong morphological and functional integration, with significant differences in linkage shape and function among waterfowl with differing feeding behaviors. In addition to exploring the processes underlying the evolutionary trajectories of functional systems, this dissertation also encompasses the broader themes of collection-based biomechanical simulation and major transitions in the evolution of waterfowl feeding ecology (chapter 6).

CHAPTER ONE: INTRODUCTION

In the dawn chorus of natural history collections, few bird clades call more loudly and prominently than waterfowl (order Anseriformes). The over 200 published dietary studies (Johnsgard 1978; Marchant and Higgins 1990; Kear 2005), the more than 2000 curated videos of waterfowl behavior (ibc.lynxeds.com), and physical representation as skin and skeleton museum specimens entice the attentive observer and invite interpretation. Waterfowl occupy a prominent place not only in the field of natural history but also as a model system for the study of basic bird biology. Waterfowl have been used to study the thermoregulatory function of the beak (Hagan and Heath 1980), digestive physiology (van Gils et al. 2007; van Gils et al. 2008), and altitudinal adaptation (McCracken et al. 2009). In evolutionary developmental biology, mallards (*Anas platyrhynchos*) have been used as a model to understand the genetic and developmental basis of beak shape variation (Wu et al. 2004; Wu et al. 2006). And we know more about the feeding apparatus of mallards than perhaps any other species of bird, including *in vivo* motor patterns of the jaw muscles during feeding and drinking (Zweers 1974; Kooloos and Zweers 1989; van der Leeuw et al. 2003), jaw muscle proprioception (Bout and Dubbeldam 1991), and three-dimensional kinematics of the cranial linkage mechanism (Dawson et al. 2011).

From this extensive foundation of previous research we have gained insights into the unique morphology, ecology, and geography characterizing each of the approximately 150 living species of waterfowl as well as a better understanding of basic waterfowl biology. However, relatively few studies have combined these data to build a more complete understanding of the evolutionary history of the waterfowl clade, which originated over 45 million years ago (Clarke et al. 2005; Prum et al. 2015). With the construction of new molecular phylogenies (Sraml et al.

1996; Johnson and Sorenson 1998; McCracken et al. 1999; Sorenson et al. 1999; Donne-Goussé et al. 2002; Hackett et al. 2008; Burleigh et al. 2015) we now have a confident understanding of the phylogenetic position of waterfowl within the bird tree of life and a reasonably confident estimate of the phylogenetic relationships among waterfowl. Thus, now is an ideal time for a synthesis of data compiled from the literature and new data from natural history collections within a phylogenetic framework.

In the second chapter I examine dietary evolution in waterfowl, focusing in particular on the evolution of herbivory. Herbivory is rare among birds and is usually thought to have evolved predominately among large, flightless birds due to energetic constraints or an association with increased body mass. Nearly all waterfowl are flighted and many are predominately herbivorous. Compiling data from over 200 published diet studies to create a continuous character for herbivory, I demonstrate that waterfowl have undergone at least five independent transitions toward herbivory and that these transitions are uncorrelated with changes in body mass when phylogeny is taken into account. This represents the most comprehensive application to date of avian diet data to phylogenetic comparative analyses. These results challenge the hypothesis that a larger body mass confers an advantage in the digestion of low-quality diets but do not exclude the possibility that shifts to a more abundant food source have driven shifts toward a larger body mass in other bird lineages. These results also shift thinking on dietary evolution from 'switching discrete categories' to 'transitioning continuous characters' and reveal an exceptional capacity of waterfowl to evolve herbivory. This exceptional capacity of waterfowl prompts a reinterpretation of the relatively infrequent origination of herbivory among flighted birds.

In the third chapter I develop a general framework to derive functional variables for biological linkage mechanisms, including the cranial linkages of bird and fish skulls. Many

musculoskeletal systems, including the skulls of birds, fishes, and some lizards consist of interconnected loops of mobile skeletal elements, analogous to human-engineered linkage mechanisms. I present three-dimensional, multiloop linkage models of kinesis in the skulls of birds and fishes and I use these models, in combination with new kinematic simulation software, to investigate structure-function relationships in these systems. The results show that kinematic transmission, the most widely used functional metric for linkages, is unsuitable for linkages in which the motions of input or output links have substantial translational components. For the cranial linkage mechanism of birds in particular, force mechanical advantage (analogous to the mechanical advantage of a lever) is a more suitable than kinematic transmission as a functional metric. By comparing the results of different functional metrics, including kinematic transmission, mechanical advantage, and a new functional metric, expansion advantage, I show that different biological linkages require different functional metrics. This is the first study to introduce a computational framework for three-dimensional linkage simulation that is integrated into a workflow for shape data collection and analysis.

In the fourth chapter I combine the diet data compiled in chapter two with three-dimensional beak shape data to examine how a performance trade-off in waterfowl between filter-feeding and grazing relates to the evolution of beak shape. Previous work has shown that performance trade-offs can influence the divergence of underlying morphological traits at the population or species level but whether and how trade-offs influence patterns of morphological diversification at longer evolutionary timescales remains less well understood. Using dietary proportions of ‘leaves’ versus ‘seeds and animals’ as a proxy for the performance trade-off in waterfowl between grazing and filter-feeding, the results show congruence between the performance trade-off and the major axis of variation in beak shape. I argue that performance

trade-offs may direct the trajectories of morphological diversification by underpinning major axes of morphological variation and promoting morphological convergence along these axes. This study represents the most comprehensive analysis to date of the relationship between beak shape and diet in birds and provides strong support for the classical, but infrequently tested, hypothesis that beak shape closely reflects diet in birds. Additionally, this study highlights the power gained by considering the three-dimensional curvature of the beak rather than traditional linear measurements (height, length, width); shape variables incorporating curvature have consistently stronger correlations with dietary differences than linear dimensions.

In the fifth chapter I expand on chapter four by examining functional evolution of the beak within the larger context of the skull. The upper and lower beak represent just two of ten mobile elements in the jaw apparatus of birds. These additional bony elements behind the beak serve as attachment sites for muscles and form a transmission system, known as a linkage or mechanism, that enables rotation of the upper beak. In this chapter I test whether the shape of the cranial linkage serves as an additional source of variation upon which selection acts in the evolution of avian jaw function. Integrating geometric morphometric analyses and biomechanical modeling the results show strong and significant evolutionary covariation between the beak and linkage, the linkage and neurocranium, but not between the beak and neurocranium. Additionally, waterfowl that differ by feeding ecology differ in linkage shape and function. Linkage modeling shows that in birds the linkage and beak are coupled in such a way that the mechanical advantage of the linkage and beak is changed simultaneously and in the same direction by changing beak height. The results support this mechanism of synergistic change in linkage and beak function across waterfowl. Interestingly, although the linkage and beak are tightly integrated they can exhibit opposing patterns of functional evolution: the evolution of

pursuit diving is associated with a decrease in mechanical advantage of the beak but an increase in mechanical advantage of the linkage. Thus, a consideration of avian cranial linkage diversity may provide additional insights into functional diversification of the beak not apparent from considerations of beak shape alone. Taken together, the correlated morphological, functional and ecological evolution between the beak and linkage point to an important role of linkage shape in the evolution of beak mechanics and behavior.

Lastly, in the final chapter I explore three broader themes of this dissertation. The first theme relates to the roles of body mass, performance trade-offs, and mechanical advantage in shaping the evolutionary trajectory of the waterfowl feeding apparatus. The second theme is a new computational workflow for collection-based biomechanical simulation. This dissertation illustrates the utility of three new open-source software packages: 'StereoMorph' for the collection of landmark and curve data using a stereo camera setup, 'linkR' for kinematic simulation and analysis of three-dimensional linkage mechanisms, and 'svgViewR' for three-dimensional, interactive visualization of shape data and biomechanical simulations. The last theme is the evolution of waterfowl feeding ecology. These dissertation chapters assemble an integrative picture of the transformations in the waterfowl feeding apparatus, including dietary, behavioral, and morphological transitions. These data, including paleontological evidence, vestigial structures among extant waterfowl, and ancestral state reconstructions of diet and morphology, support multiple, independent transitions in waterfowl to a more goose-like form from a duck-like form. In taking an integrative approach, this dissertation seeks not only to use waterfowl feeding ecology as a system in which to address broader biological questions but also to expand our knowledge of the unique processes and transformations that gave origin to a diverse order of birds adapted to sea, fresh water, and land spanning six continents.

CHAPTER TWO: EXCEPTIONAL AVIAN HERBIVORES: MULTIPLE TRANSITIONS TOWARD HERBIVORY IN THE BIRD ORDER ANSERIFORMES AND ITS CORRELATION WITH BODY MASS[1]

Abstract

Herbivory is rare among birds and is usually thought to have evolved predominately among large, flightless birds due to energetic constraints or an association with increased body mass. Nearly all members of the bird order Anseriformes, which includes ducks, geese and swans, are flighted and many are predominately herbivorous. However, it is unknown whether herbivory represents a derived state for the order and how many times a predominately herbivorous diet may have evolved. Compiling data from over 200 published diet studies to create a continuous character for herbivory, models of trait evolution support at least five independent transitions toward a predominately herbivorous diet in Anseriformes. Although a non-phylogenetic correlation test recovers a significant positive correlation between herbivory and body mass, this correlation is not significant when accounting for phylogeny. These results indicate a lack of support for the hypothesis that a larger body mass confers an advantage in the digestion of low-quality diets but does not exclude the possibility that shifts to a more abundant food source have driven shifts toward herbivory in other bird lineages. The exceptional number of transitions toward a more herbivorous diet in Anseriformes and lack of correlation with body mass prompts a reinterpretation of the relatively infrequent origination of herbivory among flighted birds.

[1]This chapter was originally published as: Olsen, A.M. 2015. Exceptional avian herbivores: Multiple transitions toward herbivory in the bird order Anseriformes and its correlation with body mass. Ecology and Evolution 5(21): 5016–5032.

Introduction

Herbivory is exceptional among dietary strategies in that it exploits one of earth's most abundant, and yet least digestible, food sources: the leaves, stems, buds and bulbs of plants, (Karasov 1990). Despite the associated digestive challenges, herbivory has evolved repeatedly in several vertebrates, including mammals (Cork 1996; Janis 2000), turtles (Bjorndal 1980), lizards (Cooper and Vitt 2002; Stayton 2006) and teleost fishes (Roberts 1987; Choat and Clements 1998; Winterbottom and McLennan 1993). Although only 2% of extant bird species have a diet that is primarily herbivorous, herbivory has likely evolved in birds at least nine times (Table 2.1). These independent origins appear to show little phylogenetic pattern. Origins of herbivory are scattered across the avian tree of life and it is commonly assumed that herbivory has evolved no more than twice within any one order. In contrast to this lack of phylogenetic pattern, there does appear to be an association between herbivory and lower flight capacity or the loss of flight entirely. Most herbivorous ratites, the Takahe (*Porphyrio mantelli*) and the Kakapo (*Strigops habroptila*) are flightless. Although Galliformes, Tinamiformes and the Hoatzin (*Opisthocomus hoazin*) are capable of flight, flight in these groups is characterized by short, explosive bouts used primarily in escape from predators (Dial 2003) or short-range travel (up to 350 m in the Hoatzin; Strahl 1988). Among avian herbivores, herbivorous Anseriformes are exceptional in being generally strong fliers with the capacity for long-range flight, albeit poor maneuverability and a narrow range of flight speeds (Dial 2003).

It is often assumed that herbivory is observed primarily among flightless and weak-flying birds due to a potential association with an increase in body mass (Morton 1978; Dudley and Vermeij 1992; Klasing 1998), which places an increased cost on flight (Masman and Klaassen 1987; e.g. Guillemette 1994). Two main hypotheses propose mechanisms by which herbivory

Table 2.1. Origins of herbivory in birds.

Order	Num Origins	Total Spp	Flight?	Examples	Reference
Ratites	1-2				
Struthioniformes[a]		<5[b]	No	Ostrich (*Struthio camelus*)	Milton et al. 1994
				Emu (*Dromaius novaehollandiae*)	Davies 1978
+ Tinamiformes		<47	Escape[c]	Andean Tinamou (*Nothoprocta pentlandii*)	Mosa 1993
Dinornithiformes (Moas)†		9	No		Wood et al. 2008
Aepyornithiformes (Elephant birds)†		2-7	No	Elephant bird (*Aepyornis*)	Clarke et al. 2006
Galliformes	1+	<19[d]	Escape[c]	Rock Ptarmigan (*Lagopus muta*)	Sedinger 1997
Anseriformes	1+	20-30	Yes	Screamers, geese, swans, moa-nalos	Morton 1978 James and Burney 1997
Opisthocomiformes	1	1	Weak[e]	Hoatzin (*Opisthocomus hoazin*)	Grajal et al. 1989
Gruiformes[a]	1	1	No	Takahe (*Porphyrio mantelli*)	Mills and Mark 1977
Psittaciformes	1	1	No	Kakapo (*Strigops habroptila*)	Trewick 1996
Passeriformes	2+	2	Yes	White-tipped Plantcutter (*Phytotoma rutila*)	Bucher et al. 2003
Totals	9+	<115		Thick-billed Saltators (*Saltator maxillosus*)	Munson and Robinson 1992

Examples include species for which leaves, stems, buds and bulbs comprise greater than 80% of stomach contents or foraging observations for at least a season. (a) Likely non-monophyletic (Hackett et al. 2008; Mitchell et al. 2014). (b) Includes all those in *Struthio*, *Rhea* and *Dromaius*. (c) Fly in brief, explosive escape bouts (Dial 2003). (d) Includes all species in Tetraoninae. (e) Observed to fly up to 350 m without rest (Strahl 1988). †Extinct.

may be positively associated with body mass. The first, based initially on the Jarman-Bell Principle (Geist 1974), posits a physiological mechanism whereby parameters that enhance digestive capacity, such food intake rate, scale with body mass at a rate greater than energy expenditure (basal metabolic rate), thus affording larger individuals an energetic advantage when feeding on low quality foods relative to smaller individuals. This hypothesis, referred to here as the 'digestive efficiency' hypothesis, predicts that within already herbivorous lineages, larger individuals will outcompete smaller individuals or reach a degree of herbivory not possible at lower body masses, leading to an observed positive correlation between herbivory and body mass. A second hypothesis proposes an ecological mechanism whereby body size is not positively associated with herbivory, per se, but rather with diets that provide sufficiently abundant and large packets of food (Hiiemae 2000; Clauss et al. 2013). This hypothesis, referred to here as the 'abundance-packet size' hypothesis, predicts that as a lineage increases in body mass, selection will act to shift the diet toward foods that are available in larger or more abundant packets, such as leaves of plants, resulting in an observed positive correlation between herbivory and body mass.

Herbivorous birds tend to have larger body masses than their closest relatives: the Takahe is among the 15 heaviest birds in the order Gruiformes, the Kakapo and swans are the heaviest members of their orders, and ostriches and emus are the heaviest and sixth heaviest extant birds, respectively (Dunning 2008). Studies in lizards (Pough 1973; Schluter 1984; Cooper and Vitt 2002) and terrestrial mammals (Price and Hopkins 2015), have found positive correlations between body mass and herbivory. However, studies in herbivorous primates (Clauss et al. 2008), reptiles (Franz et al. 2011), ungulates (Steuer et al. 2011) and herbivorous mammals more generally (Clauss et al. 2007; Müller et al. 2013) have found little or no empirical support for the

digestive efficiency hypothesis, indicating that such correlations are not due to any digestive advantage conferred by an increase in body mass.

For birds in particular, known allometries of digestive parameters do not support the digestive efficiency hypothesis. The scaling of food intake rate to body mass does not differ significantly from that of basal metabolic rate to body mass (Fritz et al. 2012) and the length of time food is retained in the gut, which is positively associated with the extent of digestion (Demment and Van Soest 1985; Prop and Vulink 1992), is uncorrelated with body mass among herbivorous birds (Fritz et al. 2012). Although larger birds have larger small intestinal volumes relative to their basal metabolic rate (Lavin et al. 2008), it is unlikely that such scaling would contribute an increase in digestive efficiency for herbivores given that large intestine and caecal volumes (for which few morphological data are available) bear greater relevance to the digestion of high fiber foods (Leopold 1953; McBee and West 1969; Gasaway 1976; Barnes and Thomas 1987). Thus, any potential correlation between herbivory and body mass in birds is more likely due to an ecological, rather than physiological, mechanism.

Birds in the order Anseriformes, which includes ducks, geese, swans and mergansers, consume a diversity of foods: seeds, fish, mollusks, aquatic insects, algae, and herbage of aquatic and terrestrial plants (Figure 2.1). While herbivory is most prevalent among those Anseriformes commonly known as geese (Lavery 1971; Middleton and van der Valk 1987; Kingsford 1989), it is also observed in screamers (Naranjo 1986), the sister group to all other Anseriformes, swans (Squires and Anderson 1995; Bailey et al. 2008) and some species of ducks, such as the American Wigeon (*Anas americana*; Wishart 1983; Havera 1998). Additionally, nearly all Anseriformes are flighted, with the exception of three species of steamer ducks and the extinct moa-nalos (Olson and James 1991; Fulton et al. 2012). It has long been recognized that ducks

Figure 2.1. Canada Geese (*Branta canadensis*) feeding on grasses in Sarpy County, Nebraska. Canada Geese have partially herbivorous diets, composed primarily of the leaves, seeds and fruits of plants.

and geese are both polyphyletic (Delacour and Mayr 1945) and this has been supported by phylogenetic studies based on morphological (Livezey 1986) and molecular (Donne-Goussé et al. 2002; Sorenson et al. 1999; González et al. 2009) characters. The polyphyly of geese and the occurrence of herbivory in several other anseriform taxa raise the question of how many times herbivory has evolved in Anseriformes. If an herbivorous diet has evolved repeatedly, this would provide an ideal system in which to test whether increased herbivory is associated with an increase in body mass in birds.

In this study I examine the evolution of herbivory in Anseriformes, using quantitative and qualitative diet data compiled from the literature to estimate the degree of herbivory for most anseriform species. I reconstruct the ancestral degree of herbivory at key nodes in the anseriform phylogeny using models of continuous trait evolution. I then test whether herbivory is significantly correlated with body mass using non-phylogenetic and phylogenetic correlation tests. I explore the effects of different phylogenetic relationships, branch lengths and definitions of herbivory. Lastly, I discuss the implications of this study's results for the origins of geese, the

relationships among body mass, flightlessness and herbivory, and the potential importance of the avian feeding apparatus and foraging behaviors in explaining dietary evolution along body mass gradients in birds.

Materials and Methods

Diet data and indices

I compiled diet data from 208 quantitative studies and 11 qualitative studies to create a continuous character representing the extent of herbivory in 14 (of 287) species of Galliformes, the sister clade of Anseriformes, and 99 (of 168) species of Anseriformes (Clements et al. 2014). These 113 species represent 13 of the 76 galliform genera and 37 of the 52 anseriform genera. Galliform taxa, which were included to better circumscribe estimates for the ancestral dietary state of Anseriformes, were chosen based on those taxa for which the most detailed diet data were available and to include representatives of all five galliform families. I used handbooks (Johnsgard 1978; Marchant and Higgins 1990; Kear 2005; Poole 2005) and Google Scholar searches to locate the 219 primary diet data sources. When the primary source was not available, I took data from a secondary source.

The data included in this meta-analysis were collected using a wide range of methodologies, including the relative proportions of items in the gut (e.g. Landers et al. 1977), the relative proportions of items in feces (e.g. Middleton and van der Valk 1987), and the percent of time animals were observed to spend feeding on particular foods (e.g. Naranjo 1986). Studies of gut contents varied in the portion of the gut from which items were removed (esophagus, crop, proventriculus, etc.) and the method used to assess the relative contribution of each item (aggregate percentage, percent volume, percent mass, frequency of occurrence, etc.). Quantitative diet data were available for 106 (94%) of the 113 species included in this study;

diets of the remaining 7 species are known only by qualitative accounts. Qualitative accounts list items consumed by a particular species, verified either by visual observation of foraging behavior or gut contents, but without a numerical quantification of the relative contribution of each item to the diet. I excluded sixty-nine species of Anseriformes owing either to insufficient diet data, a lack of body mass data, or uncertain phylogenetic position (i.e. lack of published molecular sequence data).

Avian diet data are often collected during a particular season or in a particular locality. When possible, I treated diet data from different seasons and localities as separate entries, totaling 403 entries. The total number of primary sources cited (219) is less than the number of entries as some sources contained data from multiple seasons, localities or species. Thirty species are represented by a single entry and the maximum number of entries for one species is 11. For each entry, both qualitative and quantitative, I grouped each food item consumed into one of eight non-overlapping categories (Table 2.2). I calculated the relative importance of each category as a percentage such that all categories summed to 100% for each entry.

Table 2.2. Dietary categories used in this study and the corresponding parts and taxa included in that category. The herbivory index is the sum of the proportions of leaves, plants, roots and algae. The folivory index is the sum of the proportions of leaves and plants.

Category	Parts and taxa included
Leaves	Fibrous parts of plants: leaves, stems, root stalks, needles, branches of Embryophyta ("land plants")
Roots	Roots, rhizomes and bulbs of Embryophyta
Seeds	Seeds and nuts of Embryophyta
Fruits	Fruits, flowers, catkins or spores of Embryophyta
Plants	Embryophyta, part is not specified (e.g. "15% dandelion")
Algae	Chlorophyta or charophyceae (green algae), rhodophyta (red algae), phaeophyceae (brown algae) or cyanobacteria
Animal	Metazoa
Other	Any taxon not included in the above categories or unidentified matter

For quantitative studies reporting the percentage of gut contents or percentage of feeding time, I used the raw percentages directly. For studies reporting the frequency of occurrence of gut or fecal contents, I normalized the relative frequencies such that the frequencies summed to 100%. Although qualitative studies do not quantify the relative importance of each item, importance is often indicated by descriptive adjectives (e.g. primarily leaves, rarely seeds). To take this into account, I used the qualitative descriptions to score items on a scale from 1–4, ranging from a rare to primary component of the diet. If no such description was given I scored each item equally. I then normalized the scores such that all scores for an account summed to 100 to obtain a category sum in the form of a percentage.

I averaged the percentage representation of each category across all entries for each species, giving equal weight to each entry. To calculate the extent of herbivory for each species, I summed the dietary categories that include the leaves and roots of plants and algae (Table 2.2) and divided by the sum of all categories except 'other' (since this often included unidentified matter). This produces a value between 0 and 1, referred to here as herbivory index. Items identified as a plant but for which the part of the plant was not specified ('plant' category), are assumed in most cases to represent the fibrous parts of plants and are thus included in herbivory index. Most arguments concerning the potential correlation between diet and body mass are based on the relative digestibilities of dietary components. Because roots, rhizomes and bulbs are slightly more digestible on average than leaves, stems and buds (Karasov 1990), a second dietary index was also calculated summing only the leaves and unidentified plant parts. This is referred to here as folivory index and represents a diet that is a less digestible subset of the herbivory index. Prior to all correlation tests, I logit-transformed both dietary indices to account for a skew toward small values, first changing all zeros and ones to the minimum and maximum values,

respectively (Warton and Hui 2011; Sokal and Rohlf 2012). Logit transformation yielded approximately normal distributions of dietary indices.

Phylogenetic trees

To model the evolution of herbivory in Anseriformes and account for phylogenetic relatedness in testing for a correlation between herbivory and body mass I used a published phylogeny of 6714 avian species, pruned to include the 113 galliform and anseriform species in this study (Burleigh et al. 2015). Constructed from a sparse supermatrix of 22 nuclear loci and seven mitochondrial regions, this tree represents the most current molecular phylogeny of galloanserae (the monophyletic clade comprising Galliformes and Anseriformes), incorporating data from several previous studies (Sraml et al. 1996; Johnson and Sorenson 1998; McCracken et al. 1999; Sorenson et al. 1999; Donne-Goussé et al. 2002) and with branch lengths scaled to molecular sequence divergence. To account for uncertainty in topology and branch lengths, I performed all analyses across a sample of 100 maximum likelihood bootstrap trees obtained from the Dryad data repository (Burleigh et al. 2014). The tree was made ultrametric solely for visualization purposes using the 'chronos' function in the ape package version 3.1-4 (Paradis et al. 2004); all analyses were performed on non-ultrametric trees.

Body mass data

I obtained body masses for all species except the extinct moa-nalo *Thambetochen chauliodous* from Dunning (2008), using species averages and pooling subspecies (N = 1–7608). Body masses are sexually dimorphic within the sampled taxa, with males weighing about 225 g on average more than females. However, because sex-segregated data for body mass, and to a greater extent diet, are lacking for most sampled taxa, I took the arithmetic mean of female and male body masses. I obtained the mass of *T. chauliodous*, (6227.5g) from an estimate by Iwaniuk

and colleagues (2004) based on tibiotarsal circumference. Mean body masses ranged from 166.3 g in *Callipepla californica* (California Quail) to 11.1 kg in *Cygnus buccinator* (Trumpeter Swan) with a mean across all sampled taxa of 1.71 kg and a standard deviation of 1.81 kg. I $\log_{10}$-transformed body mass averages prior to the correlation tests to account for a skew toward small body mass.

Trait models

To choose the best model for the ancestral state reconstruction of herbivory and folivory index, I compared five models of trait evolution: a Brownian motion model (Felsenstein 1973), an Ornstein-Uhlenbeck (OU) model (Butler and King 2004), a lambda model, a kappa model and a delta model (Pagel 1999). The Brownian motion model fits two parameters to the trait data: an initial trait value and a rate parameter (Felsenstein 1973). The remaining models estimate these same two parameters with an additional parameter to account for several potential scenarios such as attraction toward a particular trait value, covariance among traits that is only partially predicted by the phylogeny, a relationship between character divergence and speciation and time-dependent trait evolution (Felsenstein 1973; Butler and King 2004). I fit each model to both dietary indices using the 'fitContinuous' function in the geiger package version 2.0.3 (Harmon et al. 2008) of R version 3.1.3 (R Core Team 2015) across all 100 trees in the sample distribution and used AICc scores to compare the fit of each model.

Ancestral state reconstructions

I used the best fitting model (here the lambda model) to reconstruct the ancestral state of herbivory and folivory index for the 113 species dataset. I estimated the lambda parameter for each tree using 'fitContinuous'. I then estimated the ancestral states using the 'rescale' function in geiger and the 'ace' function in the ape package (Paradis et al. 2004), with the restricted

maximum likelihood (REML) method (Felsenstein 1973; Schluter et al. 1997). I performed ancestral state reconstruction for the 100 trees in the sample distribution using the lambda parameter specific to each tree. Since I performed ancestral state reconstruction across multiple trees of differing topology, I only recorded estimates of ancestral states (and their corresponding 95% confidence intervals) at five strict consensus nodes (nodes A-E in Figure 2.3); the ancestors of these nodes are identical across all trees. I selected these five nodes from a strict consensus tree of all 100 trees containing only the species included in this study, constructed using the 'consensus' function in the ape package (Paradis et al. 2004). I plotted the distributions of ancestral state estimates and their corresponding 95% confidence intervals using the 'density' function in R (R Core Team 2015), applying a Gaussian kernel to produce smooth probability distributions. The peak of each distribution (mode) was determined by the maximum kernel density. I plotted estimates at all nodes onto the maximum likelihood topology using the 'plot.phylo' function in ape (Paradis et al. 2004).

Non-phylogenetic and phylogenetic correlation tests

To test for a correlation between diet and body mass, I performed non-phylogenetic and phylogenetic correlation tests between $\log_{10}$ body mass and logit-transformed dietary index values (herbivory and folivory index). For non-phylogenetic correlation tests, I performed a Pearson's correlation test using the 'cor.test' function in the R stats package (R Core Team 2015). Major axis (MA) regression and standardized major axis regression, using the 'lmodel2' function in the R package lmodel2 (Legendre 2014), were performed solely for trend line visualization.

Because mass and diet data were collected from interrelated taxa, the trait values do not represent independent data points. I quantified the strength of phylogenetic signal by calculating

Blomberg's K and Pagel's λ for dietary indices and body mass using the 'phylosig' function in the phytools package (Pagel 1999; Blomberg et al. 2003; Revell 2012). To account for phylogenetic non-independence, I tested for a correlation between the standardized phylogenetic independent contrasts (PICs) of diet and body mass, assuming the evolution of the traits could be simulated by Brownian motion (Felsenstein 1985). Before performing correlational analyses, I tested for proper standardization of branch lengths by testing for a correlation between the standard deviation and absolute value of the contrasts (Garland et al. 1992). I used the 'pearson' and 'kendall' methods available in the 'cor.test' function to identify any linear or non-linear trends, respectively. If the standard deviation and absolute value of the contrasts showed a significant trend, the branch lengths were exponentially or log transformed using a range of constants until no significant trend was observed. This was performed for each trait and for each tree in the bootstrap distribution.

Once branch lengths were properly standardized, I computed the contrasts using the 'pic' function in ape (Paradis et al. 2004) and tested for a correlation (Pearson's and Kendall's) between the contrasts using 'cor.test'. PICs, as opposed to phylogenetic generalized least squares (PGLS) regression analysis, were used because a regression assumes that the independent (predictor) variable is measured without error (Sokal and Rohlf 2012), which is not appropriate for this data set. While PGLS allows for the fitting of several different evolutionary models while performing the regression, these models explain phylogenetic signal in the residuals (the fit of the tree to the regression) and do not relate directly to the test of whether the variables are significantly correlated (Freckleton et al. 2002; Revell 2010).

Results

Diet classification

Some degree of herbivory is widespread across galloanserae: of the taxa represented in this study, 71% of Anseriformes and 86% of Galliformes have an herbivory index greater than 5% (Figure 2.2). However, several different galloanserae lineages exhibit a predominately herbivorous diet (Figure 2.3). For example, I identified 25 anseriform species with an herbivory index greater than 70%. This includes species commonly called geese in the genera *Alopochen*, *Anser*, *Branta*, *Cereopsis*, *Chen*, *Chenonetta* and *Cyanochen*. Also included are Horned Screamers (*Anhima cornuta*), all swans of the genus *Cygnus*, the moa-nalo *T. chauliodous*, and three ducks of the genera *Anas*. Among the 14 Galliformes included in this study, two species, the Spruce Grouse (*Falcipennis canadensis*) and Rock Ptarmigan (*Lagopus muta*) also have predominately herbivorous diets, 76% and 74%, respectively. The results of dietary categorization using the more restricted folivory index are similar to the results with herbivory index and are not described further here but are provided in the supporting information.

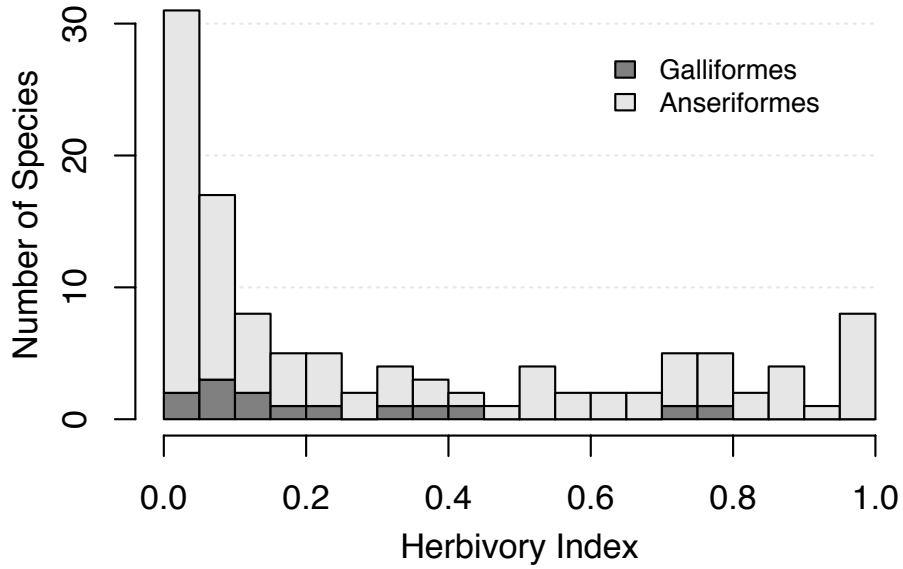

Figure 2.2. Histogram of herbivory index values for the Anseriformes (light) and Galliformes (dark) in this study.

Trait models and ancestral state reconstruction

Of the five different trait models tested for the evolution of herbivory index, the lambda model is the best fitting model, having the lowest AICc score for 78% of the sample tree distribution ($N = 100$). Of these models, the lambda model also has the least variable AICc score across all topologies with a mean AICc score of 25.7 and a standard deviation of 3.4. The remaining 22% of trees are best fit by the kappa model, with a mean AICc score of 28.7 (SD = 5.1). The results of ancestral state reconstructions of herbivory index using the lambda model across the entire tree distribution (100 trees) are summarized in Figure 2.3. Estimates of the ancestral herbivory index at the five chosen consensus nodes range from 21-58% across all topologies. At the two deepest consensus nodes, the root of Anseriformes and the root of Anatidae (nodes A and B in Figure 2.3, respectively; Clements et al. 2014), estimates of ancestral herbivory range from 42-52% but with 95% confidence intervals ranging from 3-92%, indicating the unreliability of these estimates. At the root node of all Anseriformes except *Anhima* and *Anseranas* (node C in Figure 2.3), ancestral herbivory estimates range from 33-44% and upper 95% confidence intervals do not exceed 72%. At the most recent consensus node (E in Figure 2.3), ancestral herbivory estimates range from 21-41% and upper 95% confidence intervals do not exceed 64%.

Correlation tests

A non-phylogenetic correlation test identifies a significant relationship between body mass and herbivory index ($p = 0.0001$; Figure 2.4) although there is considerable scatter in this relationship (Pearson's r = 0.36). The trend is dominated by the Anserinae (which here includes the genera *Cereopsis*, *Cygnus*, *Branta*, *Chen* and *Anser*) and *Anas* clades. Running counter to

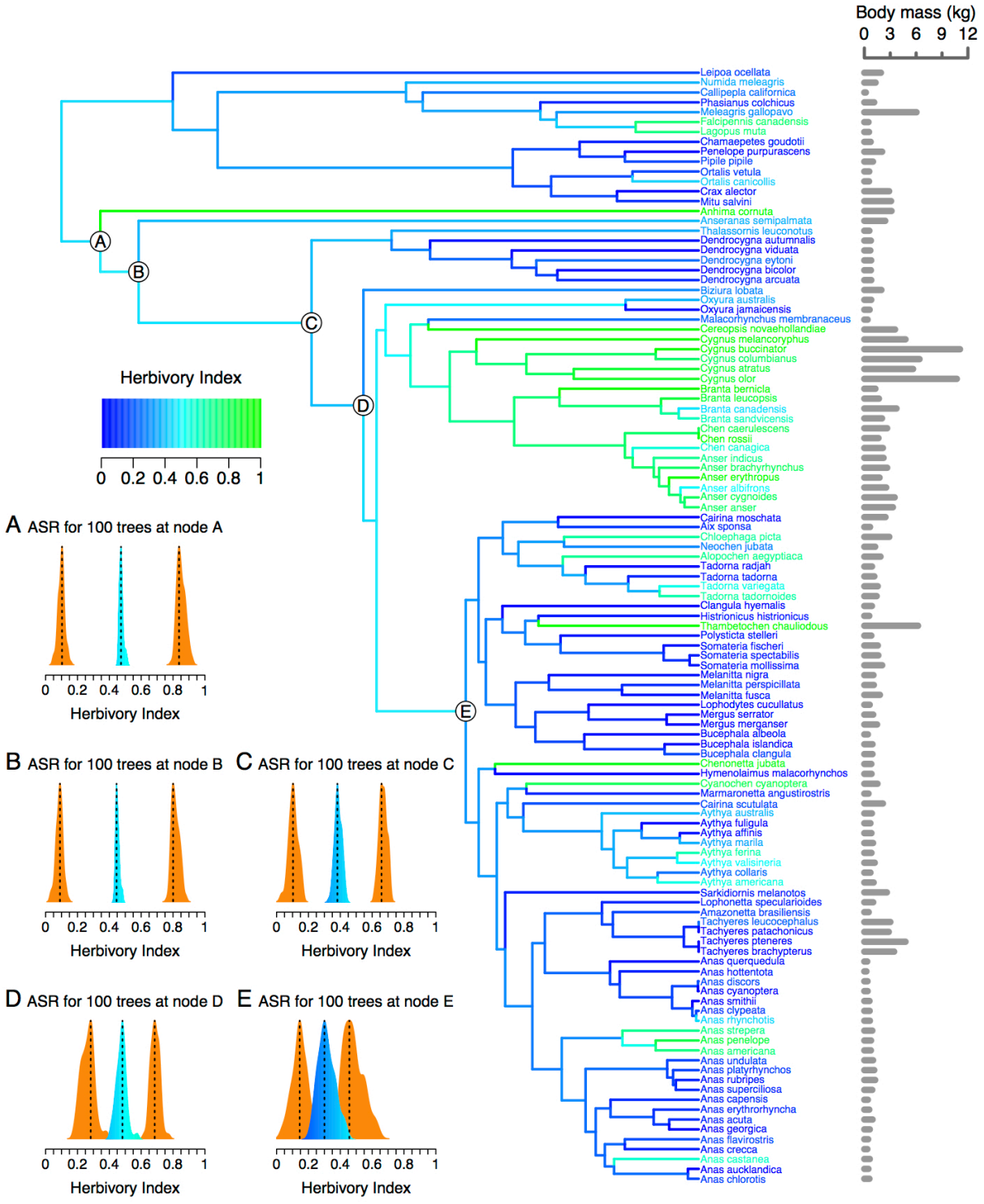

Figure 2.3. Ancestral state reconstruction of herbivory index in Anseriformes and a subset of Galliformes using a lambda model of trait evolution (Pagel 1999) on the maximum likelihood topology of Burleigh et al. (2015). Bars plotted to the right of each tip label show the mean body mass of that species in kilograms. Herbivory indices of each species are represented by branch

(**Figure 2.3, continued)** tip and label colors and estimated ancestral values of herbivory index are represented by the color of internal branches, with green being most herbivorous and blue being least herbivorous. The results for the entire tree distribution (100 trees) at strict consensus nodes A-E are summarized in the corresponding kernel density plots. For each consensus node the distribution of ancestral herbivory estimates are shown in the same color scheme as the branches and the distribution of lower and upper 95% confidence intervals are shown in orange. Peaks of each distribution are indicated by dashed lines. Node A is the root of Anseriformes, node B is the root of Anatidae and the sister clade to node A are the Galliformes.

this trend are the steamer ducks (*Tachyeres*), which have large body masses and herbivory indices of 0-20%. Exclusion of the four species in *Tachyeres* increased the linearity of the trend (Pearson's r = 0.45). Galliformes also appear to oppose the positive trend between body mass and herbivory and exclusion of Galliformes (flightless steamer ducks not excluded) also

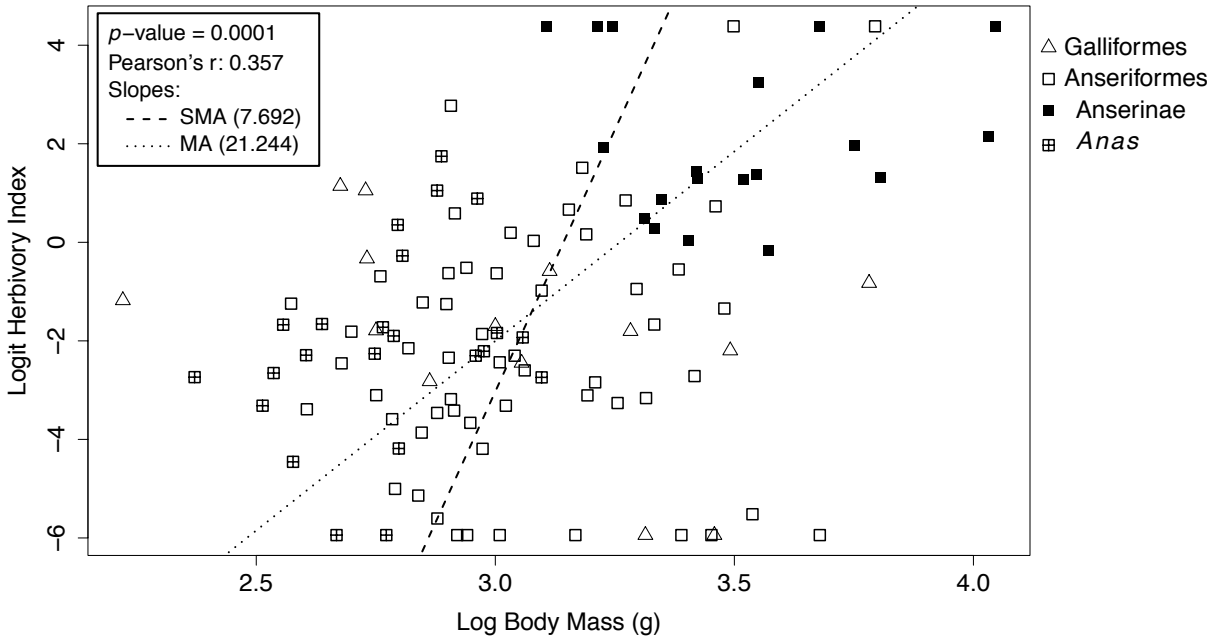

Figure 2.4. Plot of logit-transformed herbivory index versus $\log_{10}$ body mass for Anseriformes (square symbols) and a subset of Galliformes (triangle symbols). Two major clades within Anseriformes are indicated by different square symbols: filled squares for Anserinae (including the genera *Cereopsis*, *Cygnus*, *Anser*, *Branta* and *Chen*) and crossed-squares for the genus *Anas*. Significance statistics of a non-phylogenetic Pearson correlation test and slopes of non-phylogenetic major axis regressions are shown.

increased the linearity of the trend (Pearson's r = 0.45).

For all trees, significant phylogenetic signal was found in $\log_{10}$ body mass (λ = 0.98-0.99, $p < 0.001$; K = 0.286-0.527, $p < 0.001$) and logit herbivory index (λ = 0.73-0.86, $p < 0.001$; K = 0.12-0.24, $p < 0.01$), consistent with previously reported values for phylogenetic signal of ecological traits in birds (Smith 2012). Pearson's and Kendall's correlation tests between the standardized independent contrasts of body mass and herbivory recovered a significant relationship at the $\alpha = 0.05$ threshold for only 1% of trees and did not recover a significant relationship at the $\alpha = 0.01$ threshold for any trees (Figure 2.5A, B). Correspondingly, values of Pearson's r were low, ranging from -0.01 to 0.19 for all trees (Figure 2.5C).

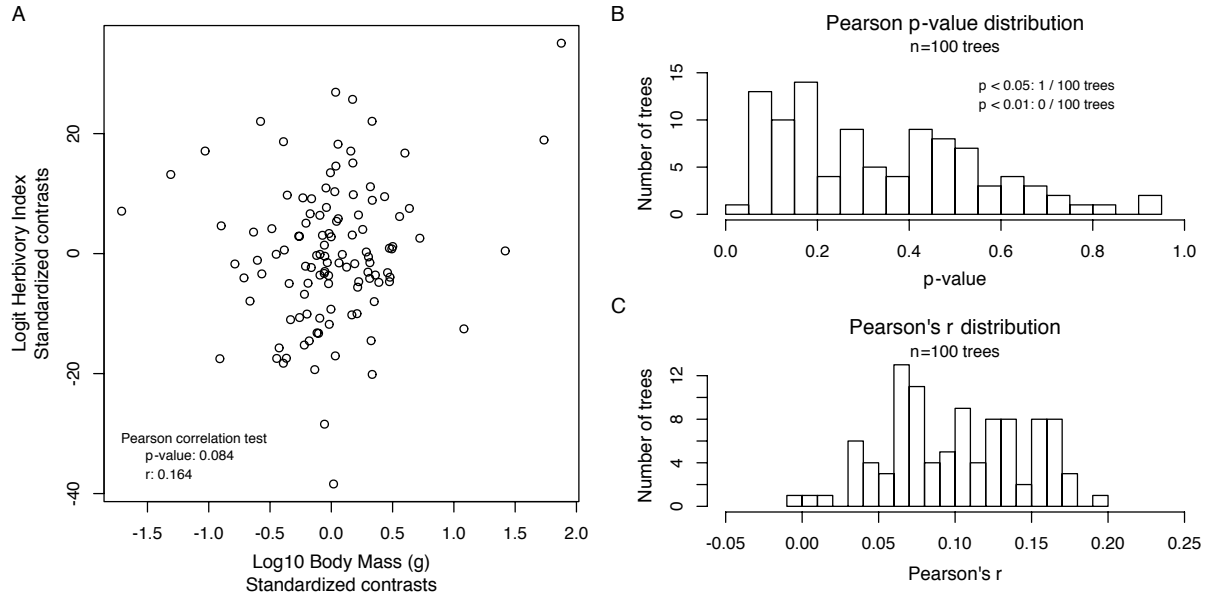

Figure 2.5. Pearson's correlation test on the standardized contrasts of logit-transformed herbivory index and $\log_{10}$ body mass. (A) Plot of the contrasts for the maximum-likelihood topology (Burleigh et al. 2015) and associated correlation statistics. Histogram of the *p*-values (B) and Pearson's r (C) resulting from correlation tests performed across the entire tree sample (n = 100). In (B), the number of trees that yielded *p*-values less than 0.05 and 0.01 are indicated.

Discussion

Compilation of diet data from 219 primary sources reveals that some degree of herbivory is widespread across galloanserae with several independent lineages exhibiting a predominately herbivorous diet. Such distributed and wide-ranging degrees of herbivory necessarily limit the potential of evolutionary trait models to confidently estimate ancestral states and, as expected, the deepest consensus nodes of the tree are characterized by wide confidence intervals. However, at consensus nodes with narrower confidence intervals, ancestral state reconstruction consistently favors an ancestor with a less herbivorous diet, with estimates ranging from 21% to 58%. In particular, ancestral estimates at the most recent consensus node within Anseriformes considered in this study support at least five independent increases to a predominately herbivorous diet from an ancestor that was likely less than 45% herbivorous. Correlation tests using phylogenetic independent contrasts show that the apparently significant positive correlation between herbivory and body mass is driven primarily by a couple of large clades. In the following discussion, I will consider limitations and assumptions in the interpretation of these results as well as explore the implications of these results for the origins of geese and the evolution of herbivory more broadly across birds.

Diet as a continuous character

With over 200 published primary sources, we know more about the diets of Anseriformes than perhaps any other order of birds, both in terms of the proportion of species studied and the quantitative nature of the data. To my knowledge, this study represents the most comprehensive compilation to date of avian diet data from the literature applied to the generation of continuous dietary characters, ancestral state reconstruction or correlation with other ecological characters. However, in representing this wealth of data as a single continuous ecological character, I have

made several simplifying assumptions. Firstly, the studies from which I compiled these data weigh the relative contributions of food items using different methods (e.g. by mass, volume, frequency of occurrence), which is known to introduce biases when comparing among studies (Swanson and Bartonek 1970; Swanson et al. 1974). By normalizing the contribution of each dietary component for each study, I sought to generate an ecological character that represents the relative importance of herbivorous or folivorous food items in the broadest sense for each species.

Secondly, anseriform diets can vary considerably between seasons and localities. For example, the diet of Canvasbacks (*Aythya valisineria*) consists of 95% animal matter during the winter in Chesapeake Bay (Perry and Uhler 1988) but shifts to 99% fibrous plant material during fall migration in Wisconsin (Korschgen et al. 1988). By taking an average across several studies (when available), each dietary index represents the relative importance of the relevant food items across seasons and localities (e.g. species that are herbivorous throughout the year have a higher herbivory index than those with an herbivorous diet for only a portion of the year).

Thirdly, I have also not accounted for any potential geographic sampling biases. Geography could introduce a bias particularly for migratory Anseriformes. Diets are better known for more accessible non-breeding grounds relative to less-accessible breeding grounds. For example, of the nine entries included in this meta-analysis to describe the diet of the Greater White-fronted Goose (*Anser albifrons*), eight document the diet on non-breeding grounds while one documents the diet on breeding grounds. In the *Anser* genus, for example, diets tend to be more herbivorous, by approximately 10%, on breeding grounds relative to non-breeding grounds. But time spent on breeding grounds may only account for one quarter of the year. Thus, lack of correction in such cases may result in a slight underestimate of the extent of herbivory. Despite

these limitations, the use of a continuous character to describe an organism's diet represents a significant advance relative to the traditional use of discrete characters: it more closely corresponds to the biological reality of a diverse character that often defies discrete categorization and it allows for direct comparisons with other continuous ecological characters (e.g. body mass, beak shape).

The evolution of herbivory in Anseriformes and the origins of geese

Most Anseriformes have been given common names that classify them as either a 'duck' or 'goose'. Such a distinction is not based on any definite or discrete character, neither ducks nor geese form a monophyletic clade, and some species are even referred to as both duck and goose (e.g. Australian wood duck or Maned goose, *Chenonetta jubata*). Yet 'duck' and 'goose' do capture unmistakable characteristics that are distinguishable across the broad spectrum of anseriform beak shapes and foraging behaviors. Ducks generally have flatter, broader and longer beaks and feed primarily in water, by dabbling or diving while geese have taller, shorter beaks and feed primarily on land by grazing and digging (Johnsgard 1978). The classification of diets across Anseriformes compiled here supports a general distinction based on herbivory: geese tend to be among the most herbivorous Anseriformes, although notable exceptions include more aquatic herbivores such as swans and herbivorous ducks in the genera *Anas* and *Aythya* (Figure 2.3). Considering this, geese are perhaps best thought of as Anseriformes possessing a collection of characters at the extremes of terrestriality and herbivory relative to other members of the order. Thus, the evolution of herbivory in Anseriformes yields important insights into the origins of geese, within the broader context of dietary evolution in Anseriformes.

Speculation on the origin of geese spans nearly a century and a half. Darwin (1872, p. 183) was perhaps the first, supposing that the finer, more numerous lamellae of ducks evolved

from an ancestral condition of coarser, less numerous lamellae observed among several geese today, a "goose-to-duck" transition. The potential phylogenetic affinity of Anseriformes to an order of aquatic shorebirds (Delacour and Mayr 1945; Sibley et al. 1969) and the discovery of the stem anseriform fossil *Presbyornis* (Olson and Feduccia 1980), with an undeniably duck-like skull and wader-like postcranial skeleton, introduced the possibility that the transition proceeded in the exact opposite direction, from duck to goose. However, from recent phylogenetic studies a clear sister relationship between Anseriformes and the exclusively terrestrial Galliformes has emerged (Sibley et al. 1988; Hackett et al. 2008), seemingly supporting a terrestrial feeding ecology as ancestral for Anseriformes and tipping the balance of evidence back in favor of the goose-to-duck hypothesis. The ancestral state reconstruction of diet presented in this study is unable to resolve the polarity of this transition by reliably estimating the diet at the root of Anseriformes (Figure 2.3). However, at a more recent node there is sufficient resolution to support several independent increases in herbivory from a primarily non-herbivorous ancestor (node E in Figure 2.3). This establishes a duck-to-goose polarity for multiple transitions giving rise to geese in the genera *Chloephaga*, *Alopochen, Thambetochen*, *Chenonetta* and *Cyanochen*. Given the remarkably convergent characteristics of geese, it is likely that a similar pattern of duck-to-goose transitions has given rise to additional lineages of geese throughout the evolutionary history of Anseriformes, including the Cape Barren Goose (*Cereopsis novaehollandiae*) and geese in the genera *Anser*, *Branta* and *Chen*.

Two additional lines of evidence support a duck-to-goose transition. The first is the near ubiquity of lamellae among Anseriformes. Lamellae are keratinous comb-like ridges that line the upper and lower bills of nearly all Anseriformes. The only Anseriformes lacking lamellae are the mergansers (*Mergus* and *Lophodytes*), which instead have keratinous, tooth-like serrations, and

the screamers (*Anhima* and *Chauna*), which may in fact possess vestigial lamellae (Olson and Feduccia 1980). Although lamellae could function in stripping seeds or grasping vegetation (van der Leeuw et al. 2003), they likely evolved originally for filter-feeding. The only other avian lineages possessing comparable structures, flamingos and prions, also use lamellae to filter-feed (Klages and Cooper 1992; Zweers et al. 1995). *In vivo* experiments have demonstrated a trade-off in performance between filter-feeding and grazing such that specialization in one is accompanied by decreased performance in the other (van der Leeuw et al. 2003). Such a trade-off and the widespread distribution of lamellae among Anseriformes supports the hypothesis that the evolution of grazing, and therefore herbivory, represents a shift away from more duck-like, primarily filter-feeding ancestor. The second line of evidence is the Lower Eocene fossil anseriform *Presbyornis* (Olson and Feduccia 1980), which has a three-dimensionally preserved beak remarkably similar to the modern Freckled Duck (*Stictonetta naevosa*) or Pink-eared Duck (*Malacorhynchus membranaceus*). In spite of a radically non-duck-like postcranial skeleton, this fossil, commonly placed at the stem of the sister group to *Anseranas* (node C in Figure 2.3; Livezey 1997; Clarke et al. 2005), establishes a definitively duck-shaped bill early in the history of Anseriformes in support of the duck-to-goose hypothesis.

These results are also consistent with the proposed theory for the origin of the moa-nalos, a lineage of recently extinct herbivorous geese in the Hawaiian Islands (Olson and James 1991). The skulls of the moa-nalos bear a strong resemblance to those of the exclusively herbivorous Cape Barren Goose of southern Australia and evidence from coprolites confirms that moa-nalos likely fed exclusively on the leaves of native vegetation (James and Burney 1997). Yet despite several goose-like features, morphological and molecular data from sub-fossils place moa-nalos as an early divergence within the subfamily of dabbling ducks Anatinae and not closely related

to any extant lineages of geese (Olson and James 1991; Sorenson et al. 1999). Thus, it has been proposed that moa-nalos evolved from a filter-feeding duck within the past 6 million years, the age of the oldest Hawaiian Island, Kauai (Sorenson et al. 1999). The results of this study support this theory by not only estimating a low degree of herbivory as ancestral for the clade from which moa-nalos are most likely to have evolved, but also by identifying moa-nalos as one example of a series of parallel shifts toward increased herbivory in the evolutionary history of Anseriformes.

The correlation between herbivory and body mass in birds

The historic expectation that body mass is positively correlated with a more herbivorous diet in birds (Morton 1978; Dudley and Vermeij 1992; Klasing 1998) likely stems from a classic 'digestive efficiency' hypothesis that a larger body mass provides advantages in the use of low quality diets (Geist 1974; reviewed in Clauss et al. 2013). Such a hypothesis invokes a physiological mechanism whereby differential scaling of digestive parameters, such as food intake rate, causes larger herbivores to outcompete smaller herbivores or increase the herbivorous portion of their diet. The 'abundance-packet size' hypothesis proposes an ecological mechanism whereby increases in body mass, for reasons perhaps unrelated to dietary shifts, causes animals to shift toward diets composed of foods that are available in increasingly abundant or large packets (Hiiemae 2000; Clauss et al. 2013). In the spectrum of food abundance and packet size, it is supposed that leaves of plants and large animals lie at the extremes of abundance and packet size, respectively. This leads to the prediction that a shift toward larger body mass in non-carnivorous lineages would lead to an increase in herbivory. While both of these hypotheses predict correlated increases between herbivory and body mass, they differ in the proposed sequence of increases: the digestive efficiency hypothesis predicts that increases in

body mass follow shifts toward herbivory while the abundance-packet size hypothesis predicts that shifts toward herbivory follow increases in body mass.

This is the first study to directly test the relationship between body mass and an herbivorous diet in birds in a phylogenetic context. The data show that while there are several predominately herbivorous Anseriformes of large body mass, these are primarily clustered in a single clade (Figures 2.3 and 2.4). Additionally, there are also herbivorous Anseriformes of small body mass which represent independent shifts toward increased herbivory: The American Wigeon (*Anas americana*), Blue-winged goose (*Cyanochen cyanoptera*) and Australian Wood Duck (*Chenonetta jubata*) are all predominately herbivorous but have average body masses between 750 and 1500 grams. Within the Galliformes, the predominately herbivorous Rock Ptarmigan (*Lagopus muta*) and Spruce Grouse (*Dendragapus canadensis*) also have low average body masses relative to both Anseriformes and other Galliformes, less than 600g (Dunning 2008). Thus, once phylogeny is taken into account and for a range of assumed phylogenetic relationships, the apparently significant correlation between herbivory and body mass observed in a non-phylogenetic correlation test is no longer significant (Figure 2.5).

The results of this study do not support the digestive efficiency hypothesis: independent transitions toward increased herbivory are not consistently associated with an increase in body mass. Other vertebrate groups, such as lizards (Pough 1973; Schluter 1984; Cooper and Vitt 2002) and terrestrial mammals (Price and Hopkins 2015) do exhibit a correlation between herbivory and larger body mass. Yet recent studies have shown that this association is not explained by increased digestive efficiency. Studies in mammals, lizards and birds investigating the relationship between food intake rate and body mass and between mean retention time and body mass, the two primary mechanisms by which the digestive efficiency is proposed to

increase, have found little or no evidence that an increase in body mass per se confers a digestive advantage (Clauss et al. 2008; Franz et al. 2011; Fritz et al. 2012; Müller et al. 2013; Steuer et al. 2014). Thus, this study contributes to a growing body of literature refuting a physiological link between body mass and herbivory or dietary digestibility more generally.

The results of this study also appear to contradict the abundance-packet size hypothesis that increases in body mass are associated with shifts toward herbivory. However, two caveats may preclude this study from drawing a strong conclusion regarding this hypothesis. First, the abundance-packet size hypothesis predicts that increases in body mass are followed by increased herbivory. Within Anseriformes, there are likely only three pronounced increases in body mass: the Anserinae, the moa-nalos (represented by *Thambetochen*) and the steamer ducks (*Tachyeres*). The Anserinae and moa-nalos conform to the ecological prediction, showing increases in body mass and shifts to predominately herbivorous diets, while steamer ducks have evolved molluscivory as their predominate feeding mode (Weller 1972; Agüero et al. 2014). Since these two hypotheses make different predictions regarding the sequence of changes in body mass and diet, there may be a sufficient number of dietary shifts to robustly test the digestive efficiency hypothesis but an insufficient number of body mass changes to robustly test the abundance-packet size hypothesis.

The second caveat that may preclude using these results to make a strong conclusion regarding the abundance-packet size hypothesis is that the entire order Anseriformes, relative to other birds, may in fact lie at the extreme of the ecological body mass-diet spectrum, characterized by large body masses and abundant or large packet food sources. In contrast to browsing or catching flying insects on the wing, filter-feeding enables Anseriformes to collect large quantities of aquatic insect larvae, bivalves and seeds en masse (Kooloos et al. 1989; van

der Leeuw et al. 2003; Gurd 2006). Piscivory and molluscivory, in *Mergus* and *Tachyeres* for example, enable the acquisition of large packets of animal food, in analogy to carnivory. And although body masses within this sample span two orders of magnitude, the sampled taxa are heavy relative to other birds: the lightest species in this study (*C. californica*, 166g) is heavier than 78% of extant birds (Dunning 2008). Thus, there may also be insufficient variation in food source abundance or packet size to test the abundance-packet size hypothesis.

Even if Anseriformes occupied a wider range of the body mass-diet spectrum to robustly test the abundance-packet size hypothesis, it is unlikely that a body mass-diet spectrum, as it is currently framed, can adequately explain dietary evolution in birds. Although a seed-eating duck and seed-eating passerine both have diets composed primarily of seeds, the packet sizes differ considerably because of differences between filter-feeding and browsing among individual seed pods and plants. Foraging behavior provides a key link between diet and packet size and likely relates more directly to body mass than diet per se. Thus, a body mass-foraging behavior spectrum may prove more useful in explaining dietary variation along body mass gradients in birds than a body mass-diet spectrum.

Exceptional avian herbivores

If herbivory in birds is not necessarily constrained by an increase in body mass, why is herbivory not more widespread in birds? And what accounts for the exceptional number of transitions toward increased herbivory in Anseriformes relative to other bird orders? An herbivorous diet is a considerable digestive challenge, owing to the low digestibility of leaves, stems and underground parts of plants relative to other foods commonly consumed by birds (Karasov 1990). Herbivorous Anseriformes appear to compensate for this low digestibility by adopting a “high-throughput” strategy: high food intake and short mean retention time (Clauss et

al. 2007; Fritz et al. 2012; Frei et al. 2014). It has been observed more generally across Anseriformes that as the quality of the food ingested increases, less time is spent engaged in food intake both across species (Paulus 1988) and as a response to seasonal shifts within species (Brodsky and Weatherhead 1985; Paulus 1984). As a consequence of higher ingestion rates, mean retention times in herbivorous Anseriformes are shorter by an order of magnitude than avian herbivores that spend less time feeding and rely more on gut fermentation such as the Hoatzin or ostriches (Grajal et al. 1989; Karasov 1990; Mayhew and Houston 1993; Fritz et al. 2012).

This high-throughput strategy poses its own challenges and requires that herbivorous Anseriformes graze continuously for several hours, in some cases over nine hours per day (Owen 1972; Ebbinge et al. 1975). Grazing involves cyclical movements of the upper and lower beak to crop the leaves of plants and the tongue to transport food items into the pharynx (van der Leeuw et al. 2003). This continuous and cyclical motion of the beak is fundamentally different from the way in which most other birds use their beak to feed. Surprisingly, filter-feeding is perhaps the most similar beak behavior among birds to grazing; the upper and lower beak also open and close cyclically in coordination with the tongue to serve as a suction pump for fluid (Zweers et al. 1995; van der Leeuw et al. 2003). Although there is a trade-off in performance between grazing and filter-feeding in Anseriformes, they are not mutually exclusive behaviors and many grazers continue to use filter-feeding to some degree (Johnsgard 1978; van der Leeuw et al. 2003).

While it is perhaps tempting to speculate that filter-feeding, with its similarities to the demands of grazing and likely ancestral distribution among Anseriformes, has facilitated the repeated evolution of herbivory in Anseriformes, empirical support for this hypothesis is lacking.

Filter-feeding has evolved two other times among birds, in flamingos and prions (Klages and Cooper 1992; Zweers et al. 1995), yet neither of these clades displays any tendency toward herbivory (although the mechanism of filter-feeding and ecological context also vary considerably). Additionally, emus have also evolved a high-throughput strategy to herbivory, in contrast to the independently evolved, low-throughput strategy of ostriches, indicating such a strategy is not unique to Anseriformes (Frei et al. 2014).

Anseriformes are also exceptional, relative to other birds, in that transitions to increasing herbivory have occurred, with the exception of the moa-nalos, without the loss of flight. Outside of Anseriformes, herbivory tends to occur in birds that have lost flight or show lower flight capacity (Table 2.1). Several of these lineages are island endemics: the elephant birds of Madagascar (Clarke et al. 2006) and the Moas, Takahe and Kakapo of New Zealand (Mills and Mark 1977; Trewick 1996; Wood et al. 2008). Although island endemism is not a direct cause of increased body mass in birds (Gaston and Blackburn 1995), it is a driving factor in the loss of flight (McNab 1994) which then lessens constraints on a subsequent increase in body mass. Given the result of this and prior studies, the digestive efficiency hypothesis is unlikely to explain the apparent associations among body mass, flightlessness and herbivory outside of Anseriformes. However, the results of this study do not exclude the possibility that the abundance-packet size hypothesis could account for increasing herbivory in large-bodied and flightless birds. Indeed, flightlessness may be an additional factor that, independent of increases in body mass, could drive shifts toward an abundant and easily accessible food source such as herbivory.

Although the underlying causes may remain unclear, the repeated evolution of a more herbivorous diet and its lack of association with a higher body mass or loss of flight in

Anseriformes prompt a reinterpretation of the relatively infrequent origination of herbivory among flighted birds. The unique and versatile feeding apparatus of Anseriformes has likely played a major role in the dietary evolution of this clade. Comparisons of the foraging behaviors, *in vivo* mechanics, and morphology of the feeding apparatus in different lineages of filter-feeding and grazing Anseriformes will shed important insights on the relationships between feeding morphology and diet, the functional analogies between these feeding strategies and the remarkable number of dietary transitions that characterize this diverse clade.

CHAPTER THREE: LINKAGE MECHANISMS IN THE VERTEBRATE SKULL: STRUCTURE AND FUNCTION OF THREE-DIMENSIONAL, PARALLEL TRANSMISSION SYSTEMS[1]

Abstract

Many musculoskeletal systems, including the skulls of birds, fishes, and some lizards consist of interconnected chains of mobile skeletal elements, analogous to linkage mechanisms used in engineering. Biomechanical studies have applied linkage models to a diversity of musculoskeletal systems, with previous applications primarily focusing on two-dimensional linkage geometries, bilaterally symmetrical pairs of planar linkages, or single four-bar linkages. Here we present new, three-dimensional, parallel linkage models of the skulls of birds and fishes and use these models (available as free kinematic simulation software), to investigate structure-function relationships in these systems. This new computational framework provides an accessible and integrated workflow for exploring the evolution of structure and function in complex musculoskeletal systems. Linkage simulations show that kinematic transmission, although a suitable functional metric for linkages with single rotating input and output links, can give misleading results when applied to linkages with substantial translational components or multiple output links. To take into account both linear and rotational displacement we define force mechanical advantage for a linkage (analogous to lever mechanical advantage) and apply this metric to measure transmission efficiency in the bird cranial mechanism. For linkages with multiple, expanding output points we propose a new functional metric, expansion advantage, to

[1]This chapter was submitted for peer review to the Journal of Morphology as: Olsen, A.M. and Westneat, M.W. 2016. Linkage Mechanisms in the Vertebrate Skull: Structure and Function of Three-Dimensional, Parallel Transmission Systems. (Minor revisions recommended)

measure expansion amplification and apply this metric to the buccal expansion mechanism in fishes. Using the bird cranial linkage model, we quantify the inaccuracies that result from simplifying a three-dimensional geometry into two dimensions. We also show that by combining single-chain linkages into parallel linkages, more links can be simulated while decreasing or maintaining the same number of input parameters. This generalized framework for linkage simulation and analysis can accommodate linkages of differing geometries and configurations, enabling novel interpretations of the mechanics of force transmission across a diversity of vertebrate feeding mechanisms and enhancing our understanding of musculoskeletal function and evolution.

Introduction

Biomechanical models link structure and function by providing quantitative hypotheses of how relevant morphological parameters relate to a particular biomechanical function (Herrel et al., 2002; Westneat, 2003; Van Wassenbergh et al., 2006; Davis et al., 2010; O'Brien and Bourke, 2015). In combination with comparative morphological datasets, such models can be used to identify patterns of functional evolution (Westneat, 1995; Wainwright et al., 2004; Nabavizadeh, 2016) or test the biomechanical hypotheses themselves (Bertram and Biewener, 1988; Druzinsky, 1993; Dumont et al., 2005; Ross et al., 2009; Soons et al., 2010). Mechanical linkages, inter-jointed chains of rigid links (Hartenberg and Denavit, 1964), provide a useful model for the motion and force transmission of musculoskeletal systems. Linkage models are particularly useful for musculoskeletal systems in which the skeletal elements interconnect to form closed chains (or loops); closed chains reduce the total mobility of the linkage, decreasing the number of input parameters required to predict the motion of all the links in a linkage.

Closed-chain mechanical linkages have been used as models for a diversity of musculoskeletal systems, including the skulls of fishes (Anker, 1974; Westneat, 1990), some lizards (Frazzetta, 1962; Metzger, 2002), and birds (Bock, 1964), the rib cages of birds (Claessens, 2009), and the striking appendages of mantis shrimps (Patek et al., 2007). These biological linkages exhibit a diversity of forms, differing in the number of links, the mobility at particular joints, and the manner in which the joints are interconnected (Wainwright et al., 2004; Westneat et al., 2005; Anderson et al., 2014). The kinetic skulls of birds and fishes, in particular, are characterized by three-dimensional geometries and skeletal elements that interconnect to form multiple chains or loops (Muller, 1989; van Gennip and Berkhoudt, 1992; Gussekloo et al., 2001; Dawson et al., 2011; Camp and Brainerd, 2014), resembling what are known in engineering as multiloop or parallel linkages (Fig. 3.1; McCarthy, 2006; Liu and Wang, 2014). Biological linkages also exhibit a diversity of functions, transmitting, amplifying, and redirecting input forces and motion into ecologically relevant behaviors (Westneat, 1994; McHenry, 2012).

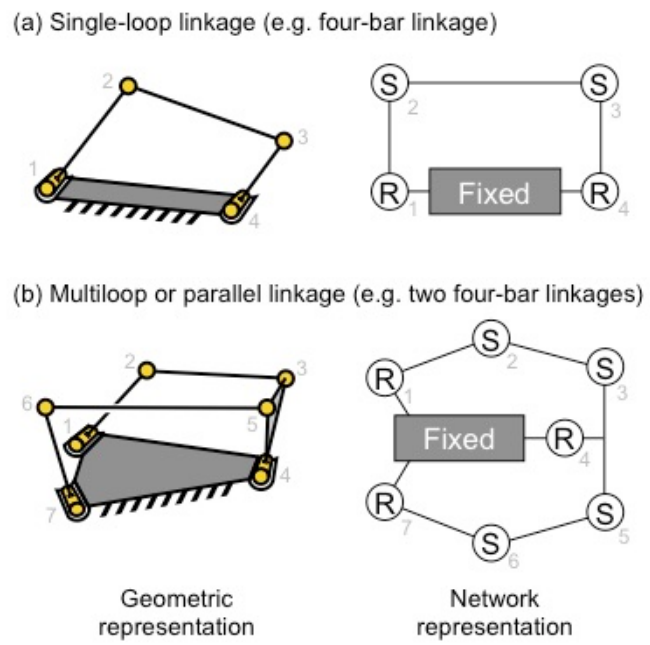

Figure 3.1. A single-chain linkage (a) versus a parallel or multiloop linkage (b), depicted geometrically (left) and as a network of interconnected joints (right), using a four-bar linkage as an example. Numbers indicate corresponding joints between the two representations.

For example, the four-bar linkage of mantis shrimps amplifies motion from an elastic element to drive forceful predatory strikes of a raptorial appendage (Patek et al., 2007) while the cranial linkages of fish skulls redirect forces from the locomotor muscles to rapidly expand the volume of the buccal cavity during suction feeding (Camp et al., 2015).

The geometry, joint constraints, and input motion of a linkage are sufficient to simulate the relative motions of links, a process known as kinematic simulation (Grubich and Westneat, 2006; Anderson and Westneat, 2009; Cooper and Westneat, 2009). Simulated kinematics can be compared against *in vivo* kinematics to test how motor systems transmit force and motion (Westneat, 1990, 1991; Hoese and Westneat, 1996; Bergert and Wainwright, 1997; Herrel et al., 2000; Van Wassenbergh et al., 2005; Roos et al., 2009) or used to calculate functional metrics such as transmission ratios (i.e. leverage or gearing ratios). The most frequently used transmission ratio for linkages is kinematic transmission (KT), which is a ratio of output link rotation relative to input link rotation and represents the extent to which a linkage amplifies angular velocity or inversely amplifies torque (Anker, 1974; Barel et al., 1977). KT has been employed as a functional trait in comparative studies to test hypotheses on the mapping between morphological and functional diversity (Hulsey and Wainwright, 2002; Alfaro et al., 2005), the differential sensitivity of linkage function to changes in underlying morphological components (Anderson and Patek, 2015), and the association between morphology and ecology (Westneat, 1995; Anderson et al., 2014).

While KT has proven utility in predicting *in vivo* kinematics (McHenry et al., 2012) and in explaining patterns of ecological diversification (Westneat, 1995; Anderson et al., 2014), in some cases it is an incomplete measure of linkage function. Most linkages have at least one link (e.g. the coupler link of a four-bar linkage) that moves with both rotational and translational

components; that is, the motion of such a link is not purely rotational. Additionally, many biological linkages, such as those in the skulls of birds and fishes, have multiple input or output links. For fish in particular, multiple output links function in expanding the buccal cavity. Since KT only measures velocity or torque amplification between two rotating links it cannot account for either translational motion or expansion. It remains unclear how these deficiencies may affect the interpretation of linkage function or whether there may be more suitable functional metrics.

Prior applications of linkage models to musculoskeletal systems have also tended to consider only two-dimensional, or planar, geometries and linkages in which all the links interconnect to form a single chain (e.g. a four-bar linkage). Exceptions to this are three-dimensional linkage models of the hyoid depression mechanism in fishes (Muller, 1989; Aerts, 1991), a three-dimensional, parallel linkage model of kinesis in birds (van Gennip and Berkhoudt, 1992), and a parallel linkage model of jaw protrusion in the slingjaw wrasse (*Epibulus insidiator*; Westneat, 1991). While some biological linkages are quite planar and can benefit from the computational simplicity of two-dimensional modeling, it has recently been shown that even for linkages traditionally assumed to be relatively planar, such as the fish opercular linkage, two-dimensional models are poor predictors of *in vivo* kinematics (Camp et al., 2015).

The assumption of planarity can distort the results of a linkage simulation in two ways. First, digitizing a three-dimensional object from a single camera view causes features at a greater distance from the camera to appear smaller relative to closer features, due to the perspective effect introduced by the camera. Second, a two-dimensional or planar linkage model makes the implicit assumption that all axes of rotation are perpendicular to the linkage plane and that all translations are parallel to the linkage plane. The magnitude of error in model predictions

introduced by flattening a three-dimensional geometry into two dimensions has not previously been quantified.

To answer these questions we constructed three-dimensional, parallel linkage models of kinesis in the skulls of birds and suction-feeding fishes. Using these new models we compared kinematic transmission (KT) with alternative functional metrics, including mechanical advantage and a new functional metric, expansion advantage, for quantifying expansion amplification. We also used these models to quantify the errors introduced by simplifying a three-dimensional linkage geometry into two dimensions. To perform kinematic simulation and analysis we introduce new, freely available linkage modeling software integrated into existing workflows for shape data collection and analysis. The central aims of this study are to (1) propose new, parallel linkage models for skull function in birds and fishes, (2) evaluate the use of transmission ratios as metrics for biological linkage function, and (3) extend biological linkage modeling to three dimensions in order to promote synthesis between linkage morphology and mechanics in comparative analyses of musculoskeletal systems.

Methods

Modeling the cranial linkages of birds

In most birds, nine mobile bones in the skull form a set of cranial linkages that enables rotation of the upper beak (Hoese and Westneat, 1996; Bout and Zweers, 2001; Dawson et al., 2011). In birds with prokinesis, the upper beak rotates as a rigid link about a hinge-like joint, in contrast to birds having other forms of kinesis (e.g. rhynchokinesis) in which the upper beak bends at long flexion zones (Zusi, 1984; Estrella and Masero, 2007). We developed a three-dimensional linkage model for a prokinetic bird, using the Great Horned Owl (*Bubo virginianus*) as an example, based on described passive and *in vivo* kinematics in other bird species (Fig. 3.2;

van Gennip and Berkhoudt, 1992; Gussekloo et al., 2001; Dawson et al., 2011) and passive manipulation of fresh Great Horned Owl skulls. Force and motion are transmitted to the upper beak through four links (the quadrate, jugal, pterygoid and palatine) arranged in parallel sets on each side of the skull. All motions are simulated relative to a fixed neurocranium. Acting through this linkage, the quadrate protractor muscle elevates the upper beak while the pterygoid

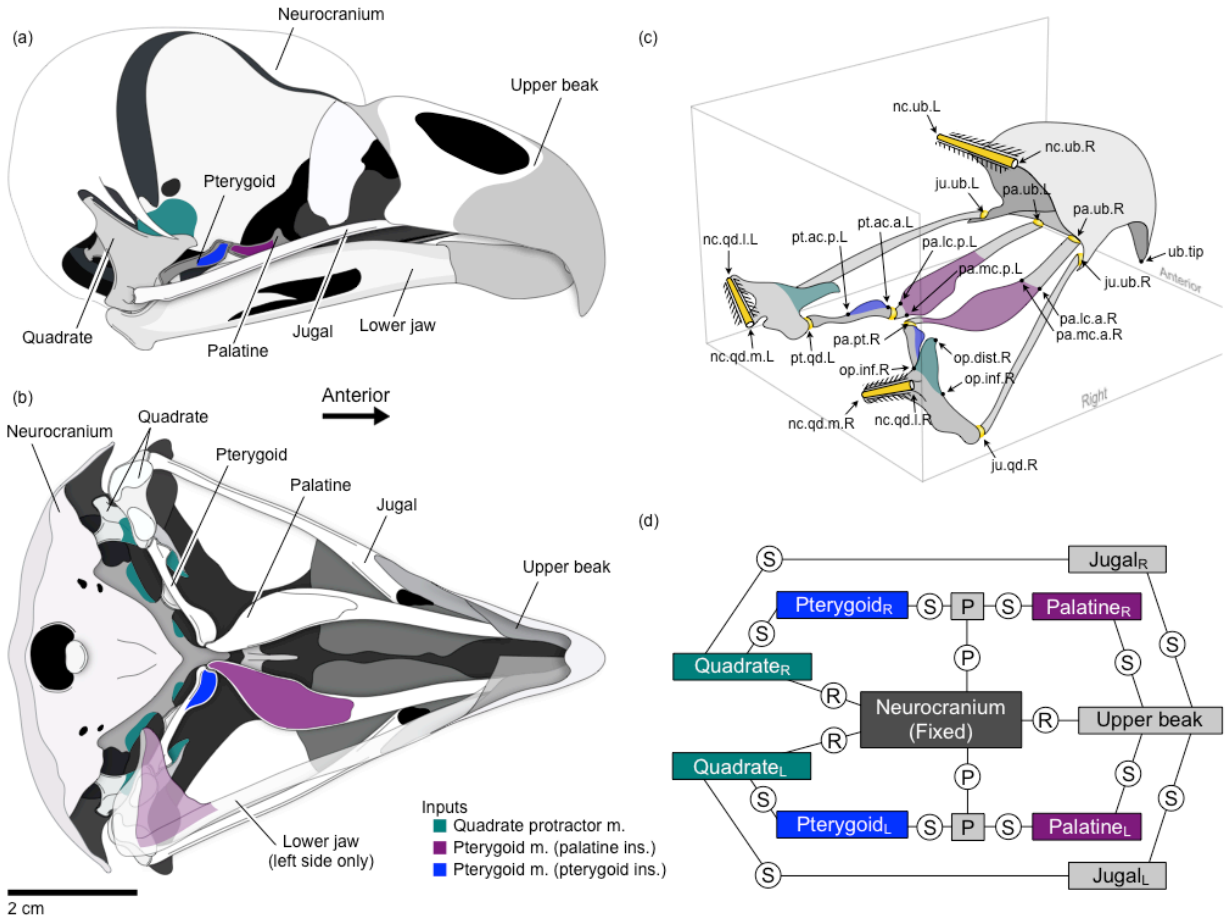

Figure 3.2. The bird cranial linkage mechanism, shown in the Great Horned Owl (*Bubo virginianus*), in lateral (a) and ventral (b) views. (c) Oblique dorso-posterior view of the three-dimensional geometry of the linkage with joints in yellow. Hatching indicates attachment to the fixed link. A key to landmark abbreviations is provided in Table 3.1. L/R refers to left/right; for clarity, not all bilateral landmarks are shown on both sides. (d) The linkage depicted as a network diagram, with links indicated by rectangles and joints by circles; letters denote constraint type (see Methods). *P*-joints and planar sliding links (not shown in c) constrain joint motion to the parasagittal plane.

Table 3.1. Key to landmark abbreviations used in figures 3.2c and 3.3c.

Abbreviation	Description
Owl	
ju.qd	Jugal-quadrate joint
ju.ub	Jugal-upper beak joint
nc.qd.m	Medial condyle of neurocranium-quadrate joint
nc.qd.l	Lateral condyle of neurocranium-quadrate joint
nc.ub	Neurocranium-upper beak joint
op.dist	Distal point of orbital process
op.inf	Inferior base of orbital process
op.sup	Superior base of orbital process
pa.lc.a	Anterior extent of lateral palatine crest
pa.lc.p	Posterior extent of lateral palatine crest
pa.mc.a	Anterior extent of medial palatine crest
pa.mc.p	Posterior extent of medial palatine crest
pa.pt	Palatine-pterygoid joint
pa.ub	Palatine-upper beak joint
pt.ac.a	Anterior limit of pterygoid anterior crest
pt.ac.p	Posterior limit of pterygoid anterior crest
pt.qd	Pterygoid-quadrate joint
ub.tip	Upper beak tip
Salmon	
ac.as	Anterosuperior corner of anterior ceratohyal
ac.pi	Posteroinferior corner of anterior ceratohyal
ac.ps	Posterosuperior corner of anterior ceratohyal
ac.hy	Anterior ceratohyal-hypohyal joint
hy.mid	Midsagittal point on hypohyal
hy.sh	Sternhyoideus muscle insertion on hypohyal
nc.ep	Epaxial insertion on neurocranium
nc.su.a	Neurocranium-suspensorium anterior joint
nc.su.p	Neurocranium-suspensorium posterior joint
lj.qd	Lower jaw-quadrate joint
lj.sy.inf	Inferior aspect of lower jaw symphysis
lj.sy.sup	Superior aspect of lower jaw symphysis
nc.vc	Neurocranium-vertebral column joint
pc.ai	Anteroinferior corner of posterior ceratohyal
pc.as	Anterosuperior corner of posterior ceratohyal
pc.su	Posterior ceratohyal-suspensorium joint
px.mid	Anterior part of premaxilla at the midline

muscle, which inserts on the pterygoid and palatine, retracts the upper beak. While the quadrate of some bird species articulates with the neurocranium by a single condyle, permitting full rotational degrees of freedom (Dawson et al., 2011), the quadrate of owls has two widely spaced condyles that likely fix a single axis of rotation *in vivo* (Fig. 3.2c).

Modeling the cranial linkages of suction-feeding fishes

The skulls of fishes are characterized by multiple interconnected chains of skeletal elements arranged in diverse geometries and configurations that grant a high degree of mobility (Lauder, 1982; Wainwright et al., 2004). The neurocranium, suspensoria, mandibular arch and hyoid arch form a central linkage that expands the buccal cavity during suction feeding (Anker, 1974; Muller, 1989; Van Wassenbergh et al., 2005; Konow and Sanford, 2008; Van Wassenbergh et al., 2013; Camp and Brainerd, 2014). We developed a three-dimensional linkage model to simulate the motion of these bones, using the Atlantic salmon (*Salmo salar*) as an example (Fig. 3.3). Our model is based on previously published models and *in vivo* kinematics in other fish species (Aerts, 1991; De Visser and Barel, 1998; Van Wassenbergh et al., 2005; Camp and Brainerd, 2014) and on passive manipulations of fresh salmon skulls.

Our linkage model incorporates the vertebral column, neurocranium, suspensoria, lower jaw, hyoid, lower jaw symphysis, hypohyal, and soft tissue connections between the hyoid arch and lower jaw. All motions are simulated relative to a fixed vertebral column. The suspensoria rotate relative to the neurocranium about broad, hinge-like axes of rotation (Fig. 3.3c; De Visser and Barel, 1998). The suspensoria are joined by the lower jaw anteriorly and the hyoid arch posteriorly. We make the simplifying assumption of rigid links, including the bones that comprise the hyoid and soft tissue in tension between the hyoid and lower jaw. The two primary

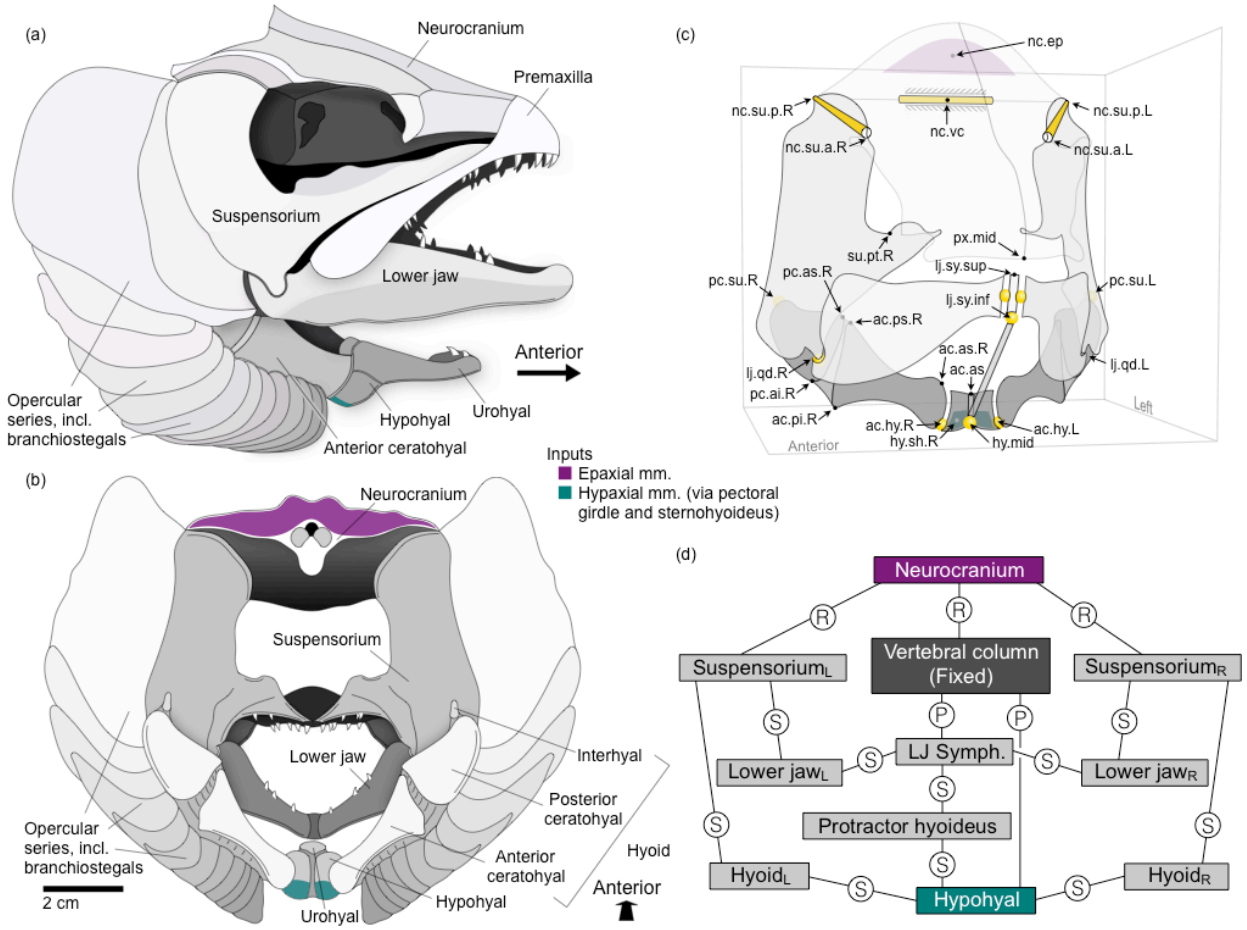

Figure 3.3. The mandibular and hyoid arch of teleost fishes, shown in the Atlantic salmon (*Salmo salar*), in lateral (a) and posterior (b) views. (c) Oblique anterior view of the three-dimensional geometry of the linkage with joints in yellow. Hatching indicates attachment to the fixed link. A key to landmark abbreviations is provided in Table 3.1. L/R refers to left/right; for clarity, not all bilateral landmarks are shown on both sides. (d) The linkage depicted as a network diagram, with links indicated by rectangles and joints by circles; letters denote constraint type (see Methods). *P*-joints (not shown in c) constrain joint motion to the midsagittal plane.

force inputs to the linkage are the epaxial and hypaxial musculature, or muscles along the dorsal and ventral aspects of the body, respectively (Camp et al., 2015). The epaxial musculature elevates the neurocranium about the vertebral column while the hypaxial musculature exerts an indirect force on the hyoid through the shoulder girdle and sternohyoideus muscle, retracting the hyoid posteriorly and ventrally.

Shape data collection

The three-dimensional coordinates (landmarks) of the joints in the bird and fish linkages were collected using a two-camera, stereo setup; camera calibration and landmark digitization, reconstruction and bilateral reflection were performed using the R package StereoMorph (Olsen and Westneat, 2015). Bird linkage landmarks were collected from three Great Horned Owl skeletal specimens from the Field Museum of Natural History and fish linkage landmarks were collected from three fresh specimens obtained from a local fish market. Two-dimensional landmarks for the planar bird linkage model were collected by digitizing a single lateral photograph of each owl specimen.

Kinematic simulation

While commercial multibody dynamic software provides a generalized framework for 3D linkages of any configuration (e.g. SimMechanics, AnyBody Modeling System), all currently require a cost to implement and none is well suited to integration with morphometric analyses. We have developed a new, free software package, linkR (Olsen, 2016a; cran.r-project.org/package=linkR), for three-dimensional kinematic simulation and analysis of parallel linkages written in the cross-platform R language (R Core Team 2015). Linkages are defined in linkR as an interconnected set of joints, each imposing a particular constraint on motion between the two links it connects (Liu and Wang, 2014). In this study we use three basic joint constraints: rotational (*R*), spherical (*S*) and planar (*P*). Rotational joints permit only rotation about a single axis, spherical joints permit rotation about all three axes (including long-axis rotation), and planar joints permit translation within a plane. The configurations of the bird and fish cranial linkages are depicted in figures 2d and 3d, respectively. Each is constructed from a set of two

different single-chain linkages; the degrees of freedom of a parallel linkage are not necessarily the same as those of the constituent linkages (Fig. 3.4).

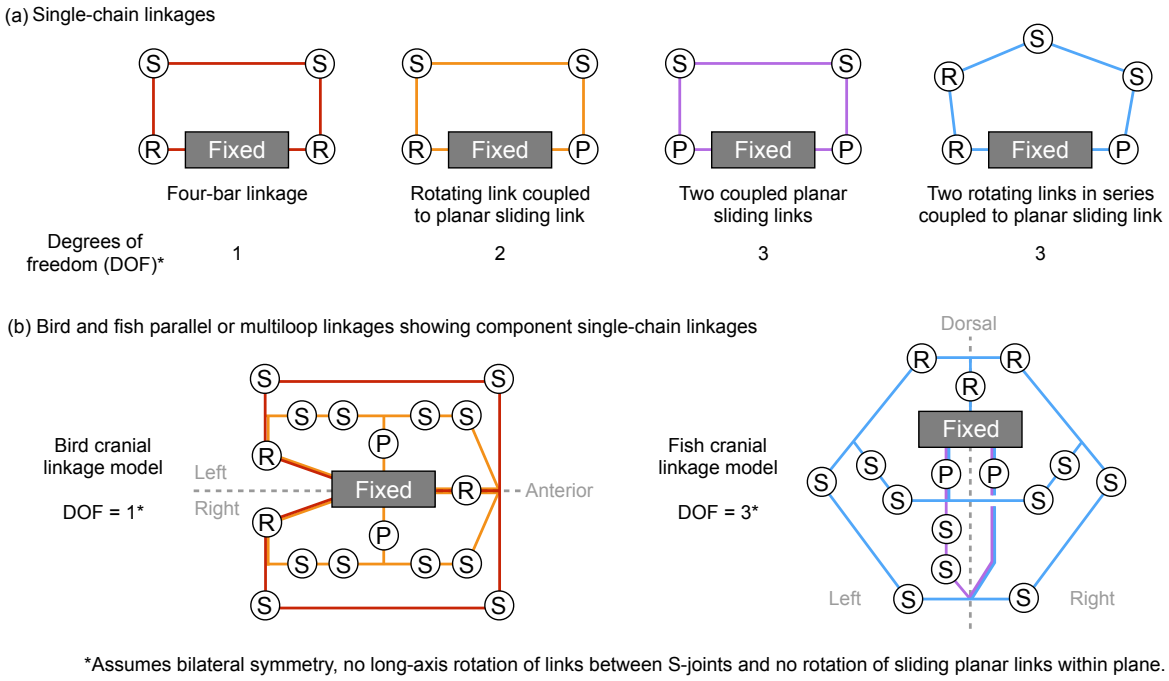

Figure 3.4. The degrees of freedom of a parallel linkage can differ from those of its constituent single-chain linkages. Four single-chain linkages (a) are combined to construct the bird and fish parallel linkages (b).

To perform kinematic simulation a set of input rotations or translations equal to the degrees of freedom (DOF) of the linkage must be specified, thus ensuring a single solution for all joint positions. Here, 'degrees of freedom' refers to the number of parameters needed to completely describe the conformation of the linkage (i.e. the shapes of the linkage through time). To reduce the degrees of freedom for each linkage we assume bilateral symmetry, no long-axis rotation of links joined at each end by S-joints and no rotation of planar sliding links within the plane. We use *P*-joints to maintain bilateral symmetry: pterygoid-palatine joint motion is

constrained to the parasagittal plane for the bird model and the hypohyal and lower jaw symphysis are constrained to the midsagittal plane for the fish model.

The simulation software then uses analytical geometry to solve for all the unknown joint positions (Supplementary Materials S2). The linkR package is not currently intended for time-dependent or dynamic simulation but rather for predicting relative motion, which is sufficient for calculating transmission ratios and other functional metrics. Our bird cranial linkage model has one degree of freedom; we specified a 5-degree rotation of the upper beak as the input. Our fish cranial linkage model has three degrees of freedom: neurocranium elevation-depression and two-dimensional translation of the hypohyal in the midsagittal plane (antero-posterior and dorso-ventral). To quantify the transmission efficiency (the ratio of relative motion in a mechanism between an input and output) of force input to the neurocranium and hypohyal independently, we performed two simulations: a 4 degree rotation of the neurocranium without hypohyal translation and a 3 mm translation of the hypohyal without neurocranial rotation. The path of hypohyal translation (i.e. the relative magnitudes of anterior-posterior and dorsal-ventral translation) affects linkage kinematics (Aerts, 1991; De Visser and Barel, 1998). We simulated multiple trajectories of the hypohyal in the form of straight-line paths varying in angle from 0 to -45 degrees relative to the anterior-posterior axis, with more negative angles corresponding to more inferiorly directed translations. Although the *in vivo* path of the hypohyal in salmon is unknown, *in vivo* kinematics collected for another salmonid taxon (*S. fontinalis*) during raking behavior, which has been characterized as a "closed-mouth strike", supports the assumption of a straight-line trajectory (Konow et al., 2008). Simulations were visualized using the R package svgViewR (Olsen, 2016b), which creates interactive, three-dimensional visualization files that can be viewed in the web browser (see Data Accessibility).

Linkage functional metrics

We used the results of the kinematic simulation to calculate linkage functional metrics, including mechanical advantage (MA) and kinematic transmission (KT). MA measures the amplification of either force or torque through a mechanism, referred to here as force MA (MA_f) and torque MA (MA_t), respectively. Mechanical advantage can be derived from the relationship between work, force and displacement. We demonstrate that KT is equal to the inverse of torque MA.

The movement of a point as a result of a force (F) is associated with an amount of work (δW), or energy, equal to the product of the force and displacement (dx) vector magnitudes.

$$\delta W = F dx \tag{3.1}$$

Assuming work is conserved across the mechanism, input work equals output work (input and output represented by subscripts i and o, respectively).

$$\delta W = F_o dx_o = F_i dx_i \tag{3.2}$$

The input and output force and displacement magnitudes can be equated as ratios, representing force MA.

$$MA_f = \frac{dx_i}{dx_o} = \frac{F_o}{F_i} \tag{3.3}$$

For a point on a rotating body, the displacement can be expressed in terms of the moment arm length (r) and the change in angular displacement ($d\theta$).

$$dx = r d\theta \tag{3.4}$$

For input and output points on rotating bodies, force MA is:

$$MA_f = \frac{r_i d\theta_i}{r_o d\theta_o} = \frac{F_o}{F_i} \tag{3.5}$$

For a single lever, the input and output angular velocities are equal. Thus, equation (5) simplifies to the familiar ratio of input moment arm to output moment arm length:

$$MA_f(lever) = \frac{r_i}{r_o} = \frac{F_o}{F_i} \tag{3.6}$$

Equations (3.2) and (3.4) can also be combined to present the conservation of work in terms of angular displacement.

$$\delta W = F_o r_o d\theta_o = F_i r_i d\theta_i \tag{3.7}$$

The torque (τ) and angular displacement vectors can be equated as the ratios of angular displacement and torque (the product of the force and moment arm length), representing torque MA.

$$MA_t = \frac{d\theta_i}{d\theta_o} = \frac{\tau_o}{\tau_i} = \frac{F_o r_o}{F_i r_i} \tag{3.8}$$

KT, a measure of angular displacement amplification, is then the inverse of torque MA.

$$KT = \frac{1}{MA_t} = \frac{d\theta_o}{d\theta_i} = \frac{\tau_i}{\tau_o} \tag{3.9}$$

Torque MA can be made equal to force MA by multiplying torque MA by the ratio of moment arms, if and only if both links move exclusively by rotation.

$$MA_t \frac{r_i}{r_o} = MA_f \tag{3.10}$$

Force and torque MA only measure force and displacement amplification at a single point or along a single rotating body, respectively. Thus, they might prove inadequate for mechanisms that generate expansion, which might be considered to have multiple output points or links. We developed a new functional metric, expansion advantage (EA), to relate time-varying changes in linkage size (due to compression or expansion) to input translation. Linkage size is measured using centroid size (CS), a commonly used metric in shape analysis to measure the size of a

landmark set (Zelditch et al., 2012). Centroid size is defined as the square root of the summed differences between all landmark coordinates and the landmark centroid (mean coordinate),

$$CS = \sqrt{\sum_{i=1}^{K}\sum_{j=1}^{M}\left(X_{ij} - C_j\right)^2} \tag{3.11}$$

where K is the number of landmarks (X), M is the number of dimensions and C is the landmark centroid. Since CS is one-dimensional, the ratio of CS change and input displacement yields a dimensionless ratio, EA, which represents the change in linkage size for a given input motion.

$$EA = \frac{dCS}{dx_i} \tag{3.12}$$

We calculated instantaneous KT, MA and EA values over a range of linkage positions for the bird and fish cranial linkage models. Kinematic simulation can be used to approximate instantaneous transmission ratios by simulating very small input displacements (e.g. dx_i, $d\theta_i$) at various linkage positions and measuring the relevant output variables (e.g. $d\theta_o$, dx_o, dCS); this is equivalent to approximating a derivative by adding small steps at different function values and computing the difference quotient. For both models we found that linear displacements of 0.0001 mm and angular displacements of 0.00001 deg were sufficient to estimate transmission ratios with errors less than 0.01%.

Results

Function in the bird cranial linkage

Kinematic simulation of the three-dimensional owl cranial linkage predicts a 5-degree rotation of the upper beak for a 6.5 degree rotation of the quadrates (Fig. 3.5a; see Data Accessibility for video). The pterygoids and palatines displace by both translation and rotation; for 5 degrees of upper beak rotation, the pterygoids translate 1.4 mm and rotate 1.2 degrees while

the palatines translate 2 mm and rotate a total of less than 0.4 degrees. Torque MA (inverse KT) and force MA yield opposite rankings of quadrate, pterygoid, and palatine transmission efficiency (Figs. 3.5b versus 5c). The small rotational components of pterygoid and palatine motion, in comparison with the quadrate, lower their corresponding torque MA relative to quadrate torque MA (Fig. 3.5b; we compare inverse KT, rather than KT, to force MA since both measure input-to-output amplification). However, taking into account total displacement (translation and rotation), insertion sites on the palatine and pterygoid show greater average displacement than those on the quadrate, causing the average force MA of the pterygoid and palatine to exceed that of the quadrate (Fig. 3.5c). Force MA values for the pterygoid and palatine show declines between 9 and 14% due to a progressive decrease in displacement with upper beak protraction. The wide range of MA and KT values are due primarily to the range of insertion points considered within each individual rather than variation among individuals. The range of force MA for the quadrate is two times that of the pterygoid and palatine owing to a greater range of in-lever lengths for the quadrate protractor muscle.

The force MA simulation results using two-dimensional, lateral landmarks recovers the same ranking by input (palatine > pterygoid > quadrate) as simulations using three-dimensional landmarks and estimates mean palatine force MA within 2% of the three-dimensional simulation results (Fig. 3.5c,e). However, two-dimensional simulations overestimate quadrate force MA by 20% and pterygoid force MA by 15% and show no apparent change in palatine or pterygoid force MA as a function of upper beak rotation. Since force MA is a more appropriate metric for comparing the transmission efficiency of different inputs in the bird cranial linkage we show only the results of force MA for the two- versus three-dimensional comparison. Torque MA using the two-dimensional model shows a similar pattern for quadrate and palatine inputs as

three-dimensional torque MA, but for pterygoid input the two-dimensional model returns a torque MA 50% less than that of the three-dimensional model (results not shown). Thus, the two-dimensional model does not capture the full rotation of the pterygoid during kinesis.

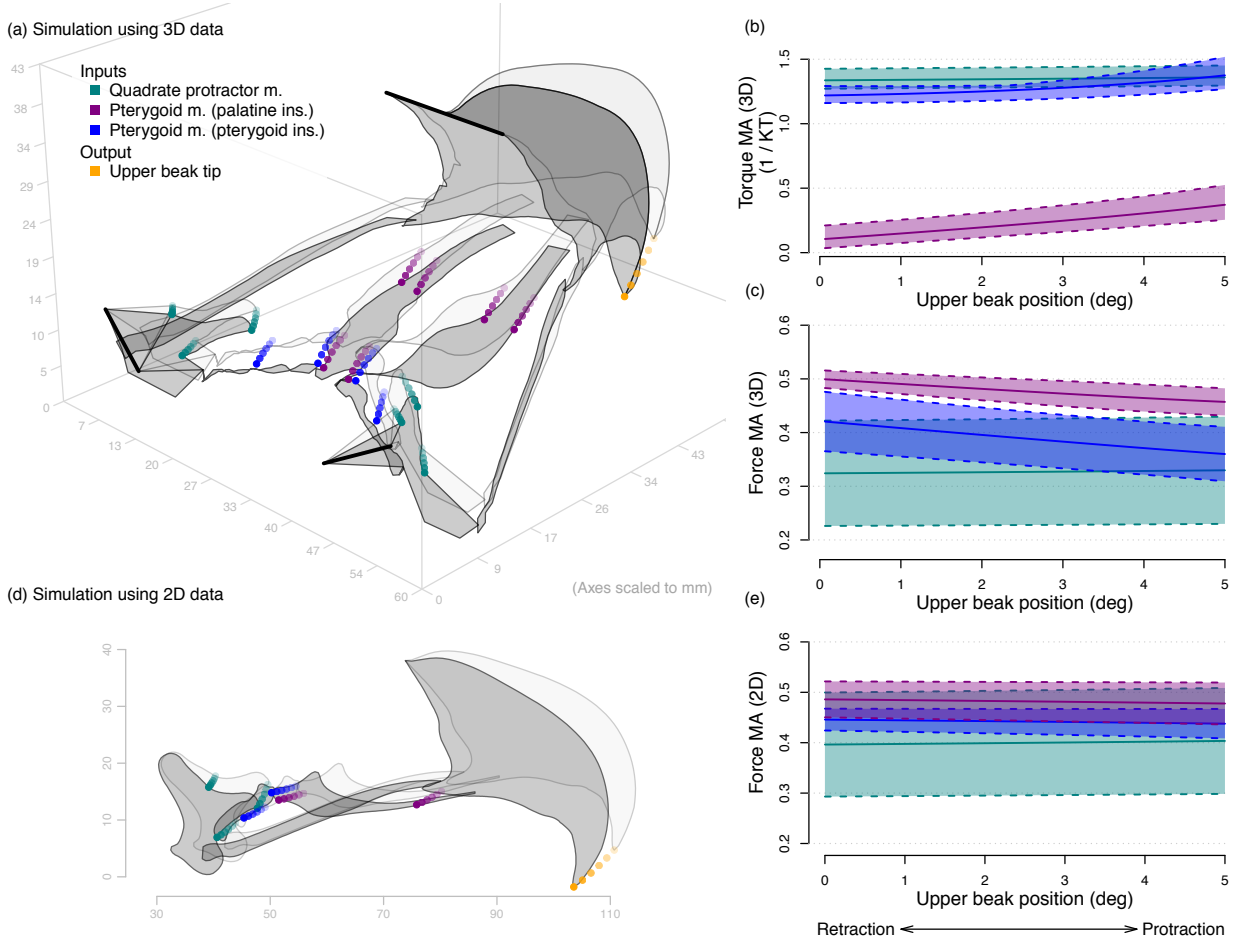

Figure 3.5. Simulation results, mechanical advantage (MA) and inverse kinematic transmission (KT) for the bird cranial linkage calculated using three-dimensional (a-c) and two-dimensional (d-e) linkage models. (a) Oblique dorso-posterior view of the three-dimensional linkage at two positions. Insertion points used to calculate force MA (c) are indicated by colored points. Lighter opacity corresponds to a more protracted upper beak. For (b-c) and (e) solid lines indicate means and dashed lines indicate the full range of values across all individuals (n = 3). Ranges also include the range of insertion sites for each muscle.

Function in the fish cranial linkage

Kinematic simulation of the salmon cranial and hyoid linkages predicts that neurocranial elevation and hypohyal retraction independently result in buccal expansion (Fig. 3.6a,e; see Data Accessibility for video), although the rate of expansion is greatest when both inputs act simultaneously. We present the results of simulating each input independently in order to compare transmission ratios for each input.

The KT ratios for different input-output pairs show differing magnitudes and patterns of angular velocity amplification (Fig. 3.6b,f). Angular velocity amplification is consistently higher for neurocranial input than for hypohyal input (as measured by hyoid rotation), at least 4-5 times greater at the start of mouth opening. For hypohyal input, the rate of lower jaw rotation relative to hyoid rotation increases with mouth opening while the rate of suspensorial rotation relative to hyoid rotation decreases with mouth opening. Consequently, lower jaw-hyoid KT increases with mouth expansion while suspensorium-hyoid KT decreases with mouth expansion (Fig. 3.6b). For neurocranial input, the rates of lower jaw and suspensorium rotation relative to neurocranial elevation both decrease as the mouth opens (Fig. 3.6f). As a result, both neurocranium-input KTs decline with mouth expansion (Fig. 3.6f).

The linkage model predicts that the buccal cavity expands relatively quickly at first followed by a subsequent decline (Fig. 3.6c,g), resulting in a decline in expansion advantage (Fig. 3.6d,h); EA decreases by approximately 50% on average with mouth opening for both hypohyal and neurocranial inputs. Similar to the KT results, the model predicts that EA (i.e. expansion amplification) for neurocranial input is at least 5 times greater than that for hypohyal input (Fig. 3.6h versus 3.6d). For hypohyal input, the combined variation in the angle of input

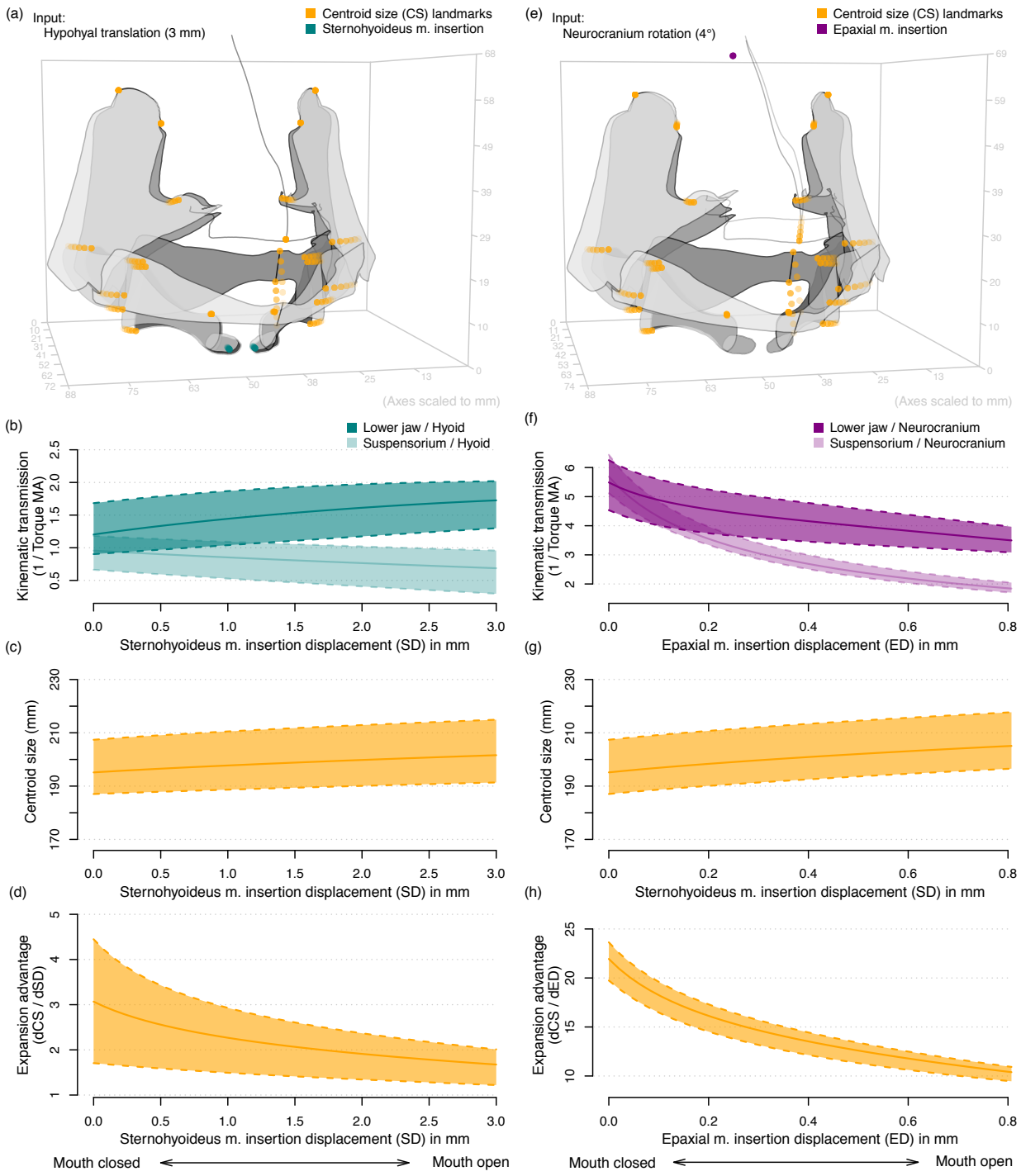

Figure 3.6. Simulation results, centroid size (CS), kinematic transmission (KT) and expansion advantage (EA) for the fish cranial linkage calculated by independently simulating posterior translation of the hypohyal (a-d) and elevation of the neurocranium (e-h). The positions of the links for a closed and open mouth are indicated in (a) and (e). Sites of force input to the hypohyal and neurocranium are indicated by teal points (a) and purple points (e), respectively. Centroid

(Figure 3.6. continued) size (CS) landmarks are indicated in orange. Lighter opacity corresponds to a more expanded position. Due to the relatively small displacements of the hypohyal and neurocranium inputs, successive iterations of these landmarks are largely superimposed. For (b-d) and (f-h) solid lines indicate means and dashed lines indicate the full range of values across all individuals (n = 3).

hypohyal translation (0 to -45 degrees) and interindividual variation accounts for the variation in KT, centroid size (CS), and EA values (Fig. 3.6b-d). For EA in in particular, more posterior (rather than inferior) translation of the hypohyal increases the rate of buccal expansion (maximum dashed line) as this produces greater lateral expansion of the suspensoria. In contrast, for neurocranial input, the ranges of KT, CS, and EA are due entirely to interindividual variation as only a single input rotation was used (Fig. 3.6f-h).

Discussion

A central conclusion of this study is that a new and versatile framework for representing, simulating and analyzing the kinematics of three-dimensional biological linkages has the potential to transform studies of linkage function in biomechanics. The new models of bird and fish cranial linkages presented here demonstrate the potential of this framework to encompass biological linkages of diverse geometries and configurations. This framework also forms the basis of open source computational tools for simulating and analyzing linkage kinematics, a product that biologists and engineers alike are encouraged to test and employ in research applications. Below we discuss the use of transmission ratios as metrics of biological linkage function, modeling parallel biological linkages in three dimensions and the use of this framework in building a greater synthesis between the study of linkage structure and function.

Functional metrics for biological linkages

Transmission ratios, such as mechanical advantage or kinematic transmission, are ideal functional metrics for biological linkages because they are dimensionless ratios and have a clear biomechanical significance as measures of the extent to which a mechanical system amplifies force or velocity (i.e. gearing or leverage). Importantly, transmission ratios alone do not predict absolute force or velocity but rather the relative difference in force or velocity between an input and output of a mechanical system (Arnold et al., 2011; McHenry and Summers, 2011). However, since the gearing of a mechanical system determines the efficiency with which potential energy is converted into kinetic energy, if the principal sources of energy loss in a mechanical system are known, transmission ratios can also be used to predict absolute force or velocity (McHenry, 2012). We show that the difference between force MA and KT, two of the most common transmission ratios for biomechanical systems, is that the former measures linear amplification between two points in a mechanical system while the latter measures angular amplification between two rotating links (Eqs. 3 and 9). Whether force MA or KT is most

Table 3.2. Recommended functional metrics for different linkage types.

Linkage attributes	Functional metric
• Single input and output link • Motion of input and output links is primarily rotational	Kinematic transmission (KT) or torque mechanical advantage (MA_t)
• Single input and output link • Input and output at particular points in system • Motion of either input or output link has large translational component	Force mechanical advantage (MA_f)
• Multiple input or output links • Motion of either input or output links is contraction or expansion	Expansion advantage (EA)

suitable for a particular system depends on the nature of the input and output forces and motions (Table 3.2).

Kinematic transmission (KT), or inverse torque MA (Eq. 9), is used to describe linkage gearing in two of the best studied biological linkages: the four-bar anterior jaw linkage of teleosts (Westneat, 1995; Hulsey and Wainwright, 2002; Alfaro et al., 2004, 2005; Wainwright et al., 2004, 2005) and the four-bar linkage of the mantis shrimp striking appendage (Patek et al., 2007; McHenry et al., 2012; Anderson, 2010; Anderson et al., 2014). KT of the anterior teleost jaw linkage relates output rotation of the maxilla to input rotation of the lower jaw (Barel et al., 1977; Westneat, 1994) while KT of the mantis shrimp linkage relates output rotation of the striking appendage to rotation of the meral-V, a spring-loaded input link (Patek et al., 2007). In both cases, the output link is the coupler link of the four-bar linkage (the link connecting the two rotating links), the motion of which can vary from pure translation to pure rotation, depending the configuration and conformation of the linkage (Hartenberg and Denavit, 1964). Thus, KT, taking into account only angular displacement, will consistently underestimate the total displacement advantage. However, for both the fish jaws and the mantis shrimp claw, biomechanical models and the KT of the linkage have been shown to accurately predict *in vivo* kinematics (Westneat, 1990, 1994; Patek et al., 2007; McHenry et al., 2012), indicating that there are cases in which the translational component of the coupler link is small.

Despite the utility of torque MA for some linkage systems, we demonstrate its limitations as a metric of force transmission from muscles to the upper beak in the bird cranial kinesis mechanism. First, input and output forces are applied at discrete points: muscle insertions and points on the upper and lower beak where items are grasped, respectively (Fig. 3.2). Second, the motions of the pterygoid and palatine relative to the neurocranium both have translation

components that are not adequately captured in torque MA, which considers only link rotation. Torque MA gives the impression that the mechanical advantage is highest for input to the quadrate, followed by the pterygoid and palatine (Fig. 3.5b). However, force MA, which takes into account the total displacement of the pterygoid and palatine, yields the opposite ranking (Fig. 3.5c). The palatine, which moves primarily by translation, has a near zero torque MA but the largest force MA relative to insertions on the quadrate and pterygoid. Thus, force MA is a more suitable functional metric for systems with input and output forces applied at discrete points or when the motion at points of input or output force has large translational components (Table 3.2).

The results of the fish linkage model show the limitations of KT in describing transmission efficiency during buccal expansion. While muscle insertions on the hypohyal and neurocranium can be taken as points of input force, there is no single output point or rotating output link (Fig. 3.3). Rather, the output of the linkage is expansion of many points simultaneously, indicated by increasing centroid size (Fig. 3.6c,g). Additionally, the KTs for different pairs of input and output links yield conflicting impressions of the rate of buccal expansion as a function of mouth opening. KT based on ratios of hyoid to lower jaw and suspensorial rotation give the impression of increasing or slightly decreasing rates of buccal expansion (Fig. 3.6b), while ratios based on neurocranial to lower jaw and suspensorial rotation give impressions of more substantial decreases in the rate of buccal expansion (Fig. 3.6f). Expansion advantage (EA) circumvents these limitations by taking into account several output points and as a consequence shows a consistent decline in the relative rate of buccal expansion for both hypohyal and neurocranial inputs (Fig. 3.6c,f).

There are, however, caveats to the use of expansion advantage as a functional metric. First, unlike mechanical advantage, expansion advantage does not have a clear biomechanical significance. A transmission ratio should account for all input and output motion. In contrast, changes in centroid size will only account for displacements toward and away from the centroid (Eq. 11). While this decreases its clear biomechanical interpretation, we argue that it enhances its use as a functional metric for buccal expansion in fishes. The principal output force during buccal expansion in fishes, that which opposes input forces from the axial muscles, is likely the negative buccal pressure exerted on the bones surrounding the mouth rather than drag (Camp et al., 2015). Since buccal pressure depends in part on the rate of mouth volume change, the rate of mouth expansion, included in expansion advantage as the instantaneous change in centroid size, should be a better proxy for output force than displacement more generally. A second caveat is that centroid size is only an approximate measure of overall linkage size, it is dependent on the number and distribution of landmarks distributed throughout the linkage and it is not entirely separable from shape (Bookstein, 1989). Because of the sensitivity of centroid size to the choice of landmarks, comparisons of expansion advantage across multiple species will be most meaningful when the same set of homologous landmarks is used for all species.

Despite these caveats we maintain that expansion advantage is a better functional metric than force MA or KT for the cranial-hyoid linkages of suction-feeding fishes. Expansion advantage better captures the function of the linkage in expanding the mouth and samples points throughout the linkage rather than at a single point or link. Additionally, because centroid size is one-dimensional and in the same units as input translation, the resulting ratio is dimensionless, like mechanical advantage. Lastly, centroid size can easily be calculated using the same set of

landmarks that one might use in geometric morphometric analyses, making expansion advantage ideal for relating structure and function in comparative studies of fish skull diversity.

Modeling parallel biological linkages in three dimensions

Previous studies of biological linkages have primarily considered linkage models in which all the links interconnect to form a single, closed chain. As a consequence, musculoskeletal systems consisting of multiple interconnecting skeletal elements, such as the skulls of birds and fishes, are divided up into several single-chain linkages, each of which is studied in isolation. We demonstrate that these more complex musculoskeletal systems can be modeled as parallel linkages, while maintaining or even decreasing the number of input parameters required for kinematic simulation (Fig. 3.4). In the case of the bird linkage model, the lateral four-bar linkages and medial sliding-link linkages share the same rotating links (Fig. 3.2d). As a result, the solution of the single degree of freedom four-bar linkage can be used to solve the position of the planar sliding joint, resulting in single degree of freedom for the entire mechanism (Fig. 3.4). In the case of the fish linkage model, the assumption of coupling between the hyoid and lower jaw during mouth opening via a tensed protractor hyoideus muscle makes it possible to predict lower jaw rotation from hyoid rotation (Fig. 3.3d). Thus, although each single-chain linkage has three degrees of freedom when simulated independently, the combined parallel mechanism also has just three degrees of freedom (Fig. 3.4). Both cases show that parallel linkage models present advantages over a single-chain approach by constraining the possible conformations of models with greater numbers of links and enabling the investigation of how coupling mechanisms influence overall linkage kinematics.

Previous studies of biological linkages have also primarily considered two-dimensional linkage models, with the notable exception of work simulating the hyoid linkage of fishes in

three dimensions (Aerts, 1991; De Visser and Barel, 1998) and a three-dimensional linkage model of kinesis in birds (van Gennip and Berkhoudt, 1992). While the use of two-dimensional models to represent three-dimensional geometries simplifies both data collection and simulation it also distorts the true joint coordinate positions and does not permit out-of-plane motion. We used the owl cranial linkage to quantify the error resulting from the use of a simpler two-dimensional linkage model rather than the full three-dimensional model. Owls have exceptionally wide skulls among birds, causing the two-dimensional landmarks collected from a lateral view to be more distorted from their actual three-dimensional position in comparison with other bird species. Thus, by using an owl skull as the basis of the bird linkage model we present a worst-case example of the inaccuracies introduced by flattening a three-dimensional geometry to two dimensions. Since three-dimensional landmarks more accurately represent the true geometry of the skull, the results of the two-dimensional model can be compared against those of the three-dimensional model to quantify the magnitude of these inaccuracies.

Surprisingly, the planar model recovers the same overall pattern of force transmission results as the three-dimensional model (Fig. 3.5c,e), including the same ranking of force MA by input and an average palatine force MA within 2% of the three-dimensional model (Fig. 3.5c,e). However, the planar model also introduces two main inaccuracies. First, the planar model overestimates the average force MA for two of the three input links by 15-20% (Fig. 3.5e). Second, the planar model falsely predicts that the force MA values for the pterygoid and palatine remain constant as a function of upper beak rotation. In the three-dimensional model, the palatine and anterior pterygoid follow an arcing trajectory as they displace superiorly and anteriorly, causing relative input displacement and force MA to decrease with upper beak protraction (Fig. 3.5a,c). The magnitude and direction of errors resulting from assumptions of planarity will

depend on the particular geometry of the linkage and may in some cases be trivial. In particular, given that the results presented here represent a worst-case example, the errors resulting from planar linkage models applied to other bird species will likely be less than those found in this study. Nevertheless, these results do encourage caution when interpreting the results of two-dimensional linkage models applied to biological linkages with substantially three-dimensional geometries or motions.

We have limited the comparison of two- and three-dimensional models to the bird linkage model because it is not possible to construct a two-dimensional linkage model for buccal expansion that incorporates both suspensorial and lower jaw rotation. The rotation of the suspensorium about the neurocranium and of the lower jaw about the suspensorium occur within orthogonal planes (the coronal and sagittal planes, respectively). Thus, a planar model cannot incorporate both rotations. Previous studies (e.g. Westneat, 1990; 1994) have shown planar four-bar models, consisting of the hyoid, suspensorium, and pectoral girdle, to accurately predict *in vivo* kinematics in fishes. However, in these models the suspensorium and neurocranium were treated as a single link and suspensorium rotation followed neurocranial elevation-depression within the same plane as lower jaw depression. Three-dimensional models of buccal expansion have the advantage of enabling simultaneous simulation of suspensorial abduction-adduction and neurocranial elevation-depression.

Integrating linkage form and function

A better understanding of the morphological and functional diversity of biological linkages will be gained in pairing functional simulations and analyses of biological linkages with geometric morphometric approaches (e.g. Cooper and Westneat, 2009). The relatively infrequent application of three-dimensional linkage models to musculoskeletal systems is due in part to the

difficulty of collecting three-dimensional landmark or shape data. For linkage modeling, this is further compounded by the high cost of current software for simple three-dimensional kinematic simulation. In this paper we demonstrate a workflow for the analysis of biological linkages based entirely on freely accessible R packages: StereoMorph for the collection of three-dimensional shape data (Olsen and Westneat, 2015), linkR for kinematic simulation of linkages (Olsen, 2016a), and svgViewR for interactive, animated visualization (Olsen, 2016b).

Additionally, this workflow integrates seamlessly with R packages for shape analysis, such as geomorph (Adams and Otárola-Castillo, 2013), with the potential for mutually beneficial contributions between geometric morphometrics and linkage analysis. Commonly the first step in geometric morphometric analysis is generalized Procrustes superimposition, in which shape sets are optimally aligned by translation and rotation to minimize differences among shapes in position and orientation (Rohlf and Slice, 1990; Zelditch et al. 2012). This step assumes that the relative position among landmarks remains fixed, at most allowing semilandmarks to slide within a curve or surface. The analysis of musculoskeletal system shape as a whole challenges this assumption because the relative positions of shape coordinates are not fixed. Instead, shape coordinates are able to move relative to one another according to the particular joint mobilities among elements. The kinematic simulation procedure described here could be combined with current Procrustes superimposition algorithms to provide a superimposition method that minimizes differences in linkage system conformation, in addition to position and orientation.

Likewise, geometric morphometrics benefits the analysis of linkage systems by providing a means of comparing different linkage conformations (O'Higgins et al., 2011). In such an approach, kinematic simulation could be performed on linkages having one or more degrees of freedom to yield all possible conformations. The shape differences among these conformations

could then be reduced into major axes of shape variation using ordination methods such as principal components analysis to produce a “conformation morphospace”. The new framework presented here, capable of encompassing biological linkages of diverse configurations and integrated with existing tools for shape analysis, provides an accessible workflow with which to explore the morphological and functional diversity of musculoskeletal systems.

CHAPTER FOUR: CONGRUENCE OF A PERFORMANCE TRADE-OFF, A MAJOR AXIS OF SHAPE VARIATION, AND MORPHOLOGICAL CONVERGENCE IN THE EVOLUTION OF THE WATERFOWL FEEDING SYSTEM (AVES: ANSERIFORMES)

Abstract

Performance trade-offs are considered to be an important constraint on the trajectories of evolutionary diversification. In particular, previous work has shown how performance trade-offs can influence the divergence of underlying morphological traits at the population or species level. But precisely how trade-offs influence patterns of morphological diversification at longer evolutionary timescales remains poorly understood. I tested the relationship between a performance trade-off and patterns of morphological diversification in the feeding system of waterfowl (Aves: Anseriformes). I collected diet and three-dimensional beak shape data for 49 species waterfowl, which experience a performance trade-off between filter-feeding and grazing. The first major axis of variation in beak shape separates duck-like beaks from goose-like beaks and is strongly correlated with dietary differences that relate to filter-feeding versus grazing behavior. Although relative linear dimensions of the beak correlate strongly with diet, shape variables incorporating curvature consistently have the strongest correlations with dietary differences. Additionally, waterfowl exhibit at least 8 independent transitions along this same axis of beak shape variation, resulting in convergence of a goose-like beak from a more duck-like form. These results demonstrate congruence between a performance trade-off at the level of the individual and a major axis of morphological variation and convergence at the order level. This is consistent with previous observations of the relationship between performance trade-offs and morphological evolution at the population or species level. I argue that performance trade-

offs may direct the trajectories of morphological diversification by underpinning major axes of morphological variation and promoting morphological convergence along these axes.

Introduction

Performance trade-offs are a central force behind most of the best understood examples of evolution (Stearns 1989; Boag & Grant 1984; Arnold 1992; Podos 2001; Ghalambor, Reznick & Walker 2004; Herrel et al. 2009). The inverse relationship among two or more performance variables (Fig. 4.1a) plays an important role in the evolutionary divergence of traits by promoting alternative strategies in response to selection (Schluter 1995; Robinson, Wilson & Shea 1996; Robinson 2000; O'Steen, Cullum & Bennett 2002; Svanbäck & Eklöv 2003; Cummings 2007; Konuma & Chiba 2007; De Paepe et al. 2011; Ellerby & Gerry 2011; Projecto-Garcia et al. 2013).

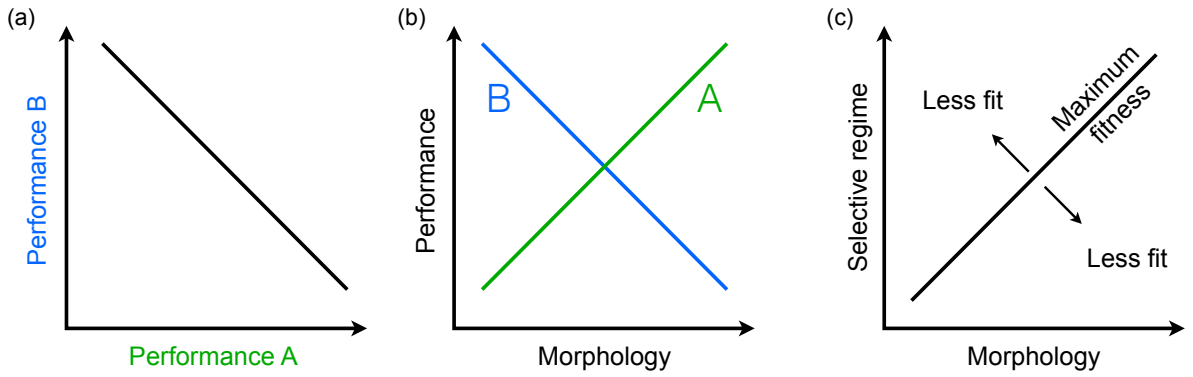

Figure 4.1. (a) If two performance traits exhibit a trade-off then maximum performance of each will be inversely correlated. (b) If a morphological axis of variation is associated with the performance trade-off, performance traits will exhibit opposite slopes in relation to this axis. (c) Shifts in the selective regime are predicted to shift morphology along this axis such that the fitness of the organism is closer to the maximum fitness for that particular selective regime.

For example, a trade-off between fecundity and offspring size in Trinidadian guppies leads to alternative strategies in response to different levels of predation (Reznick & Endler 1982; Reznick et al. 1996), a trade-off between feeding and vocal performance in Darwin's finches

mediates beak size divergence in response to differing size distributions of available seeds (Grant et al. 1976; Podos 2001; Huber and Podos 2006; Herrel et al. 2009), and a trade-off between pelagic and benthic feeding performance drives divergence of sympatric sticklebacks (Larson 1976; Schluter 1993).

A key morphological trait or set of traits often underlie whole-organism or phenotypic performance trade-offs (Fig. 4.1b), such as coloration brightness in Trinidadian guppies (Endler 1980), beak size in Darwin's finches (Grant et al. 1976), or mouth width and gill raker length in sticklebacks (Schluter 1993). These morphological traits often reflect basic physical constraints such as the trade-off between aerobic versus anaerobic in muscle mechanics (Vanhooydonck et al. 2014), between conspicuousness and camouflage in visual perception (Endler 1980), or between relative force and velocity in biomechanical systems (Westneat 1994; McHenry & Summers 2011). Selection acts on the morphological traits either directly (e.g. sexual selection) or indirectly through the effect of morphology on behavior, performance, and fitness (Endler 1980; Arnold 1983; Kingsolver et al. 2001; Kaplan and Phillips 2006; Irschick et al. 2008). As a result, a shift in the selective regime drives a shift in a key morphological trait such that the organism acquires a unique combination of performance aspects better suited to that particular selective regime (Fig. 4.1c).

While performance trade-offs may be associated with striking differences in morphology, even at microevolutionary timescales, identifying the axis of morphological variation that best corresponds to a particular performance trade-off often requires a detailed understanding of how morphology relates to function and performance (Wainwright 1996). Dimensionality reduction methods (e.g. principal component analysis) are often applied to define the axes of greatest morphological variation separating members of a population or clade. One might expect a priori

that performance trade-offs would drive the major axes of variation in the relevant functional system due to intercorrelated and relatively large changes of multiple traits in response to selection. Indeed, there appears to be a general alignment of performance trade-offs and major axes of variation in several systems for which both have been identified, including beak shape in Darwin's finches (Foster, Podos & Hendry 2008), head shape in African cichlids (Cooper et al. 2010), and body shape in South American geophagine cichlids (Arbour & López-Fernández 2013), sticklebacks (Walker & Bell 2000), and *Anolis* lizards (Irschick et al. 1997). Given the prevalence of performance trade-offs, this suggests that trade-offs, in concert with other constraints such as development or genetic covariances (Arnold 1992; Futuyma, Keese & Scheffer 1993; Schluter 1996), could be a principal determinant of major axes of variation.

If performance trade-offs are a principal determinant of morphological divergence at the level of a species or genus, they may also leave a prominent signature in macroevolutionary patterns of diversification. Importantly, from population- or species-level studies in which morphology is known to diverge in correspondence to performance trade-offs, morphological evolution shows repeated, bidirectional shifts along the same axis over time (Endler 1982; Price et al. 1984; Schluter & McPhail 1992; Grant & Grant 2006). If this pattern of independent transitions along a consistent axes of morphological variation, directed or constrained by a performance trade-off, were to play out at longer timescales one would predict parallel trajectories of divergence on shorter timescales and convergence at longer timescales (Losos 2011; Stayton 2015). Taken as a whole, one would predict congruence of performance trade-offs, major axes of morphological variation, and macroevolutionary trajectories of convergence.

The evolution of the feeding in the bird order Anseriformes (waterfowl) is an ideal system in which to test this prediction. Waterfowl have evolved a diversity of feeding strategies,

including pursuit diving, aquatic browsing, filter-feeding, and grazing with an associated diversity of feeding morphologies and diets (Johnsgard 1978; Li & Clarke 2015). While many waterfowl both filter-feed and graze, there is a performance trade-off between the two behaviors such that species that exhibit higher filter-feeding performance also exhibit lower grazing performance, and *vice versa* (van der Leeuw et al. 2003). Filter-feeding is used to capture seeds and invertebrates from water while grazing is used to crop the leaves of aquatic or terrestrial plants (Kear 2005). This performance trade-off is related to differences in feeding morphology, with more duck-like waterfowl specializing in filter-feeding and more goose-like waterfowl specializing in grazing. Lastly, waterfowl show several independent transitions toward increased folivory (Olsen 2015), making it possible to test whether these patterns of convergence are associated with the performance trade-off between filter-feeding and grazing.

The objective of this paper is to test whether a performance trade-off aligns with the major axes of morphological variation and convergence in the feeding system of waterfowl. If performance trade-offs are a central force driving and constraining the direction of morphological evolution, then the trade-off between filter-feeding and grazing should align with the major axes of variation and convergence in this clade. I test this hypothesis by integrating continuous characters representing dietary composition, compiled from the literature, and 3D beak curvature, collected from museum specimens, in a phylogenetic context. I test the relationship between morphology and dietary characters representing the extent of filter-feeding versus grazing and I examine patterns of morphological evolution using a phylomorphospace approach and convergence tests.

Materials and Methods

Dietary characters

I used dietary composition as an indirect measure of the performance trade-off between filter-feeding and grazing given that, in waterfowl, a diet consisting of seeds and animals is generally associated with filter-feeding while a diet consisting of leaves is generally associated with grazing (van der Leeuw et al. 2003; Kear 2005). I compiled diet data from the published literature using data sources and methodologies similar to a previous study of waterfowl dietary evolution (Olsen 2015). The data compiled for this study include 147 quantitative studies and 9 qualitative studies, representing 42 anseriform species and 37 anseriform genera. These studies used a wide range of methodologies to quantify dietary composition, including percent gut content (e.g. Landers et al. 1977), percent fecal content (e.g. Veltman et al. 1995), and the percent of time animals were observed to spend feeding on particular foods (e.g. Naranjo 1986). Studies of gut contents varied in the portion of the gut from which items were removed (esophagus, crop, proventriculus, etc.) and the method used to assess the relative contribution of each item (aggregate percentage, percent volume, frequency of occurrence, etc.). When possible, I treated diet data from different seasons and localities as separate entries.

I categorized each recorded food item from each study to create three dietary characters: 'animal and seeds', 'leaves', and 'terrestrial'. 'Animal and seeds' indicates the proportion of each species' diet composed of animals, seeds and nuts and represents approximately the extent to which a species filter-feeds. 'Leaves' indicates the proportion of leaves or unidentified plant parts and represents the extent to which a species grazes. The third category, 'terrestrial', indicates the proportion of the diet likely acquired in a terrestrial (versus aquatic) environment.

‘Terrestrial’ classifications were made using a combination of plant and invertebrate references (Cook et al. 1974; Brusca & Brusca 1990) and the original diet studies.

The dietary character for each species is a proportion from 0 to 1 (i.e. 0% to 100%). For quantitative studies reporting the percentage of gut contents or percentage of feeding time, I used the raw percentages. For studies reporting the frequency of occurrence of gut or fecal contents, I normalized the relative frequencies such that the frequencies summed to 100%. For the 9 qualitative studies I used qualitative descriptions (e.g. primarily leaves, rarely seeds) to score items on a scale from 1–4, ranging from a rare to primary component of the diet. If no such description was given I scored each item equally. I then normalized the scores such that scores summed to 100 to obtain a category sum in the form of a percentage. I took the arithmetic mean of proportions across all entries for each species, giving equal weight to each entry, to arrive at a mean proportion for each species and each of the three dietary characters.

Morphological characters

To quantify beak morphology I measured 3D curvature of the culmen (the dorsal curvature of the beak at the midline) and tomium (the biting margin of the beak) from 131 museum skeletal specimens representing a broad sampling of 49 anseriform species and 44 anseriform genera. This includes two extinct taxa: the Lower Eocene *Presbyornis sp.* (Olson & Feduccia 1980) and the recently extinct moa-nalo *Thambetochen chauliodous* (Olson & James 1991). I collected 3D curvature of the culmen and tomium using stereo camera reconstruction implemented with version 1.5.0 of the R package StereoMorph (Olsen & Westneat 2015). I calibrated two standard digital cameras with a checkerboard pattern using the StereoMorph function ‘calibrateCameras’. I photographed each specimen and manually digitized the tomium in each camera view using the StereoMorph digitizing application. I then reconstructed the

digitized curves into 3D using the StereoMorph function 'reconstructStereoSets'. I digitized the culmen from a lateral view and aligned the culmen and tomium using additional cranial landmarks. Once reconstructed, I placed 50 evenly spaced points (semilandmarks) along each curve (i.e. culmen, right tomium and left tomium). Each specimen was aligned to the midline plane, reflected, and averaged (Klingenberg, Barluenga & Meyer 2002) to produce a bilaterally symmetric set of 150 semilandmarks used in subsequent shape analyses.

For each species, I aligned semilandmarks from different individuals by Procrustes superimposition using the 'gpagen' function in version 3.0.0 of the R package geomorph (Adams & Otárola-Castillo 2013) and then averaged each aligned set to produce a single mean semilandmark set for each species. I aligned all species mean sets by a second Procrustes superimposition to obtain Procrustes coordinates, which minimize differences due to translation and rotation. Trait values collected from interrelated taxa do not represent independent data points. Thus, I performed phylogenetic principal component analysis (pPCA) on the Procrustes coordinates using the 'phyl.pca' function in the R package phytools (Revell 2009; Revell 2012) and a published phylogeny of 6714 avian species, pruned to the 49 species with shape data in this study (Burleigh, Kimball & Braun 2014, 2015). Constructed from a sparse supermatrix of 22 nuclear loci and seven mitochondrial regions, this tree represents the most current molecular phylogeny of Anseriformes, incorporating data from several previous studies (Sraml et al. 1996; Johnson and Sorenson 1998; McCracken et al. 1999; Sorenson et al. 1999; Donne-Goussé, Laudet & Hänni 2002). To this tree, I added *Presbyornis* as sister to the family Anatidae based on previous hypotheses (Livezey 1997; Clarke et al. 2005). Using the semilandmark sets I also measured standard linear dimensions of the beak (depth, width, and length) relative to beak centroid size for each species.

To visualize shape variation I used the backtransformation method (Lohmann & Schweitzer 1990; MacLeod 2009). In principal component analysis, the original input matrix can be recovered by multiplying the PC score matrix by the inverse of the eigenvector matrix. This procedure can be adapted to visualize the shape change along a particular PC axis or axes by constructing a score matrix of evenly distributed scores along the PC axis or axes of interest, within the range of the empirical PC scores, and mean scores for all other PC axes. These backtransform shapes represent the theoretical shape corresponding to a particular PC score or pair of PC scores in multivariate space. The use of backtransformation on the results of phylogenetic PCA requires the additional step of adding the product of a vector of ones and the vector of phylogenetic means (Revell 2009). I plotted the shape changes along individual PC axes using 3D coordinate axes. To visualize the distribution of shapes along two PC axes I plotted lateral silhouettes at evenly distributed points along each axis to create backtransform morphospace plots. I used lateral silhouettes for simplicity of visualization; all shape analyses were performed using 3D data.

Correlation and evolutionary trajectory estimation

For this study, the objective of the correlation tests was to identify which morphological axes of variation correlate with the three selected dietary characters and to quantify the direction and relative strength of these correlations. Before testing for correlations among the dietary and morphological characters I quantified phylogenetic signal in the characters and in the residuals of the correlations among characters by calculating Blomberg's K and Pagel's λ using the 'phylosig' function in the phytools package (Pagel 1999; Blomberg, Garland & Ives 2003; Revell 2012). I then tested for correlations using phylogenetic independent contrasts (PIC) and phylogenetic generalized least squares (PGLS) regression analysis. Each makes different

assumptions about the manner in which each character has evolved and the nature of the relationship between characters. The PIC method assumes a Brownian motion model of character evolution and compares sister tips and nodes to generate an independent character set (Felsenstein 1985). PGLS assumes a particular evolutionary model for the residuals of the regression with the ability to estimate additional evolutionary parameters (Freckleton et al. 2002; Revell 2010), including the λ parameter of Pagel (1999), a measure of phylogenetic signal, and an α parameter to simulate trait evolution toward a particular optimum (an Ornstein–Uhlenbeck model; Martins and Hansen 1997).

I performed PIC correlations using the 'pic' function in the R package ape (Paradis et al. 2004). I tested for adequate standardization and positivized contrasts (Garland et al. 1992) before assessing correlations by regressions through the origin using the 'lm' function (R core team 2016). I performed PGLS regression analyses using the 'corClasses' structures in ape and the 'gls' function in the R package nlme (Pinheiro et al. 2016) using three different evolutionary models: a model in which λ and α are fixed at 1 and 0, respectively, and two models in which λ and α were estimated simultaneously with the regression parameters (Freckleton et al. 2002; Revell 2010). The results of first model (λ=1, α=0) are identical to that of a PIC regression without branch length transformation (Garland and Ives 2000). I used the same phylogeny for regression analyses as for pPCA (Burleigh, Kimball & Braun 2015), except that the tree was pruned to the 42 species for which both diet and beak shape data were collected.

To identify patterns of morphological diversification within waterfowl I applied a phylomorphospace approach (Sidlauskas 2008; Uyeda, Caetano & Pennell 2015), simulating trait evolution within a morphospace defined by the first two pPC axes of beak shape. I compared five models of continuous trait evolution: a Brownian motion model (Felsenstein 1973), an

Ornstein-Uhlenbeck (OU) model (Butler and King 2004), a lambda model, a kappa model and a delta model (Pagel 1999). I fit each model to each pPC axes using the 'fitContinuous' function in the R package geiger (Harmon et al. 2008) and used the AICc values to determine the best fitting model. I used the best fitting model, determined by AICc values, to reconstruct the ancestral states of the first two pPC axes using the 'ace' function in the R package ape (Paradis et al. 2004) with the restricted maximum likelihood (REML) method (Felsenstein 1973; Schluter et al. 1997). I constructed the phylomorphospace by plotting the 49 species phylogeny into morphospace, using the ancestral state estimates to position the internal nodes and the pPC scores to position the tips. To quantify convergence I used the package convevol (Stayton 2015). The convevol package estimates five measures of convergence for a user-defined group of taxa: four distance-based measures, $C_{1\text{-}4}$, which represent different relative measures of phenotypic distances among the selected taxa and a frequency-based measure, C_5, which quantifies the number of transitions into a region of morphospace defined by the selected taxa. The functions 'convratsig' and 'convnumsig' use randomization tests to assess the significance of each measure (Stayton 2015).

Results

Morphological variation

The 3D curvature of the culmen and tomium in waterfowl are highly integrated: the first 2 phylogenetic principal component (pPC) axes explain 80% of the total variation in beak shape and the first 3 pPCs explain 88% of the total variation. The first pPC axis, which explains 46% of the total variation, separates characteristically 'duck-like' beaks (low pPC1 values) from more 'goose-like' beaks (high pPC1 values; Fig. 4.2a-b). Duck-like beaks exhibit a ventrally arcing culmen and tomium, high relative length, and low relative depth and width while goose-like beaks exhibit a dorsally arcing culmen and tomium, low relative length, and high relative depth

(i.e. height) and width at the base. This is reflected in positive correlations of pPC1 with relative beak depth and width and a strong negative correlation with relative length (Table 4.1).

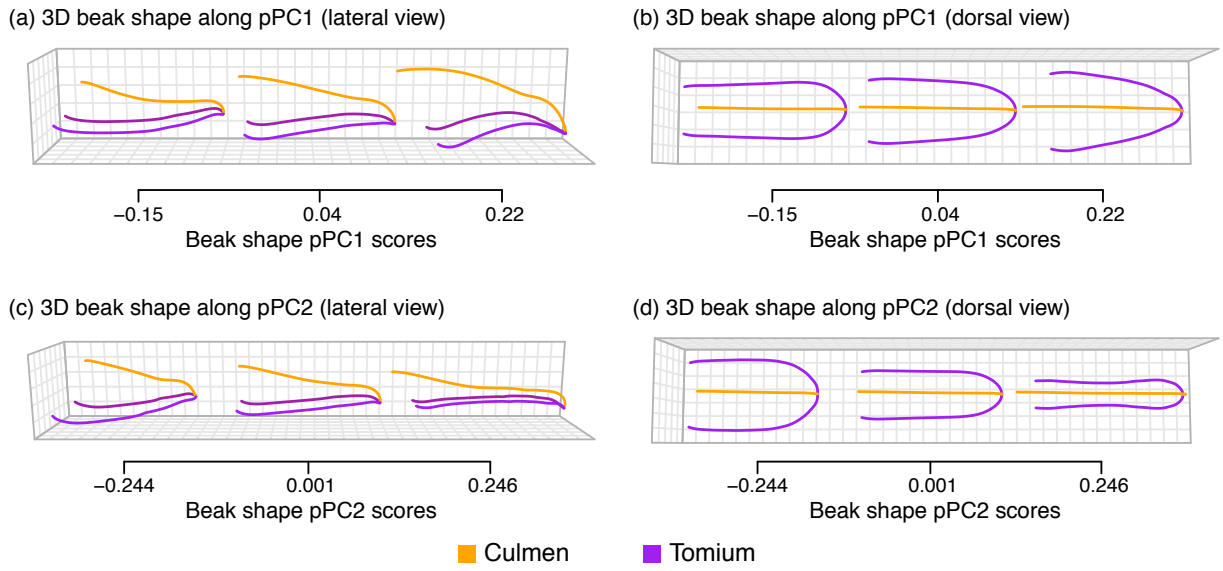

Figure 4.2. Variation in 3D beak curvature visualized using three backtransform shapes evenly spaced along the first (a-b) and second (c-d) pPC axes. The same three shapes are shown in (a) and (b) from a lateral and dorsal view, respectively. Likewise, the same three shapes are shown in (c) and (d) from a lateral and dorsal view, respectively. Orange lines indicate the culmen and purple lines indicate the tomium.

All waterfowl commonly known as geese, including the extinct moa-nalo *T. chauliodous*, have pPC1 scores greater than 0 with the exception of the magpie goose (*Anseranas semipalmata*) which has a more duck-like beak.

Relative beak	Beak curvature		Beak size
	pPC1	pPC2	
depth	**(+) 0.47**	**(-) 0.23**	0.02
width	**(+) 0.29**	**(-) 0.49**	0.05
length	**(-) 0.80**	0.07	0.09
Beak size	0.04	0.01	**(+) 1.00**
Variance explained	46.2%	33.8%	

Table 4.1. Correlations among standardized contrasts of beak curvature, relative linear dimensions, and size. Values are adjusted R^2. Correlations significant at $\alpha < 0.01$ are indicated by bold and sign of slope. Relative beak dimensions are scaled to beak centroid size.

The second pPC axis, which explains 34% of the total variation, separates the tall, broad beaks of browsing divers, such as the musk duck (*Biziura lobata*), from the slender beaks of piscivorous pursuit divers, such as mergansers (Fig. 4.2c-d). This is reflected in negative correlations of pPC2 with relative depth and width; pPC2 is uncorrelated with relative length (Table 4.1). The third pPC axis, which only explains 8% of the total variation, is related to the varying preservation in the skeletal specimens of the rhamphotheca, a layer of keratin overlaying the beak, and is not correlated with any of the relative beak dimensions. Given the artifactual, rather than biological, significance of pPC3, a clear inflection point in the pPCA scree plot between pPC2 and pPC3, and the fact that all subsequent pPC axes individually explained less than 5% of the total variation, only pPC1 and pPC2 were considered in further analyses (Zelditch et al. 2004). Based on the first two pPC axes, the beak shape of the extinct *Presbyornis* is closest to that of the extant marbled teal (*Marmaronetta angustirostris*) while the beak shape of the extinct moa-nalo *T. chauliodous* was closest to that of the extant upland goose (*Chloephaga picta*).

Relationship between morphology and diet

Not surprisingly, all dietary characters are significantly correlated with each other (all *p*-values < 0.0001; Table 4.2). The strongest correlation is an inverse relationship between 'animal and seeds' and 'leaves' ($R^2 = 0.89$; Fig. 4.3), consistent with the performance trade-off in waterfowl between filter-feeding and grazing (van der Leeuw et al. 2003). 'Animal and seeds' is also negatively, albeit more weakly, correlated with a more terrestrial diet ($R^2 = 0.38$) while a folivorous diet is positively correlated with a more terrestrial diet ($R^2 = 0.54$).

	Animal & seeds	Leaves	Terrestrial
Animal & seeds	-	**<0.0001**	**<0.0001**
Leaves	**(-) 0.89**	-	**<0.0001**
Terrestrial	**(-) 0.38**	**(+) 0.54**	-

Table 4.2. Correlations among standardized contrasts of diet characters. Above the diagonal are *p*-values, below the diagonal are R^2 values with sign of the slope indicated.

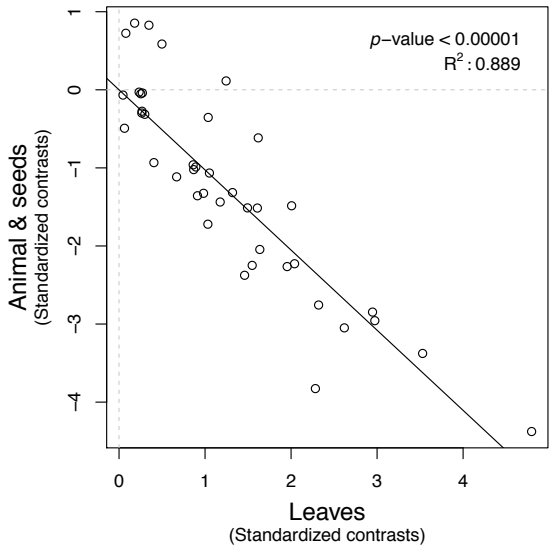

Figure 4.3. Correlation between standardized contrasts of diet characters 'animal & seeds' and leaves (regression through the origin: $P < 0.0001$; $R^2 = 0.89$; $N = 42$).

	p-value	R^2	Slope
Animal & seeds			
Beak shape pPC1	***<0.001**	**0.49**	**-2.80**
Beak shape pPC2	0.34	-0.01	-0.64
Relative beak depth	***0.002**	**0.20**	**-12.1**
Relative beak width	0.075	0.05	-6.30
Relative beak length	***<0.001**	**0.32**	**15.0**
Terrestrial			
Beak shape pPC1	***<0.001**	**0.48**	**2.70**
Beak shape pPC2	0.84	-0.02	0.13
Relative beak depth	***0.02**	**0.11**	**9.00**
Relative beak width	***0.02**	**0.12**	**8.00**
Relative beak length	***<0.001**	**0.41**	**-16.0**
Leaves			
Beak shape pPC1	***<0.001**	**0.59**	**2.90**
Beak shape pPC2	0.51	-0.01	0.40
Relative beak depth	**<0.001**	**0.23**	**12.0**
Relative beak width	***0.02**	**0.11**	**7.50**
Relative beak length	***<0.001**	**0.45**	**-16.0**

Table 4.3. Correlations of diet and beak shape standardized contrasts. Asterisks indicate significance after multiple comparison correction (*: $\alpha < 0.05$; ** <0.01; *** <0.001).

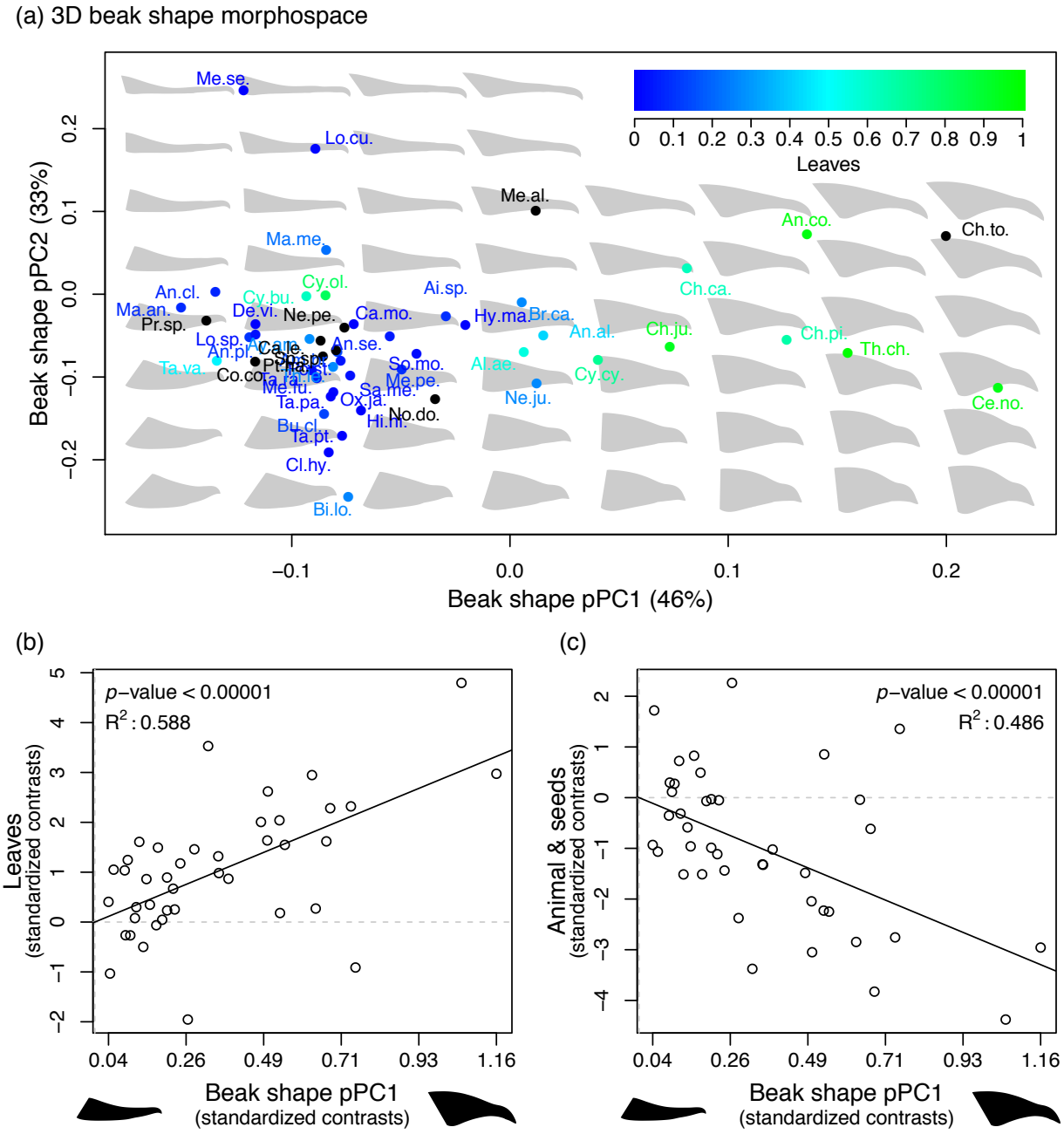

Figure 4.4. (a) Morphospace of 3D beak shapes for all species ($N = 49$) with a color gradient to indicate the leaves value for the subset species with diet data ($N = 42$). (b) Correlation between the standardized contrasts of the proportion of leaves in the diet and of beak shape pPC1 scores. (c) Correlation between the standardized contrasts of the proportion of animals and seeds in the diet and of beak shape pPC1 scores.

The first pPC axis of beak shape is strongly correlated with all of the diet characters (Table 4.3). In particular, pPC1 is positively correlated with a more folivorous diet ($R^2 = 0.59$; Fig. 4.4a-b) and negatively correlated with the dietary proportion of animal and seeds ($R^2 = 0.49$; Fig. 4.4c); pPC1 is also positively correlated with a more terrestrial diet ($R^2 = 0.48$; Table 4.3). In contrast, pPC2 is not correlated with any of the diet characters. The relative beak dimensions are also strongly correlated with the dietary characters in a manner consistent with the correlations between the relative dimensions and pPC axes (Table 4.3). Relatively deeper and shorter beaks are correlated with a folivorous and terrestrial diet and a smaller dietary proportion of animal and seeds. Although both are significant, the pPC1 scores consistently show stronger correlations with diet than the relative beak dimensions.

Evolutionary trajectories

The fits of all trait evolution models for the first two pPCs of beak shape, determined by AICc, do not differ by more than 3 indicating no obvious best fit model. The best fitting model for pPC1 is the Brownian motion model (AICc = -92). For pPC2, the best fitting model is the kappa model (AICc = -110) although this does not differ significantly from the Brownian motion model AICc value (AICc = -109). Thus, I used a Brownian motion model to reconstruct ancestral values of both pPC1 and pPC2.

Most waterfowl fall in the region of 3D beak morphospace defined by low to intermediate pPC1 and pPC2 scores (Figs 4a and 5b). Simulated trait evolution supports two main patterns of diversification from this region of morphospace. The first pattern is a single evolutionary trajectory from low to high pPC2 values in the origin of the piscivorous pursuit diving clade that includes the genera *Mergus*, *Lophodytes*, and *Mergellus*.

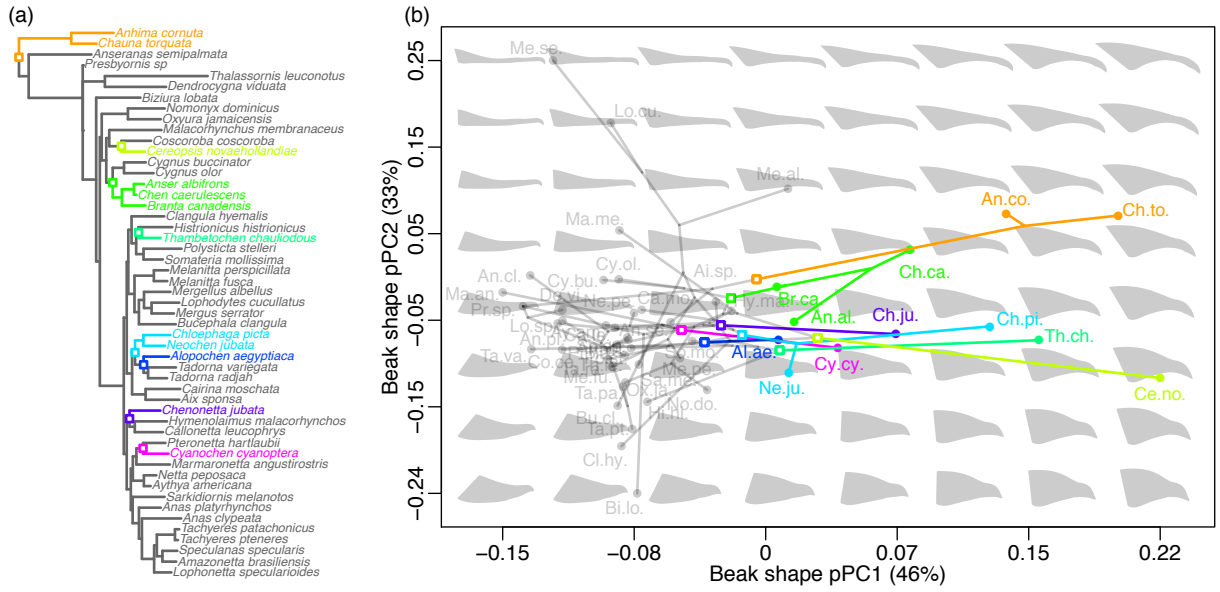

Figure 4.5. (a) Anseriform phylogeny (Burleigh, Kimball & Braun 2015) pruned to the taxa sampled in this study ($N = 49$). (b) Anseriform phylomorphospace, highlighting the screamers (orange) and 7 potentially independent 'goose' lineages. Internal nodes labeled with squares and branch colors correspond to the indicated nodes and colors in (a).

The second pattern comprises several independent and parallel transitions along pPC1 from a more duck-like beak to a more goose-like beak (i.e. from low to high pPC1 values; Fig. 4.5). The lineages undergoing these transitions include the screamer lineage, the sister group to all other Anseriformes (genera *Anhima* and *Chauna*), as well as 6-7 independent lineages of 'geese' (genera *Cereopsis*, *Anser*, *Chen*, *Branta*, *Thambetochen*, *Chloephaga*, *Neochen*, *Alopochen*, *Chenonetta*, and *Cyanochen*). These lineages are highlighted by separate colors in Fig. 4.5.

	Estimate	*p*-value
C_1	0.41	**<0.005**
C_2	0.10	**<0.005**
C_3	0.02	**<0.005**
C_4	0.02	**<0.005**
C_5	8	0.154

Table 4.4. Results of convergence tests for the screamer and goose lineages highlighted in Fig. 4.5 ($N = 200$ simulations).

Taken together, these screamer and goose lineages were found to be significantly convergent using the distance-based measures $C_{1\text{-}4}$ (Table 4.4). Evolution has closed 41% of the maximum distance among these taxa ($C_1 = 0.41$) and convergence is responsible for 2% of the total evolution among the lineages leading from the most recent common ancestor to the tips ($C_3 = 0.02$; Stayton 2015). In contrast, these taxa were not found to be significantly convergent using the frequency-based measure C_5, indicating that the number of transitions into the elliptical region defined by these taxa, 8, is not significantly greater than would be expected by chance.

Discussion

These results reveal the congruence of a performance trade-off, the major axes of morphological variation, and convergence in the feeding system of waterfowl. The inverse relationship between an 'animal and seeds' diet and a folivorous diet observed in this study (Fig. 4.3) confirms the results of *in vivo* feeding trials that show waterfowl experience a performance trade-off between filter-feeding and grazing (van der Leeuw et al. 2003). This performance trade-off is strongly associated with the first major axis of variation in 3D beak shape, as shown by the opposing correlations between beak shape pPC1 and a filter-feeding versus grazing diet (Fig. 4.4). Moreover, waterfowl beak shapes exhibit multiple, independent transitions along this performance trade-off, most notably in the convergent evolution of a more goose-like beak from a more duck-like beak (Fig. 4.5). While performance trade-offs are known to be a key driver of trait diversification (Schluter 1995; Robinson, Wilson & Shea 1996; Svanbäck & Eklöv 2003; Cummings 2007; Konuma & Chiba 2007; De Paepe et al. 2011; Ellerby & Gerry 2011; Projecto-Garcia et al. 2013), this is the first study to show that a performance trade-off at the level of the individual underlies both a major axis of morphological variation and patterns of convergence at a macroevolutionary scale.

This congruence of a performance trade-off with a major axis of morphological diversification can be explained by considering trade-offs as a constraint on the trajectory of morphological evolution in response to shifting selective regimes. A key morphological trait or set of traits underlie nearly all documented cases of whole-organism performance trade-offs (e.g. Endler 1980; Grant et al. 1976; Meyer 1989; Schluter 1993; Westneat 1994; Schondube & del Rio 2003; Konuma & Chiba 2007; Gurd 2008; Herrel et al. 2009; Ellerby & Gerry 2011; Vanhooydonck et al. 2014). Selection then acts on performance, indirectly constraining the evolution of a suite of morphological traits to shift a population toward a combination of performance variables better adapted to that particular selective regime. That the resulting major axes of morphological variation would in some way reflect this performance trade-off is not only expected on theoretical grounds (the broad, sweeping force of selection would result in intercorrelated changes of large effect) but is consistent with several previous observations of major axes of morphological variation paralleling performance trade-offs (Irschick et al. 1997; Walker & Bell 2000; Foster, Podos & Hendry 2008; Cooper et al. 2010; Arbour & López-Fernández 2013). Given sufficient time and varying selective regimes a performance trade-off can direct repeated, bidirectional shifts along the same morphological axis over time (Endler 1982; Price et al. 1984; Schluter & McPhail 1992; Grant & Grant 2006), leading to parallel trajectories of divergence on shorter timescales and convergence at longer timescales.

In the evolution of waterfowl one can find trajectories of both morphological divergence and convergence. The moa-nalos, a recently extinct clade of goose-like waterfowl endemic to the Hawaiian Islands, provide an example of rapid divergence away from a duck-like form (Olson & James 1991). The clade split from their closest mainland relative, most likely a dabbling duck in the genus *Anas*, approximately 3.6 million years ago (Sorenson et al. 1999) and rapidly evolved

into flightless, terrestrial grazers specializing on the leaves of native vegetation (James & Burney 1997) with a definitively goose-like beak (*T. chauliodous* in Fig. 4.5). Within waterfowl as whole, there have been at least 6 additional independent transitions toward a more goose-like beak and folivorous diet (Fig. 4.5; Olsen 2015). Thus, in waterfowl the performance trade-off between filter-feeding and grazing has driven parallel trajectories of divergence at Hawaiian Island timescales and convergence at the timescale of the entire order, the origin of which dates to at least 66 million years ago (Clarke et al. 2005).

These parallel and convergent trajectories, with intermediate forms along the pPC1 axis is consistent with the proposed mechanism of trade-offs constraining morphological evolution along a particular axis without necessarily lower performance in intermediate forms. Intermediate forms may in fact gain versatility with intermediate performance in both filter-feeding and grazing. The significant result for distance-based measures of convergence ($C_{1\text{-}4}$; Table 4.4) but lack of significance for the frequency-based measure of convergence (C_5) for geese can be explained by the particular pattern of convergence. Because geese occupy intermediate morphologies along the pPC1 axis, the total region of morphospace occupied by the selected taxa is relatively large, decreasing the chance that the total number of entries into that region (C_5) is significantly greater than would be expected by chance. In contrast, these parallel transitions, though varying in their extent, have made geese significantly more similar to one another than would be expected by chance.

Although evolution along a morphological axis associated with a performance trade-off could proceed in either direction, several factors could favor one direction over another (e.g. the strength and frequency of different selective regimes, relative fitness of different states). In waterfowl, the broad phylogenetic distribution of a duck-like beak causes the ancestral state

reconstruction to favor transitions predominately from duck to goose (Fig. 4.5b). While the result of such reconstructions near the base of the tree are likely unreliable, there are two lines of evidence that support filter-feeding as the primary ancestral feeding behavior for Anseriformes. The first is the widespread presence among waterfowl of lamellae, keratinous comb-like ridges lining the upper and lower beak. The only other avian lineages possessing comparable structures, flamingos and prions, also use lamellae to filter-feed (Klages and Cooper 1992; Zweers et al. 1995). The second line of evidence is the beak shape of the stem anseriform fossil *Presbyornis* (Olson and Feduccia 1980; Livezey 1997). In 3D beak shape, *Presbyornis* most closely resembles the marbled teal (*M. angustirostris*; Fig. 4.4a), a specialized filter-feeder (Fuentes et al. 2004), establishing the potential for filter-feeding as the predominate feeding mode early in the history of Anseriformes. Thus, for waterfowl, an initial state of filter-feeding specialist could explain why transitions proceed predominately from primarily filter-feeding to primarily grazing.

I have made the assumption that dietary differences, principally the difference between a diet consisting of animal and seeds versus one consisting of leaves, adequately reflect the performance trade-off between filter-feeding and grazing. Although there are notable exceptions (e.g. mergansers primarily consume fish but do not filter-feed, waterfowl can consume seeds by terrestrial browsing), I would argue that diet represents a reasonable proxy of filter-feeding versus grazing performance. First, these dietary categories generally correspond to differences in feeding behaviors in waterfowl (van der Leeuw et al. 2003; Kear 2005). Secondly, as expected by a performance trade-off, the 'animal and seeds' and folivorous characters are strongly and inversely correlated (Fig. 4.3). Thirdly, the proportion of terrestrial foods consumed, an alternative measure of the extent of grazing, is inversely correlated with the proportion of animal

and seeds (Table 4.2) and also strongly correlated with the pPC1 of beak shape in the same direction as a folivorous diet (Table 4.3).

The strong correlation between the first major axis of beak shape variation and diet uncovered in this study (Fig. 4.4), along with the central role of beak shape in bird feeding more broadly (Price 1991; Suhonen, Alatalo & Gustafsson 1994; Schondube & Martinez del Rio 2003; Herrel et al. 2005), points to beak shape as a key determinant of feeding performance in waterfowl. During filter-feeding the beak and tongue function as a piston pump to draw in water and suspended food particles at the tip of the beak (Zweers 1974). The food particles are then filtered by the lamellae and transported under the tongue into the oropharynx (Kooloos et al. 1989; van der Leeuw et al. 2003; Gurd 2006). During grazing in specialized grazers (i.e. geese) leaves are transported over the tongue where pronounced spines on the roof of the mouth enable the tongue to progressively transport food items by catching items during successive cycles of tongue protraction and retraction (van der Leeuw et al. 2003). While differences in tongue and hyoid morphology certainly play a key role (Li & Clarke 2015), in the performance trade-off between these two behaviors, differences in beak shape are also likely to play a central role.

The upper beak in waterfowl, as in most birds, rotates about a joint with the neurocranium (Hoese & Westneat 1996; Dawson et al. 2011). Jaw muscles protract and retract the upper beak by exerting force indirectly through a series of interlinked bones attached to the ventral base of the upper beak (Bock 1964). As a consequence, the upper beak is subject to the same principles of lever mechanics as the lower beak. In comparison to the beaks of ducks, goose beaks are relatively taller at the base, relatively shorter in length, and have more upwardly arcing tomium (Fig. 4.2a) all of which increase the mechanical advantage of the beak both at the beak tip and along the length of the tomium. The evolution of a higher mechanical advantage in

the upper beak of geese may function to more efficiently transmit force from the jaw muscles and generate relatively higher bite forces during grazing. Interestingly, many of these changes parallel changes in the beak shape of Darwin's finches associated with an increase in bite force, in particular greater relative beak depth and width (Herrel et al. 2005; Foster, Podos & Hendry 2008).

Conversely, a more duck-like beak bears features that likely increase filter-feeding performance. The relatively wider tip of duck beaks increases the aperture through which water and food particles can enter the mouth for filtering. Additionally, the downward arcing curvature of the tomium ensures broad overlap between the lamellae of the upper and lower beak margin while the relatively longer beak length increases the total filtering surface. For both grazing and filter-feeding, beak curvature appears to play an important role as indicated by the consistently stronger relationship between diet and morphological characters based on curvature rather than simple linear dimensions (Table 4.3).

While the hypothesis presented here predicts that performance trade-offs drive major axes of diversification, the converse is not necessarily true: major axes of variation or convergence along particular morphological axes may not necessarily reflect performance trade-offs. Major axes of variation (i.e. patterns of morphological covariances) can result from factors such as genetic covariances (Futuyma, Keese & Scheffer 1993; Schluter 1996; Walker & Bell 2000; McKinnon & Rundle 2002) or developmental constraints (Kaplan & Phillips 2006). Similarly, convergence can emerge from influences such as correlated developmental processes (Jaekel and Wake 2007), limitations on the total evolvable forms (Wake 1991), or even chance (Stayton 2015). Moreover, this hypothesis is not inconsistent with a performance trade-off acting simultaneously with additional constraints to bias the trajectory of morphological evolution (e.g.

Albertson, Streelman & Kocher 2003). Work in ducks and chickens (in the order Galliformes, the sister order to Anseriformes) has identified two independent developmental modules, one driving increased beak depth and width the other driving increased beak length (Abzhanov et al. 2004; Wu et al. 2004; Abzhanov et al. 2006), a pattern reminiscent of the changes along the first major axis of beak shape variation in waterfowl (Table 4.1). Performance trade-offs, developmental modules and yet additional constraints may thus operate simultaneously but at different levels in shaping the ultimate trajectories of morphological diversification.

It should be noted that there are cases in which one would not observe a clear relationship between a whole-organism performance trade-off and a single axis of morphological variation, even an axis composed of multiple intercorrelated traits. First, when many independently varying traits influence fitness (functional complexity), multiple alternative designs can produce equal fitness (Law & Blake 1996; Alfaro et al. 2005; Marks & Lechowicz 2006), weakening the relationship between a performance trade-off and a single axis of morphological variation. Secondly, functional complexity can weaken performance trade-offs themselves by providing individuals flexibility to match multiple performance demands with alternative strategies (Holzman et al. 2011; Oufiero et al. 2012; Vanhooydonck et al. 2014). Thirdly, sampling morphology across functional units that underlie different performance trade-offs could obscure the morphology-trade-off relationship. For example, the spacing between lamellae is known to influence a performance trade-off between prey size selection and water filtration rate during filter-feeding (Nudds & Bowlby 1984; Gurd 2008). If lamellar spacing were combined with beak shape, a clear relationship with the trade-off between filter-feeding and grazing may not emerge. Lastly, sampling too broad taxonomically could also obscure the morphology-trade-off

relationship as the same morphology in different clades will likely be subjected to different trade-offs and selective regimes.

In this paper I have proposed a role for performance trade-offs in underlying major axes of morphological variation and directing the trajectory of morphological divergence at short timescales and convergence at longer timescales. This explanation is not only consistent with patterns of morphological diversification within waterfowl but also with previous observations of the relationship between performance trade-offs and morphological evolution in a broad range of taxonomic groups and functional systems and across a range of timescales (Irschick et al. 1997; Walker & Bell 2000; Foster, Podos & Hendry 2008; Cooper et al. 2010; Arbour & López-Fernández 2013). Further studies coupling an understanding of the mechanistic and morphological basis of performance trade-offs at the level of the individual with a mapping of how the underlying morphologies have diversified at a broad phylogenetic level will determine the relative frequency and importance of trade-offs in determining evolutionary trajectories. Given the central role of performance trade-offs in biology, trade-offs may also be a central determinant of the axes along which the traits underlying those trade-offs evolve. If so, this would provide a key mechanism linking a microevolutionary process to macroevolutionary patterns of diversification.

CHAPTER FIVE: BEAK DIVERSIFICATION IS CORRELATED WITH MORPHOLOGICAL AND FUNCTIONAL EVOLUTION OF THE BONES UNDERLYING CRANIAL KINESIS IN WATERFOWL[1]

Abstract

Bird beaks are a classic model system for the study of ecological and evolutionary processes. However, the upper and lower beak represent just two of ten mobile elements in the jaw apparatus of birds. These additional bony elements behind the beak serve as attachment sites for muscles and form a transmission system, known as a linkage or mechanism, that enables rotation of the upper beak. Although many studies have focused on the role of beak shape in ecological diversification, it remains unknown whether the shape of the cranial linkage serves as an additional source of variation upon which selection acts in the evolution of avian jaw function. Integrating geometric morphometric analyses and biomechanical modeling we explore patterns of morphological and functional diversitfication of the beak and cranial linkage in the ecologically diverse waterfowl clade (Anseriformes). We find strong and significant evolutionary covariation between the beak and linkage, the linkage and neurocranium, but not between the beak and neurocranium. We also find significant differences in linkage shape and function among waterfowl that differ by feeding ecology and correlated evolution of beak function and linkage function. These results support the hypothesis that linkage shape, in addition to beak shape, is an important locus of evolutionary change among birds in the adaptation to new feeding ecologies. We also show that in birds the linkage and beak are coupled

[1]This chapter has been prepared for submission as: Olsen, A.M. and Westneat, M.W. 2016. Beak diversification is correlated with morphological and functional evolution of the bones underlying cranial kinesis in waterfowl.

in such a way that the mechanical advantage of the linkage and beak is changed simultaneously and in the same direction by changing the length of their shared link, represented approximately by beak height; we find evidence for this mechanism of synergistic change in linkage and beak function across waterfowl. In spite of the strong integration between the linkage and beak, they can exhibit opposing patterns of functional evolution: the evolution of pursuit diving is associated with a decrease in mechanical advantage of the beak but an increase in mechanical advantage of the linkage. Thus, a consideration of the avian cranial linkage diversity may provide additional insights into functional diversification of the beak not apparent from considerations of beak shape alone. Taken together, these patterns of correlated morphological, functional and ecological evolution between the beak and linkage point to an important role of linkage shape in the evolution of beak mechanics and behavior.

Introduction

Bird beaks are a classic model system for the study of ecological and evolutionary processes. The remarkable diversity of beak sizes and shapes among birds often reflects not only their diverse feeding strategies (Grant 1981; Gosler 1987; Price 1991; Barbosa and Moreno 1999; Bardwell et al. 2001; Marquiss and Rae 2002; Yanega and Rubega 2004; Herrel et al. 2005; Gurd 2007) but also the beak's demonstrated function in modulating the vocal tract during vocalization (Hoese et al. 2000; Podos 2001; Derryberry et al. 2012), preening (Barbosa 1996; Clayton et al. 2005), and thermoregulation (Hagan and Heath 1980; Tattersall et al. 2009; Greenberg et al. 2012). Owing to this remarkable morphological diversity, evolutionary malleability, and functional versatility, bird beaks have contributed to our understanding of intraspecific competition (Smith 1987; Smith 1990), character displacement (Grant and Grant 2006), evolutionary novelty (Benkman and Lindholm 1991), selection (Smith 1993; Benkman

2003), plant-animal coevolution (Parchman and Benkman 2002; Temeles and Kress 2003), hybrid fitness (Grant and Grant 1982), and performance trade-offs (Clayton and Cotgreave 1994; Moyer et al. 2002; Schondube and del Rio 2003; Herrel et al. 2009).

Although not entirely obvious from external observation of a bird, the upper and lower beak are in fact only two of ten mobile elements of the avian jaw apparatus. Just behind the upper beak and under the eye are a series of four paired bones (the quadrate, pterygoid, jugal and palatine) that interconnect to form a series of parallel loops, known as a linkage mechanism (Fig. 5.1a; Hérrisant 1748; Bock 1964; Bühler 1981; Zusi 1984; Bout and Zweers 2001). In many birds this mechanism is fully mobile such that force inputs to this mechanism, via muscles inserting on the quadrate, pterygoid, and palatine or where the lower jaw articulates with the quadrate, cause coordinated movement of the linkage elements and active protraction (raising) or retraction (lowering) of the upper beak (Fig. 5.1b; Van Gennip and Berkhoudt 1992; Gussekloo et al. 2001; Westneat et al. 1993). In this way, the upper and lower beak function as dual (and in some cases uncoupled) levers, with the cranial linkage functioning as the actuator of the upper beak (Hoese and Westneat 1996; Dawson et al. 2011).

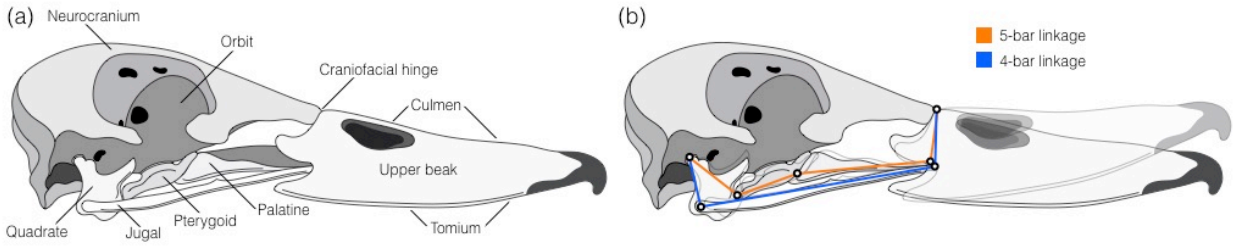

Figure 5.1. The waterfowl skull and cranial kinesis mechanism (lateral view). The linkage bones of the avian skull (a) are positioned posterior to the beak and ventral to the neurocranium. These bones interconnect to form closed loops of links (b) or linkage mechanisms. The quadrate, jugal and upper beak form a four-bar linkage (blue) while the quadrate, pterygoid, palatine, and upper beak form a five-bar linkage (orange). Motion of the linkage results in retraction or protraction (superimposed with lower opacity) of the upper beak.

Although the cranial linkage bones clearly function in transmitting force and motion to the upper beak, it is unknown whether the particular shape, or geometry, of the linkage serves as an additional source of variation upon which selection acts in the evolution of jaw function.

Just as differences in lever length (e.g. length of the jaw, a limb element) lead to differences in lever mechanics, differences in linkage geometry lead to differences in the linkage mechanics. Such mechanical differences include the extent to which the linkage amplifies relative force or velocity (mechanical advantage) or the linkage range of motion (Hartenberg and Denavit 1964). Analogous structures to the linkages of bird skulls have evolved in the skulls of fishes (Anker 1974; Westneat 1990) and the striking appendage of mantis shrimps (Patek et al. 2007). In both cases, the evolution of linkage geometry tracks evolution of the organism's ecology. Evolution of a more evasive prey diet in labrid fishes is correlated with linkage geometries that more efficiently amplify relative velocity (Westneat 1994; Westneat 1995). Mantis shrimps with faster and more forceful strikes have linkage geometries that most efficiently increase both absolute force and speed in water (McHenry 2012; Anderson et al. 2014). Additionally, previous studies have shown a relationship between skull shape and bite force in birds, in at least one case stronger than the relationship between bite force and beak dimensions (Herrel et al. 2005; van der Meij and Bout 2008). These results support the prediction that cranial linkage shape in birds evolves in relation to beak function.

However skulls are subject to multiple constraints, not least among them housing the brain, eyes, and other sensory systems (Iwaniuk and Nelson 2001; Hall and Ross 2007). In birds, relative brain size is known to have an important influence on skull shape (Marugán-Lobón and Buscalioni 2009). Because the linkage bones are situated directly under the neurocranium, it is possible that linkage geometry more closely reflects differences in brain size and shape rather

than differences in beak mechanics. In support of this, changes in the shape of the facial skeleton (including part of the linkage but excluding the beak) across birds show strong covariation with changes in neurocranium shape (Klingenberg and Marugán-Lobón 2013). At the same time, beak shape variation in crows also covaries strongly with changes in the shape of the neurocranium and orbit (Kulemeyer et al. 2009), suggesting that these observed covariances may reflect a high degree of overall integration (low modularity) in the avian skull. Whether this strong integration acts as a constraint on linkage shape evolution or reflects a strong functional, evolutionary covariation between the linkage and beak remains untested.

Waterfowl (order Anseriformes) are an ideal group in which to test whether cranial linkage geometry evolves in concert with beak function. The group exhibits a diversity of feeding strategies, including dabbling (filtering food items from water), underwater browsing of sessile food items (e.g. mussels), pursuit diving (i.e. piscivory), and grazing (Fig. 5.2; Johnsgard

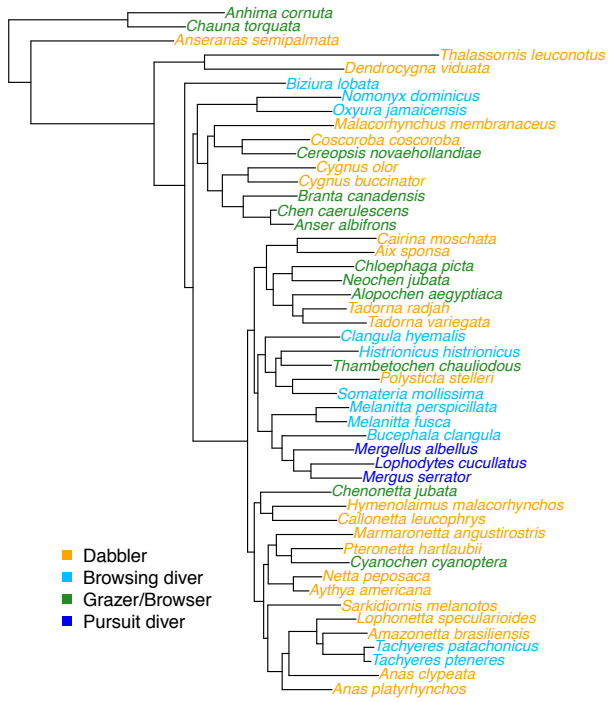

Figure 5.2. Phylogenetic relationships among the sampled taxa and assigned ecological categories based on feeding behavior. Tree from Burleigh and colleagues (2015).

1978; Marchant and Higgins 1990; Kear 2005; Li and Clarke 2015). Previous work has shown that dabbling is likely ancestral for most waterfowl with a single origin of pursuit divers and several independent transitions toward greater herbivory in the form of "geese" (Olsen 2015). These independent transitions toward increased herbivory are associated with the repeated convergence of a more goose-like beak (Olsen, in prep.), enabling a phylogenetically informed test for an association between linkage and beak function. Additionally, previous work in mallards documenting *in vivo*, jaw muscle activity patterns (Zweers 1974), feeding performance (van der Leeuw et al. 2003), and three-dimensional motion of the linkage bones and beak (Dawson et al. 2011), informs the application of biomechanical linkage modeling (Olsen and Westneat, in review) to simulate cranial kinesis in a comparative sample of skulls across the clade.

In this paper we use three-dimensional morphometric data from the skulls of waterfowl to test the hypothesis that the cranial linkage geometry in birds evolves in association with feeding ecology and beak mechanics. If linkage shape evolution is associated with beak function, we predict that linkage shape and beak shape will show a significant pattern of evolutionary covariation. We test this by quantifying morphological integration and modularity among the beak, linkage, and neurocranium. We predict that species that differ in feeding ecology will differ in linkage shape and function. To quantify linkage function we combine the morphometric data with a computational model of cranial kinesis to define two measures of linkage mechanical advantage. We then apply phylomorphospace and function-space approaches to examine patterns of morphological and functional diversification of the beak and linkage. We predict that changes in beak function will be associated with changes in linkage function. We test this by examining the relationship between mechanical advantage of the linkage and beak. By taking a broader

view of the avian jaw apparatus that encompasses the shape and function of both the upper beak and cranial linkage, this study seeks to shed insights into the function of cranial kinesis, examine the functional and evolutionary interplay between the linkage and beak, and test whether this broader consideration changes our interpretation of beak shape diversification.

Methods

Morphometric data collection

To quantify differences in skull and beak shape among waterfowl we collected 3D landmark and curve (semilandmark) data from 134 museum skeletal specimens representing 49 anseriform species and 44 anseriform genera. Specimens were obtained from collections at the Field Museum of Natural History (Chicago, IL), Natural Museum of Natural History (Washington, DC), and the Museum of Vertebrate Zoology (Berkeley, CA). All computational methods for this study were conducted in R computing framework (version 3.2.4; R Core Team 2016). Morphometric data were collected using stereo camera reconstruction implemented with version 1.5.0 of the R package 'StereoMorph' (Olsen & Westneat 2015). Two digital cameras (Nikon SLR D5000) were arranged in stereo such that their views converged on the same volume and calibrated with a checkerboard pattern using the StereoMorph function 'calibrateCameras'. Each specimen was photographed and landmarks and curves (Fig 3a) were manually digitized in both camera views using the StereoMorph digitizing application. Landmark and curve points were reconstructed into 3D using the camera calibration and the StereoMorph function 'reconstructStereoSets'. The midsagittal curvature of the upper beak (the culmen) and of the neurocranium were digitized from a single lateral view and then aligned with the 3D shape dataset using overlapping landmarks. The 3 curves (sagittal neurocranium, culmen, and tomium) were defined using 50 points evenly spaced along each curve (this number was

reduced for integration and modularity tests). Each specimen was aligned to the midline plane, reflected to fill in missing landmarks, and averaged (Klingenberg, Barluenga & Meyer 2002).

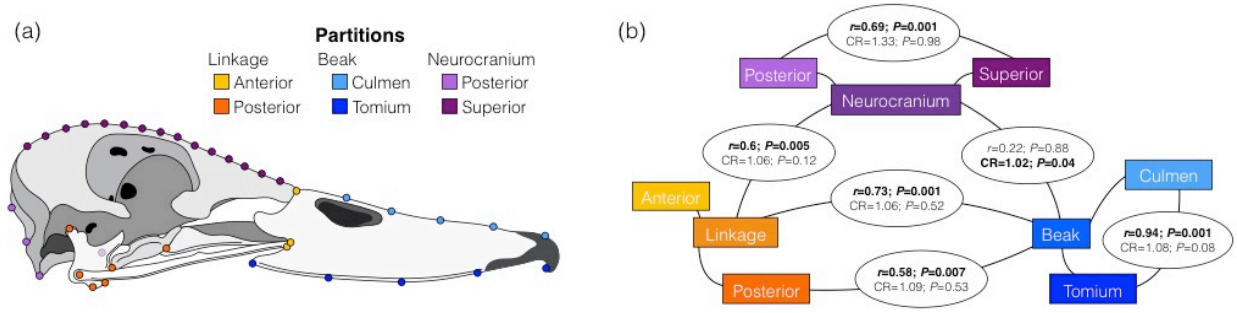

Figure 5.3. Integration and modularity of the waterfowl skull. (a) Landmarks and corresponding partitions used for integration and modularity tests (in lateral view) and (b) the resulting correlation coefficients and significance statistics. Each ellipse (b) shows the PLS correlation coefficient (*r*-PLS) and associated *P*-value above and covariance ratio (CR; Adams 2016) and associated *P*-value below. Significance of $P < 0.05$ is indicated in bold. A significant *r*-PLS correlation indicates significant integration between partitions; a significant CR indicates that the partitions vary as independent modules.

Geometric morphometric analyses

The 3D morphometric data for different portions of the skull were separated into four different sets for subsequent analyses: beak, linkage, neurocranium, and the beak and linkage together (beak+linkage). For each skull portion we first obtained a consensus shape for each species using generalized Procrustes analysis, to remove the effect of differences in centroid size, position, and rotation. This was implemented using the 'gpagen' function in the R package 'geomorph' (Adams and Otárola-Castillo 2013) to slide semilandmarks, when applicable, and a custom function to account for some missing landmarks in 1-2 species. The resulting consensus shape for each species was then scaled to mean species centroid size. A second Procrustes step was performed to align sets across species, again removing the effect of centroid size, position, and rotation. This resulted in a Procrustes coordinate set for each species and each of the four

skull portions. Relative skull dimensions were measured from the landmark data as the maximum height, width, and length of the skull (including the linkage but excluding the beak) relative to skull centroid size (also excluding the beak).

Morphometric data collected from interrelated taxa likely do not represent independent data points due to shared ancestry (Blomberg et al. 2003). To test whether morphometric data among more closely related species is more similar than would be expected under an assumption of independence we tested for phylogenetic signal using the geomorph function 'physignal' (Adams 2014). For all phylogenetic analyses in this study we used the maximum likelihood topology of a molecular phylogeny of 6714 avian species, pruned to the 49 sampled species (Fig. 5.2; Burleigh, Kimball & Braun 2014, 2015). Constructed from a sparse supermatrix of 22 nuclear loci and seven mitochondrial regions, this tree represents the most current molecular phylogeny of Anseriformes, incorporating data from several previous studies (Sraml et al. 1996; Johnson and Sorenson 1998; McCracken et al. 1999; Sorenson et al. 1999; Donne-Goussé, Laudet & Hänni 2002). Tree reading and pruning were performed using functions in the R packages 'ape' (Paradis et al. 2004) and 'phytools' (Revell 2012).

Although, shapes are scaled to the same centroid size during Procrustes superimposition, shape variation across samples can still retain a correlation with size (allometry). To test for allometry we used the geomorph function 'procD.lm' (Goodall 1991) using log centroid size for each skull portion as the size metric. For those landmark sets that showed significant allometry, the 'procD.lm' function was also used to compute size-adjusted residuals, which were added to the consensus shape to obtain size-corrected Procrustes coordinates.

To quantify the strength of covariation among the different skull portions we tested for morphological integration and modularity (Olson and Miller 1958; Cheverud 1996; Klingenberg

2008) using the geomorph functions ‘phylo.integration’ and ‘phylo.modularity’, respectively, both of which take into account phylogenetic relatedness (Adams and Felice 2014; Adams 2016). The ‘phylo.integration’ function uses partial least squares to calculate a correlation coefficient (*r*-PLS) between landmark sets. The ‘phylo.modularity’ function quantifies modular structure using a covariance ratio (*CR*). The *CR* provides a better measure of modularity than the RV coefficient, as the latter has been shown to be biased by sample size and number of variables (Adams 2016). *CR* ranges from zero to positive, with values between zero and one expressing greater modularity (lower covariation) than expected by chance (random sets of variables) and values greater than one expressing less modularity (higher covariation) than expected by chance. Both use resampling to estimate a corresponding *P*-value.

For the integration and modularity tests we divided the morphometric data into three primary partitions corresponding to three of the four landmark sets: linkage, beak, and neurocranium (Fig. 5.3a). Additionally, we used secondary partitions within each primary partition to compare covariances within and among partitions: anterior versus posterior landmarks within the linkage partition, the culmen versus tomium within the beak partition, and superior versus posterior landmarks within the neurocranium partition. As the landmark data are bilaterally symmetric, we only included left and midline landmarks in the integration and modularity tests. We observed an effect of the number of curve points on the modularity tests due to the autocorrelation among points on the same curve. If too many points were used for a particular curve it was detected as an independent module despite high levels of integration (the number of curve points had little to no effect on the integration tests). Using too many curve points would render the modularity tests less informative as each partition with curves would invariably be identified as independent. We used modularity tests between the secondary

partitions to identify an appropriate number of curve points (i.e. a number that resulted in a lack of significant modularity within each primary partition; Fig. 5.3a).

Biomechanical analysis

For force transmission systems with relatively constrained motion, such as levers and linkages, the geometry of the system has direct consequences for system function. In particular, the geometry determines the relative motion between points of force input and output which, in turn, determines the amplification of relative force or velocity. The amplification of relative force or velocity is commonly quantified using mechanical advantage (*MA*), which can be calculated by dividing the change in position where force is input into the system (dx_i) by the change in position at a point where force is output from the system (dx_o; Eq. 5.1). This ratio is also equal to the ratio of output force (F_o) to input force (F_i) at those same points in the system.

$$MA = \frac{dx_i}{dx_o} = \frac{F_o}{F_i} \tag{5.1}$$

The *MA* of a lever can be calculated by describing the motion of the input and output point as the motion of a point on a rotating body: the product of the moment arm (*r*, i.e. the minimum distance to the axis of rotation) and the change angular rotation ($d\theta$; Eq. 5.2). Since the angular rotation is the same for any point on a lever, the changes in angle cancel to yield the familiar equation of in-lever length (r_i) divided by out-lever length (r_o).

$$MA_{lever} = \frac{r_i d\theta_i}{r_o d\theta_o} = \frac{r_i}{r_o} \tag{5.2}$$

Systems with a higher *MA* amplify output force relative to input force but necessarily have reduced output velocity relative to input velocity, resulting in a trade-off between relative force and velocity (Westneat 1994).

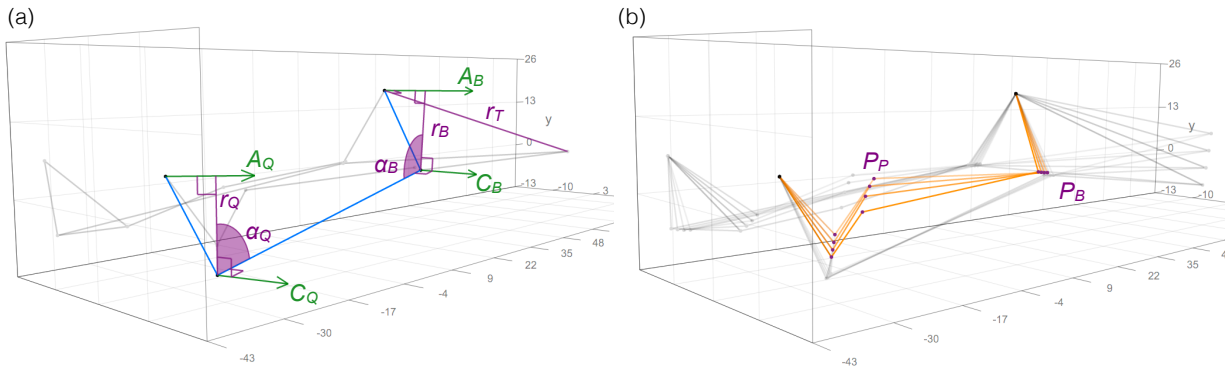

Figure 5.4. Three-dimensional geometry of the waterfowl cranial linkage and upper beak (example taken from the mallard, *Anas platyrhynchos*). (a) Geometric definitions of parameters used to quantify torque mechanical advantage through the four-bar cranial linkage (blue), from the quadrate to the beak (MA_{QB}; Eq. 5.5). Parameters use the following naming convention: moment arms (r), angles (α), axes of rotation (A), cross product vectors (C). (b) The four mobile links of the cranial five-bar linkage (orange) and associated joints (purple). P_P indicates the pterygoid-palatine joint, P_B indicates the palatine-upper beak joint. Four iterations of simulated motion of the cranial linkage elements and beak are superimposed. Force MA from the palatine to upper beak (MA_{PB}; Eq. 5.7) is approximated by taking the ratio of P_P translation to P_B translation for small input rotations of the quadrate (Olsen and Westneat, in review).

Importantly, *MA* alone does not predict absolute force and velocity; a higher *MA* can in fact lead to a higher absolute output velocity (McHenry and Summers 2011; McHenry et al. 2012). The primary sources of energy loss in a system and the system *MA* are necessary to predict absolute force and velocity output (McHenry 2012). Nonetheless, *MA* is still a key determinant of absolute force and velocity output.

To characterize beak function we calculated two different measures of mechanical advantage from the species averaged landmark data. The first, MA_{BT}, measures force advantage from an input where the jugal attaches to the beak (in-lever) to the distal tip of the beak (out-lever; Fig. 5.4a). This can also be described as a retraction (or protraction) *MA* as it represents the force advantage of the beak during the hinge-like rotation of the upper beak at the

craniofacial joint; accordingly, the moment arms are measured using the transverse axis as the axis of rotation (Eq. 5.3).

$$MA_{BT} = \frac{r_B}{r_T} \tag{5.3}$$

In contrast, our second *MA* measure, torsional MA or MA_{ML}, represents transmission due to rotation of the upper beak about the anterior-posterior axis of the skull (i.e. roll). For MA_{ML} we measured the moment arms as the minimum distance from the input (r_M, jugal-upper beak joint) and output (r_L, midpoint along the tomium) to the midline plane.

$$MA_{ML} = \frac{r_M}{r_L} \tag{5.4}$$

There is very little effective rotation of the beak about this axis (Dawson et al. 2011). However, when bite forces are not balanced between the left and right side, such as when geese grasp leaves along the side of the beak rather than at the tip (van der Leeuw et al. 2003), a torque is created on the beak that twists the beak about the anterior-posterior axis. MA_{ML} represents the force advantage of the beak in countering these torques and stabilizing the beak against roll. For both beak *MA* measures we only considered input to the upper beak from the jugal because in waterfowl the palatine and jugal bones attach to the upper beak at nearly the same location; use of the palatine as input rather than the jugal yields nearly identical *MA* values.

To characterize linkage function we also calculated two different linkage mechanical advantages from the species averaged landmark data. The first, MA_{QB}, measures torque advantage from the quadrate to the upper beak through the jugal bone. These three bones form a four-bar linkage with the neurocranium as the fixed link (Fig. 5.1b). To calculate this mechanical advantage we derived an equation for the mechanical advantage of a three-dimensional four-bar linkage and applied this to the avian cranial four-bar linkage (Eq. 5.5), where β_Q is the angle

between A_Q and C_Q and β_B is the angle between A_B and C_B (Fig. 5.4a). This equation is equivalent to the ratio of quadrate (input) rotation, $d\theta_Q$, to beak (output) rotation, $d\theta_B$, over an infinitesimally small angle (Olsen and Westneat, in review).

$$MA_{QB} = \frac{d\theta_Q}{d\theta_B} = \frac{r_B}{r_Q}\frac{\sin\alpha_B}{\sin\alpha_Q}\frac{\cos\beta_B}{\cos\beta_Q} \tag{5.5}$$

Because MA_{QB} and MA_{BT} share a common term (r_B), we also used a second measure of quadrate-to-beak *MA*, MA_{QJ} (Eq. 5.6), that excludes r_B. As this is no longer a dimensionless ratio we used linkage centroid size as a covariate in the regression analysis.

$$MA_{QJ} = \frac{1}{r_Q}\frac{\sin\alpha_B}{\sin\alpha_Q}\frac{\cos\beta_B}{\cos\beta_Q} \tag{5.6}$$

There are at least three potential mechanisms for force input to the quadrate (Zweers 1974). The first originates from adductor muscles that originate on the skull and insert more anteriorly on the lower jaw. During contraction, the posterior component of these muscle forces is transmitted to the quadrate through its articulation with the lower jaw, causing the quadrate to rotate backward and retract the upper beak. The second input force comes from the quadrate protractor muscle, which originates on the neurocranium, anterior and medial to the quadrate and inserts on the quadrate. Contraction of this muscle causes the quadrate to rotate forward and protract the upper beak. Third, the depressor mandibulae muscle, which originates on the posterior neurocranium and inserts on the retroarticular process of the mandible, forms an additional four-bar linkage with the quadrate, lower jaw, and postorbital ligament. Through the mechanism, contraction of the depressor mandibulae is thought to indirectly contribute to forward rotation of the quadrate and upper beak protraction (Bock 1964).

We calculated a second *MA* measure for the linkage, MA_{PB}, to represent the force advantage of transmission from the palatine to the upper beak. The palatine and pterygoid bones

are the insertion sites of the pterygoid muscle, which originates on the medial aspect of the lower jaw (Zweers 1974). Contraction of the pterygoid muscle pulls the palatine inferiorly and posteriorly relative to the lower jaw and retracts the upper beak. Rather than derive an equation for MA_{PB}, we used a simulation-based approach (Olsen and Westneat, in review) to approximate the ratio of instantaneous change in positions of the input and output points, P_P and P_B (Fig. 5.4b; Eq. 5.7), respectively.

$$MA_{PB} = \frac{dP_P}{dP_B} \tag{5.7}$$

Kinematic simulation was performed using the function 'animateLinkage' in the R package 'linkR' (Olsen and Westneat, in review). The linkage was defined using the 'defineLinkage' function in linkR, specifying the three-dimensional position and constraints at each joint for each species. We simulated motion of the linkage at 30 points over a 10-degree rotation of the quadrate. Unlike the *MA* of a lever, the *MA* of a linkage is non-constant for different positions or conformations of the linkage. This is the case for both MA_{QB} and MA_{PB}. We used the linkage simulation to calculate MA_{QB} and MA_{PB} at each iteration and then took the minimum value of each for subsequent analysis.

The general linkage configuration used was identical to the bird model described by Olsen and Westneat (2016, in review) except for the quadrate axis of rotation. In waterfowl, the quadrate articulates with the neurocranium via a unicondylar joint that permits three degrees of rotational freedom (Dawson et al. 2011). Thus, the morphology could not be used to establish a definite quadrate axis of rotation. Instead we defined quadrate rotation for all species to match the *in vivo* kinematics reported by Dawson and colleagues for mallards (2011), in which the quadrate rotates equally about the transverse and anterior-posterior axes (i.e. within the coronal

plane at an approximately 45 degree angle to the midline plane). While different waterfowl species likely have differing orientations of the quadrate axis of rotation, by using a consistent rotational axis we are effectively testing for variation independent of differences in the quadrate axis of rotation.

Correlation and group difference analyses

To reduce the dimensionality of the Procrustes coordinate data for visualization and regression analyses we performed phylogenetic principal component analysis using the 'phyl.pca' function in the R package 'phytools' (pPCA; Revell 2009). Correlations among shape and function variables were examined using the phylogenetic generalized least squares regression (PGLS), implemented with the 'pgls' function in the R package 'caper' (Orme et al. 2013). The delta and kappa parameters were fixed at 1 while the λ parameter (phylogenetic signal) was estimated using maximum likelihood (Revell 2010). In this way, the correlation tests takes into account phylogenetic relatedness, varying levels of phylogenetic signal, and correlations among the independent variables of the regression. The 'pgls' function corrects for unequal tip variances resulting from our use of a non-ultrametric tree.

To test whether shape and function differ with ecology we grouped the taxa into ecomorphological types (Fig. 5.2). We based these groupings on descriptions in the natural history literature (Johnsgard 1978; Marchant and Higgins 1990; Kear 2005) but also on beak shape. As the division of waterfowl into discrete ecological groups will always be somewhat arbitrary our objective with the ecological categories was to test whether groupings that intentionally produce clear divisions based on beak shape and function are similarly well discriminated by linkage shape and function. Additionally, it should be noted that most waterfowl do not conform perfectly to discrete behavioral categories – many grazing waterfowl

continue to filter-feed to some extent (van der Leeuw et al. 2003). Rather, these categories should be regarded simply as a primary feeding mode.

Differences in shape and functional variables among ecomorph groups (Fig. 5.2) were examined using phylogenetic analyses of variance, implemented using the 'aov.phylo' function in the R package 'geiger' (Harmon et al. 2008). We used 'aov.phylo' to perform both phylogenetic MANOVA on beak and linkage shape variables (multiple pPCs as dependent variables) and phylogenetic ANOVA on each of the four mechanical advantage metrics. The *P*-values for unique pairwise group difference tests were corrected for multiple hypothesis testing using the 'p.adjust' function (Holm method) in the R package 'stats' (R Core Team 2016). All shape pPC scores and mechanical advantage metrics were tested for normality using the function 'shapiro.test', also in the 'stats' package. Those with nonnormal distributions were log-transformed prior to analysis to achieve more normal distributions.

Visualizing patterns of shape and function diversification

To visualize patterns of morphological and functional diversification we applied a phylomorphospace approach, in which the evolution of two or more traits is simulated and the ancestral state estimates and tips are plotted within morphospace (Sidlauskas 2008). We simulated trait evolution using the 'ace' function in the R package 'ape' (Paradis et al. 2004) and the restricted maximum likelihood method (Felsenstein 1973; Schluter et al. 1997). To visualize shape variation along pPC axes we used the backtransformation method (Lohmann & Schweitzer 1990; MacLeod 2009; Olsen, in prep.). In principal component analysis, the original input matrix can be recovered by multiplying the PC score matrix by the inverse of the eigenvector matrix. This procedure can be adapted to visualize the shape change along a particular PC axis or axes by constructing a score matrix of evenly distributed scores along the PC axis or axes of interest,

within the range of the sample PC scores, and mean scores for all other PC axes. When plotted within morphospace, these backtransform shapes represent the theoretical shape at each pair of PC scores in morphospace for the two PC axes of interest and the mean of all other PC axes. We use lateral and ventral silhouettes to portray the backtransform shapes solely for ease of visualization; all shape analyses were performed using three-dimensional data.

Lastly, we combined PC backtransformation and biomechanical analysis to produce heat maps of *MA* across morphospace. We used backtransformation to generate a high density of backtransform shapes across morphospace (20x20), calculated the beak and linkage mechanical advantages for each backtransform shape, and plotted color-coded magnitudes using the 'graphics' R package (R Core Team 2016). Thus, like the backtransform shapes, the magnitudes in the heat maps represent the theoretical mechanical advantage at each pair of PC scores in morphospace for the two PC axes of interest and the mean of all other PC axes.

Results

Morphological integration and modularity

The cranial linkage of waterfowl is tightly integrated with both the neurocranium and beak while the neurocranium and beak are weakly integrated and show evidence of evolution as independent modules (Fig. 5.3). Significant centroid size allometry ($P < 0.05$; 1000 iterations) was detected only in the neurocranium landmark set ($R^2 = 0.10$, P-value = 0.005); prior to integration and modularity tests we regressed neurocranium landmarks on neurocranium centroid size and used the residuals in subsequent analyses. Significant phylogenetic signal ($P < 0.02$; 1000 iterations) was detected in all landmark sets, necessitating the use of analyses that take into account covariation due to phylogenetic relatedness.

Between the linkage and beak we detected strong and significant integration (*r*-PLS=0.73; *P*=0.001; 1000 iterations) and did not detect significant modularity (CR=1.06; *P*=0.52; 1000 iterations). Even when excluding the anterior landmarks of the linkage, which contact the upper beak directly, we still detected highly significant, but weaker, integration (*r*-PLS=0.58; *P*=0.007) and did not detect significant modularity (CR=1.09; *P*=0.53). The linkage is also tightly integrated with the neurocranium (*r*-PLS=0.6; *P*=0.005) with no detection of significant modularity (CR=1.06; *P*=0.12). In contrast, between the neurocranium and beak we detected moderately significant modularity (CR=1.02; *P*=0.04) and did not detect significant integration (*r*-PLS=0.22; *P*=0.88). Secondary partitions within the neurocranium and beak, the two primary partitions with curve points, recover high integration and non-significant modularity tests (Fig. 5.3b), indicating an appropriate number of curve points to compare each primary partition as a module.

Beak shape and function

Beak shapes in waterfowl display convergent and divergent transitions along opposing gradients of mechanical advantage (Fig. 5.5). The first two pPCs explain 46% and 35% of the variation in beak shape, respectively, and 81% of the variation cumulatively (the remaining pPCs explain less than 7% of the variation and are not discussed further here). Ancestral trait estimates

Figure 5.5 (next page). Phylomorphospace (a), backtransform morphospaces (b,d), and function morphospaces (c,e) showing diversification of beak shape and function in a morphospace defined by beak shape pPC1-2. Symbols and colors indicate feeding ecology groups shown in Fig. 5.2. Waterfowl show multiple independent transitions to grazing and a single transition to pursuit diving (a). The transition to grazing is associated with the evolution of a more "goose-like" beak while the transition to pursuit diving is associated with the evolution of a beak that is longer, narrower, and shorter in height (in lateral view, b, and in dorsal view, d). The MA of force transmission from the jugal to the upper beak tip (MA_{BT}) is greater for beaks that are relatively taller and shorter in length (c) while the MA for resistance to torsion (MA_{ML}) is greater for beaks that are relatively wider at the base and narrower at the tip (e).

Figure 5.5, continued.

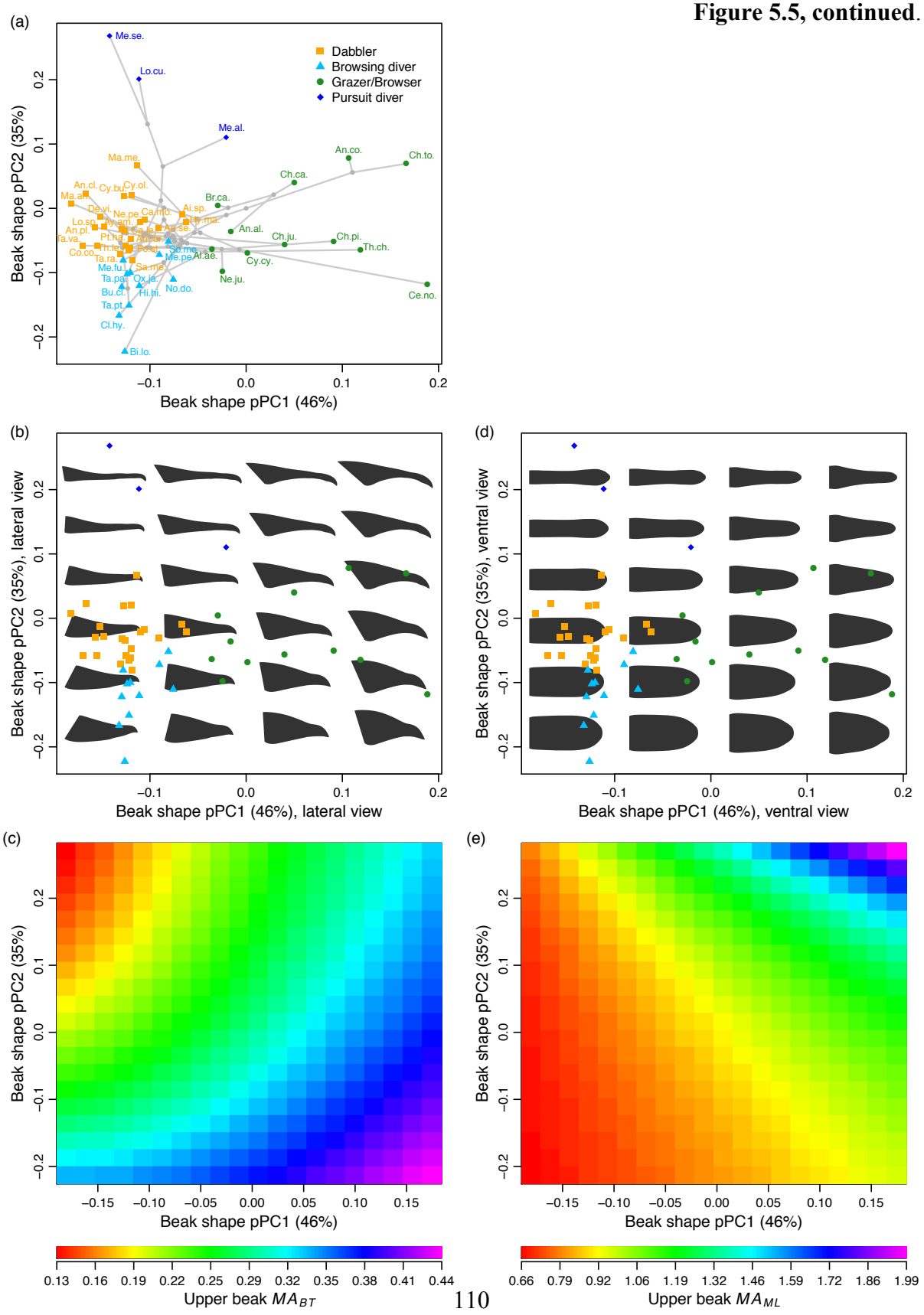

reveal convergent transitions in beak shape along pPC1 from a dabbling, or more 'duck-like', beak to a grazer/browser, or more 'goose-like', beak (Fig. 5.5a), consistent with a previous study of waterfowl beak shape and dietary evolution (Olsen, in prep.). In particular, these transitions are associated with a more dorsally arcing culmen and tomium (in lateral view, Fig. 5.5b), and a beak that is relatively wider and taller at the base, shorter in length, and narrower at the tip (in ventral view, Fig. 5.5d).

Ancestral trait estimates also reveal a single divergent transition along pPC2 (Fig. 5.5a) from a dabbling beak shape to a pursuit diving beak shape, characteristic of mergansers and smews: shorter in height, more elongate, and narrower (Fig. 5.5b,c). Beak shape variation in waterfowl is strongly and significantly associated with orthogonal gradients of retraction and torsional mechanical advantage, MA_{BT} and MA_{ML}, respectively (Fig. 5.5c,e; Table 5.1). While beak MA_{BT} and MA_{ML} increase in the same direction along pPC1, MA_{BT} decreases while MA_{ML} increases along pPC2 (Table 5.1). The transition to a grazing, more goose-like beak increases both MA_{BT} and MA_{ML} while the transition to a pursuit diver beak decreases MA_{BT} and increases MA_{ML}.

Table 5.1. Results of PGLS analysis relating beak functional variables to the first two major axes of beak shape variation.

y-Variable	*x*-Variable	Estimate	*P*-value
Log beak shape pPC1 ($\lambda = 1$, $R^2 = 0.63$)	**Intercept**	**-0.14**	**<0.0001**
	Beak MA_{BT}	**0.47**	**<0.0001**
	Log beak MA_{ML}	**0.11**	**0.01**
Log beak shape pPC2 ($\lambda = 0.9$, $R^2 = 0.63$)	**Intercept**	**0.15**	**<0.0001**
	Beak MA_{BT}	**-0.49**	**<0.0001**
	Log beak MA_{ML}	**0.23**	**<0.0001**

Linkage shape and function

A phylogenetic principal components analysis of linkage shape identifies three major patterns of variation in waterfowl linkage shapes associated with overall skull shape, the force transmission properties of the linkage, and beak shape (Fig. 5.6). The first pPC axis (41% of the variation) is strongly and significantly associated with differences in relative skull dimensions (relative height, width, and length, all excluding the beak) but is not significantly associated with either metric of linkage *MA* (Table 5.2). Additionally, none of the ecological groups show a consistent evolutionary trend along pPC1, leading to an low level of discrimination among groups along that axis (Fig. 5.6a).

In contrast, the second pPC axis of linkage shape (17% of the variation) is significantly correlated with variation in MA_{QB} and is not significantly correlated with either variation in relative skull dimensions or MA_{PB} (Table 5.2). The increase in MA is a consequence of an increase in the four-bar outlink length (r_B) relative to the inlink length (r_Q; Eq. 5.6; Fig. 5.6b). Pursuit divers and some of the lineages that evolve a more goose-like beak show parallel trajectories in linkage shape change along this axis, toward increasing MA_{QB} (Fig. 5.6c). Lastly, the third pPC axis of linkage shape (10% of the variation) is significantly correlated with MA_{PB}, as well as the relative width and height of the skull (Table 5.2). Along this axis, pursuit divers

Figure 5.6 (next page). Phylomorphospace (a,d), backtransform morphospaces (b,e), and function morphospaces (c,f) showing diversification of linkage shape and function in a morphospace defined by linkage shape pPC1-3. Symbols and colors indicate feeding ecology groups shown in Fig. 5.2. Waterfowl show differentiation in linkage shape by ecology although the pattern is weaker than for beak shape and is strongest along pPC2 and pPC3 (a,d). Grazers and pursuit divers show parallel trajectories along pPC2 (a), toward increasing MA_{QB} (c) and opposing trajectories along pPC3 (d), toward increasing and decreasing MA_{PB}, respectively. Increasing MA_{QB} is primarily associated with increase in beak height relative to quadrate height (b,c; Eq. 5.5) while increasing MAPB is associated with a decrease in overall relative linkage height and increase in relative linkage width (e,f; Table 5.2).

Figure 5.6, continued.

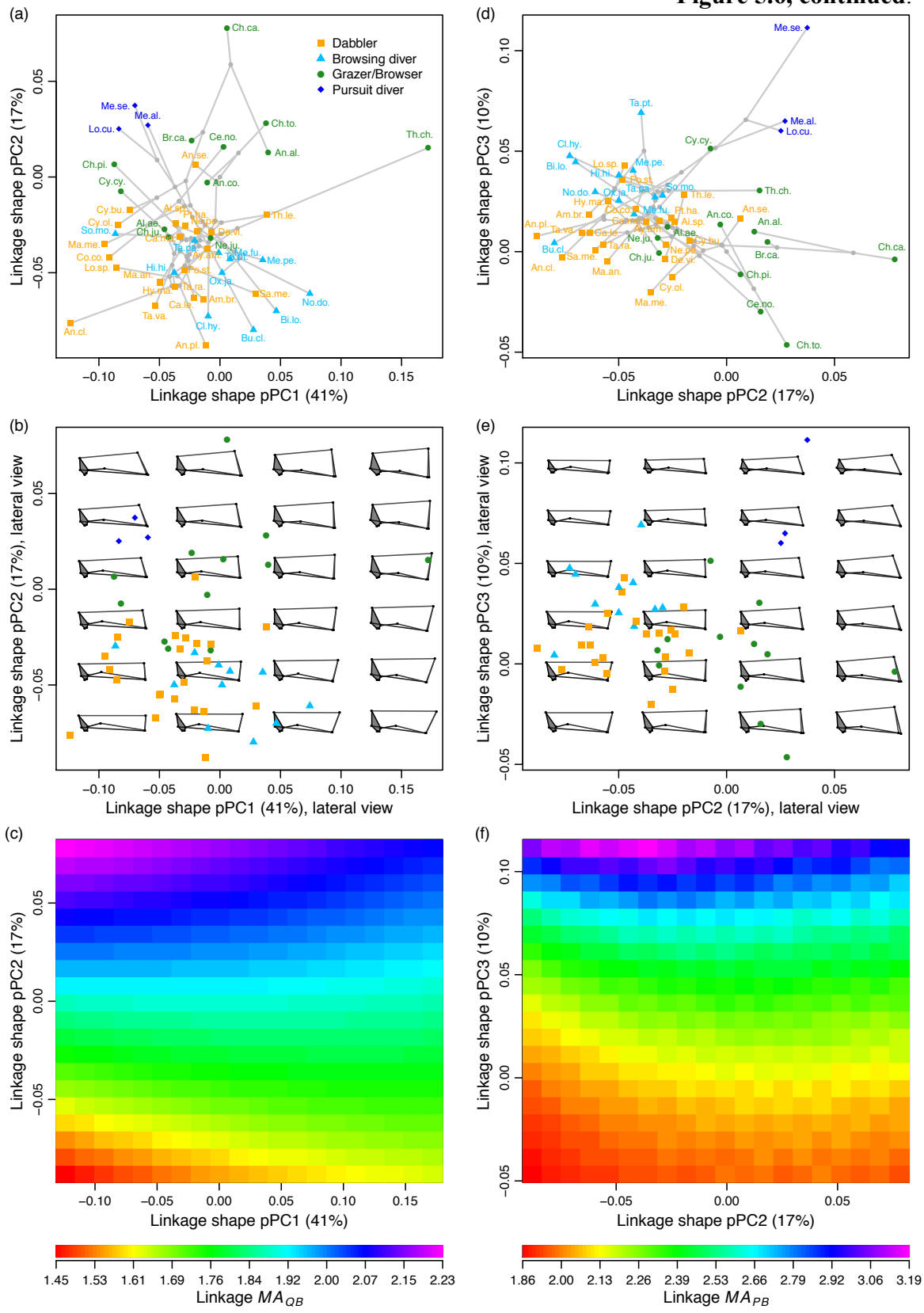

and most grazers show diverging trajectories (Fig. 5.6d), with pursuit divers evolving toward greater MA_{PB} and grazers evolving toward lower MA_{PB} (Fig. 5.6f). Consistent with the results of the integration tests, the first 3 pPCs of linkage shape, particularly linkage pPC2, all show strong correlations with beak shape pPC1, pPC2, or both (Table 5.3).

Table 5.2. Results of PGLS analysis relating linkage functional variables and relative skull dimensions to the first three major axes of linkage shape variation.

y-Variable	*x*-Variable	Estimate	*P*-value
Linkage shape pPC1 ($\lambda = 0.51$, $R^2 = 0.84$)	**Intercept**	**0.49**	**<0.001**
	Log linkage MA_{QB}	-0.04	0.4
	Log linkage MA_{PB}	-0.04	0.43
	Log skull RH	**0.37**	**<0.0001**
	Log skull RW	**0.97**	**<0.0001**
	Log skull RL	**-1.02**	**<0.0001**
Linkage shape pPC2 ($\lambda = 0.83$, $R^2 = 0.31$)	Intercept	0.15	0.31
	Log linkage MA_{QB}	**0.23**	**<0.01**
	Log linkage MA_{PB}	0	0.97
	Log skull RH	-0.03	0.8
	Log skull RW	0.14	0.18
	Log skull RL	0.26	0.29
Linkage shape pPC3 ($\lambda = 0.41$, $R^2 = 0.42$)	Intercept	0	0.99
	Log linkage MA_{QB}	0	0.94
	Log linkage MA_{PB}	**0.1**	**0.02**
	Log skull RH	**-0.18**	**0.02**
	Log skull RW	**0.2**	**0.01**
	Log skull RL	0.03	0.88

Table 5.3. Results of PGLS analysis relating major axes of linkage shape and beak shape variation.

y-Variable	*x*-Variable	Estimate	*P*-value
Log beak shape pPC1 ($\lambda = 0.88$, $R^2 = 0.6$)	Intercept	0	0.87
	Linkage pPC1	**0.21**	**<0.01**
	Linkage pPC2	**0.76**	**<0.0001**
	Linkage pPC3	**-0.41**	**<0.01**
Log beak shape pPC2 ($\lambda = 0.99$, $R^2 = 0.44$)	Intercept	0	0.95
	Linkage pPC1	**-0.25**	**<0.001**
	Linkage pPC2	**0.48**	**<0.0001**
	Linkage pPC3	-0.06	0.65

Relationship between beak function and linkage function

Across waterfowl, the *MA* of torque transmission from the quadrate to the beak through the jugal, MA_{QB}, is strongly correlated with the *MA* from the jugal to the tip of the beak, MA_{BT} ($P < 0.0001$; Table 5.4). Although MA_{QB} and MA_{BT} share the term r_B (Eq. 5.3 and 5.5), neither is determined by this term alone. Thus, a correlation indicates that the additional parameters that determine *MA* do not vary so as to obscure a positive association between linkage and beak *MA*. To test whether the correlation between MA_{QB} and MA_{BT} is driven entirely by the shared term r_B, we also regressed beak MA_{BT} on MA_{QJ}, MA_{QB} excluding the r_B term, with linkage centroid size as a covariate (Eq. 5.6). MA_{BT} is more weakly, but still significantly (P=0.02), correlated with MA_{QJ}, indicating that aspects of linkage shape in addition to r_B contribute to the correlation between linkage and beak *MA*.

Table 5.4. Results of PGLS analysis relating beak function and linkage function.

y-Variable	*x*-Variable	Estimate	*P*-value
Beak MA_{BT} ($\lambda = 1$, $R^2 = 0.31$)	**Intercept**	**0.24**	**<0.0001**
	Log linkage MA_{QB}	**0.41**	**<0.0001**
	Log linkage MA_{PB}	-0.1	0.32
Log beak MA_{ML} ($\lambda = 1$, $R^2 = 0.07$)	Intercept	-0.12	0.19
	Log linkage MA_{QB}	0.25	0.17
	Log linkage MA_{PB}	0.20	0.32
Beak MA_{BT} ($\lambda = 0$, $R^2 = 0.15$)	Intercept	0.33	0.11
	Log linkage MA_{QJ}	**0.23**	**0.02**
	Log Linkage Centroid size	-0.15	0.3

Ecological differences in shape and function

Waterfowl that employ feeding strategies differ significantly in linkage shape and function (Table 5.5-5.6). A MANOVA of the first two axes of beak shape variation on the four ecological groups verified that, as expected, the chosen assignments were sufficiently distinct in beak shape so as to differ significantly in all group pairwise comparisons (Table 5.5, top). Using

Table 5.5. Group differences in beak and linkage shape. *P*-values, after multiple hypothesis correction, of phylogenetic MANOVA with posthoc comparisons among groups (1000 simulations). Values are symmetrical across the diagonal. Bold indicates *P*-values less than 0.05.

Log beak shape pPC1-2	Browsing diver	Dabbler	Grazer/Browser	Pursuit diver
Browsing diver		**0. 006**	**0.006**	**0.006**
Dabbler	**0.006**		**0.006**	**0.006**
Grazer/Browser	**0.006**	**0.006**		**0.008**
Pursuit diver	**0.006**	**0.006**	**0.008**	

Linkage shape pPC1-3	Browsing diver	Dabbler	Grazer/Browser	Pursuit diver
Browsing diver		**0.012**	**0.012**	**0.012**
Dabbler	**0.012**		**0.006**	**0.006**
Grazer/Browser	**0.012**	**0.006**		**0.029**
Pursuit diver	**0.012**	**0.006**	**0.029**	

Table 5.6. Group differences in beak and linkage function. *P*-values, after multiple hypothesis correction, of phylogenetic ANOVA with posthoc comparisons among groups (1000 simulations). Values are symmetrical across the diagonal. Bold indicates *P*-values less than 0.05.

Beak MA_{BT} (*F*=30, *P*=**0.001**)	Browsing diver	Dabbler	Grazer/ Browser	Pursuit diver
Browsing diver		**0.006**	0.068	**0.009**
Dabbler	**0.006**		**0.006**	0.65
Grazer/Browser	0.068	**0.006**		**0.006**
Pursuit diver	**0.009**	0.65	**0.006**	

Log beak MA_{ML} (*F*=33, *P*=**0.001**)				
Browsing diver		0.89	**0.006**	**0.006**
Dabbler	0.89		**0.006**	**0.006**
Grazer/Browser	**0.006**	**0.006**		**0.006**
Pursuit diver	**0.006**	**0.006**	**0.006**	

Log linkage MA_{QB} (*F*=4.2, *P*=0.07)				
Browsing diver		0.55	1	1
Dabbler	0.55		**0.036**	1
Grazer/Browser	1	**0.036**		1
Pursuit diver	1	1	1	

Log linkage MA_{PB} (*F*=10.6, *P*=**0.002**)				
Browsing diver		0.12	0.09	**0.04**
Dabbler	0.12		0.38	**0.006**
Grazer/Browser	0.09	0.38		**0.006**
Pursuit diver	**0.04**	**0.006**	**0.006**	

these same groupings, waterfowl with different feeding strategies also show significant differences in the first three pPCs of linkage shape ($P < 0.05$) by all pairwise comparisons (Table 5.5). Waterfowl with different feeding strategies also differ significantly for all four measures of beak and linkage *MA*, although not for all pairwise comparisons (Table 5.6; Fig. 5.7). With regard to beak *MA*, significant differences in beak MA_{BT} ($P < 0.01$) were found among all groups except between grazers and browsing divers and between dabblers and pursuit divers; among waterfowl, grazers have the highest MA_{BT} (Fig. 5.7b). Also, grazers and pursuit divers differ significantly in beak MA_{ML} ($P < 0.01$) from each other and from all other groups, with pursuit divers having the highest MA_{ML} among waterfowl (Fig. 5.7b). With regard to linkage *MA*, grazers have significantly higher MA_{QB} ($P < 0.05$) than dabblers while pursuit divers have significantly higher MA_{PB} relative to all other groups ($P < 0.01$; Fig. 5.7a).

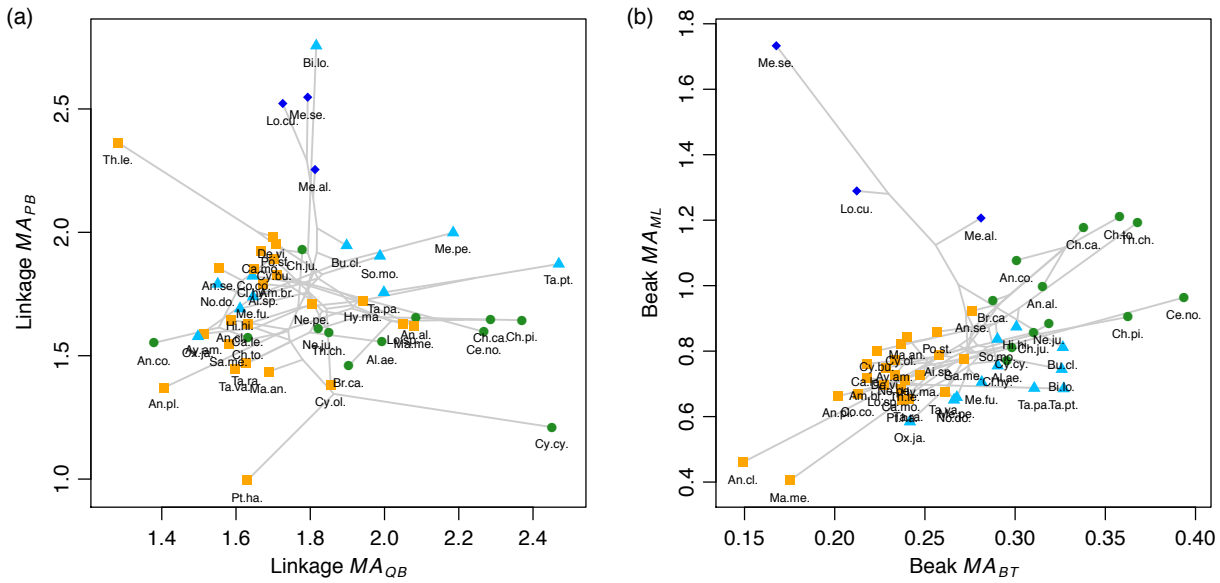

Figure 5.7. Diversification of waterfowl through linkage (a) and beak (b) function space. (a) Waterfowl do not show strong divergence by feeding behavior in *MA* of torque transmission from the quadrate to upper beak (MA_{QB}). However, pursuit divers and musk ducks (*Biziura lobata*) have evolved higher force transmission from the palatine to upper beak (MA_{PB}). (b) Waterfowl show strong divergence by feeding behavior in both measures of beak *MA*. Grazers have evolved higher *MA* for jugal to tip transmission (MA_{BT}) and torsional resistance (MA_{ML}) while pursuit divers have evolved a lower MA_{BT} and higher MA_{ML}.

Discussion

The patterns of diversification in waterfowl cranial form and function support the hypothesis that linkage shape, in addition to beak shape, is an important locus of evolutionary change among birds in the adaptation to new feeding ecologies. The pattern of morphological integration within the waterfowl skull identifies the cranial linkage as a non-independent module strongly related to both the upper beak and neurocranium. The strong evolutionary covariation of linkage shape and beak shape, in addition to significant differences in linkage shape among waterfowl that differ by feeding ecology, implies that linkage shape variation in waterfowl relates, in part, to differences in the function of the feeding apparatus. Indeed, we found that grazers tend to have higher force advantage for transmission from the quadrate to the beak than dabblers while pursuit divers have a higher force advantage for transmission from the palatine to the beak. Additionally, we show that in bird skulls the quadrate-jugal linkage and upper beak are coupled in such a way that mechanical advantage of both can be changed simultaneously and in the same direction by changing the length of their shared link (r_B, Eq. 5.3 and 5.5). The strong correlation between beak MA_{BT} and linkage MA_{QB} confirms this mechanism of synergistic change in linkage and beak function. And the persistence of a correlation after taking into account the effect of the shared link length indicates that additional aspects of linkage shape contribute to this correlation. Taken together, these patterns of correlated morphological, functional and ecological evolution between the beak and linkage point to formerly underappreciated role of linkage shape in the evolution of beak mechanics and behavior.

The observed associations between mechanical advantage and feeding ecology are consistent with the differing biomechanical demands of waterfowl feeding behaviors, particularly in the transitions from dabbling toward grazing and pursuit diving. Dabbling, or

filter-feeding, likely represents the ancestral feeding mode for most waterfowl, based on both ancestral state reconstructions of diet (Olsen 2015), beak shape (Olsen, in prep.), and limited fossil evidence (Olson and Feduccia 1980). During dabbling, the upper and lower beak open and close cyclically in coordination with the tongue, in some cases up to 20 times per second, to pump fluid through the oral cavity and filter out suspended food particles (Zweers et al. 1995; Kooloos et al. 1989; van der Leeuw et al. 2003). During grazing, the upper and lower beak also open and close cyclically but the lateral margin and tip of the beak are used in biting and cropping grasses, stripping seeds, and pecking (van der Leeuw et al. 2003). Thus, the evolutionary transition from dabbling to grazing represents a shift from a more displacement-based behavior to a more force-based behavior. A higher *MA* of either the beak, linkage, or both would enable a bird to achieve a higher static bite force given the same input (e.g. muscle) force. Additionally, a higher torsional *MA* of the beak (MA_{ML}) would enable a bird to counter a higher torsion from a unilateral bite given the same input force. Consistent with these expectations, MA_{BT}, MA_{ML} and MA_{BT} all increase in the transition from dabbling to grazing (Table 5.6; Fig. 5.7).

Although pursuit diving (in this case primarily piscivory) has likely evolved only once within waterfowl (in the clade that includes mergansers and smews), the skull shapes of anseriform pursuit divers are remarkably convergent with those of other bird lineages that have independently evolved pursuit diving (e.g. cormorants, loons). Pursuit diving imposes a number of conflicting biomechanical demands on the feeding system: the beak must close rapidly and have a relatively long reach to catch prey but it must also grasp forcefully to retain prey. Additionally, previous work in the striking appendage and associated linkage of mantis shrimps (i.e. a lever coupled to a linkage) has shown that a linkage with a higher MA (higher force

advantage) produces absolutely faster lever rotation through water because the higher linkage MA more efficiently opposes the large drag force imposed on the lever by the water (McHenry 2012; McHenry et al. 2012). The net result of these demands in the transition toward pursuit diving appears to be relative elongation of the beak to increase reach and relative velocity at the beak tip (lower MA_{BT}), relative narrowing of the beak, potentially to decrease drag but which also increases MA_{ML}, and an increase in linkage MA. In contrast to grazers, linkage MA_{PB} increases while MA_{QB} remains unchanged relative to dabblers, suggesting the force advantage is directed at the pterygoid muscles rather than through the quadrate mechanism.

Our results of integration in the waterfowl skull (Fig. 5.3) both agree and contrast with previous investigations of avian cranial integration. Consistent with our results, a previous study of cranial integration in 160 species across all bird orders found strong integration between 2D (lateral) cranial linkage shape ("facial skeleton") and neurocranial shape (beak shape was not included; Klingenberg and Marugán-Lobón 2013). In contrast with our results, a study of integration in corvid skulls found strong integration between the beak and neurocranium (Kulemeyer et al. 2009). However, unlike our study Kulemeyer and colleagues also collected orbit landmarks and included these in the neurocranium landmark set. The authors point to correlated changes between orbit orientation and beak shape as a primary driver of neurocranium-beak integration: because corvids use visual cues when grasping items with the beak, changes in beak shape are accompanied by reorientation of the orbits to maintain the beak tip within the visual field. Since grazing waterfowl primarily use visual cues whereas dabbling waterfowl primarily rely on tactile cues (Guillemain et al. 2002), it is likely that orbit shape is also strongly integrated with beak shape in waterfowl.

Also in contrast to our results a recent study of cranial integration in raptors (e.g. hawks, falcons, vultures, eagles but excluding owls) found strong integration between the beak and braincase (orbit shape not included) and a strong allometric signal in skull shape overall, with allometry explaining more variation in raptor skull shape than integration (Bright et al. 2016). Although the stronger neurocranium-beak integration pattern observed by Bright and colleagues may be explained in part by the inclusion of some "linkage landmarks" in the braincase set (the quadrate-jugal and pterygoid-palatine joints), a more likely explanation is a fundamental, clade-specific difference in patterns of cranial shape variation between raptors and waterfowl. We observe neither strong signals of allometry nor integration between waterfowl beak and neurocranium shape. This suggests the intriguing possibility that the breaking of a "genetic lock" on strong integration in size and shape within the avian skull occurred not just at the origin of modern songbirds but several times throughout the avian tree of life in association with the adaptation of beak shape to new foraging ecologies.

Although we have demonstrated a role for linkage shape the evolution of feeding behavior, changes in jaw muscle architecture are also likely to have played a prominent role in the evolution of waterfowl beak mechanics. Previous studies have found that variation in beak and skull shape in birds, after accounting for differences in body mass, either does not correlate with bite force (Sustaita and Hertel 2010) or leaves a sizeable portion of bite force variation unexplained (Herrel et al. 2005a; van der Meij and Bout 2008), indicating a major role for variation in jaw musculature. Because most of the cranial linkage bones also function as attachment sites for the jaw musculature, it is likely that the evolution of waterfowl linkage shape is also a consequence of changes in muscle architecture. For example, while the first major axis of variation in linkage shape does not correlate with either measure of linkage *MA*, it does

correlates with increases in both the relative width and height of the skull (Table 5.2). Interestingly, relative skull width and height are strongly and positively correlated with bite force in Darwin's finches (Herrel et al. 2005b), likely as a correlate of increase jaw muscle mass. However, waterfowl do not appear to be strongly differentiated in linkage shape along pPC1 (Fig. 5.6a) so it is unclear how changes in linkage shape along this axis relate to jaw function. A more detailed understanding of how muscle architecture differs among waterfowl with differing feeding ecologies would inform our understanding of how muscle architecture evolution may influence the evolution of linkage shape and vice versa.

The patterns of morphological and functional covariation within the waterfowl skull demonstrated by this study have several broader implications for our understanding of the ecological diversification of birds. Although prior studies have largely studied beak shape evolution in isolation from the cranial linkage, if the strong morphological integration between the beak and linkage shown here for waterfowl holds across other bird orders, the inclusion of linkage shape would likely not yield a fundamentally different pattern of jaw morphological evolution. However, in spite of strong morphological evolution, the linkage and beak can exhibit different patterns of functional evolution, as evidenced by decreasing beak MA_{BT} but increasing linkage MA_{PB} in the transition to pursuit diving in waterfowl (Fig. 5.7). Thus, a consideration of the avian cranial linkage diversity may provide additional insights into functional diversification of the beak not apparent from a consideration of beak shape alone. Additionally, previous studies have shown that greater morphological integration is predicted to increase the range of morphological diversity and drive evolution along paths determined by trait covariances rather than along paths determined by selection, thereby decreasing evolutionary flexibility (Goswami et al. 2014). In the context of beak evolution, particular beak shapes may be less likely to evolve

within clades having a particular range of linkage shapes because this would break the pattern of covariance. Thus, a consideration of avian cranial linkage diversity may additionally help to illuminate why different clades of birds exhibit radically different ranges and trajectories of beak diversification.

CHAPTER SIX: BROADER THEMES AND FUTURE DIRECTIONS

A central objective of this dissertation has been to integrate dietary, morphological, and functional data within a comparative framework to test hypotheses on the evolution of functional systems. The preceding chapters have focused on the testing of particular functional hypotheses or the application of particular computational approaches. In this final chapter, I will highlight three broader themes that recur throughout this work with the intention of unifying the diverse approaches and ideas herein and justifying the value of collections-based research. I will first discuss the insights this dissertation has provided into some general principles that have been proposed to shape the evolutionary trajectories of functional systems. Second, I will discuss how the computational approaches developed here advance an improved workflow for collection-based biomechanical simulation. Third, I will discuss the implications of these results for the origins of geese and the evolution of feeding ecology in waterfowl more broadly.

Evolutionary trajectories of functional systems

A common theme throughout this dissertation are general principles or mechanisms that may influence the evolution of functional systems. One commonly hypothesized mechanism that appears in both chapters two and five is functional evolution through the evolution of body size. Size is an all-encompassing measure of organismal morphology that is often strongly associated with organismal performance (e.g. basal metabolic rate, bite force) and is frequently the first major axis of interspecific morphological variation. Partly for this reason, the evolution of body size is commonly hypothesized to be a major pathway in the evolution of functional systems (e.g. Bright et al. 2016). For the evolution of waterfowl feeding, however, the body size

hypothesis does not appear to have particularly high explanatory power. Chapter two showed that shifts toward increased herbivory in waterfowl are not associated with increased body mass, as predicted by the hypothesis that body mass affects digestive efficiency. And chapter five showed that differences in cranial size do not explain much, if any, of the variation in beak shape. Rather, much of the variation in waterfowl beak shape can be explained by differences in diet (chapter four). This contrasts with a recent finding that beak shape variation in raptors is strongly related to variation body size and not variation in diet (Bright et al. 2016).

It seems, however, premature to rule out a relationship between ecology and body mass in waterfowl given the profound influence of body mass on organismal physiology. A study of the waterbird clade (a non-monophyletic clade including pelicans, cormorants, herons, penguins, etc. but not waterfowl) found a relationship, though somewhat indirect, between body mass and foraging ecology (Smith 2012). In particular, diving birds with higher body mass also have more bone pneumatization (invagination of bone by air sacs that lightens the skeleton) and birds with more pneumatization are less likely to engage in pursuit diving behavior. When a similar investigation was made for waterfowl, the results were less conclusive; diving waterfowl exhibit lower skeletal pneumatization than their nondiving relatives however body mass was not found to correlate significantly with pneumatization (O'Connor 2004). Thus, diving or buoyancy considerations do not appear to be good candidates to explain patterns of body mass evolution for waterfowl. Chapter two investigated only the relationship between body mass and the extent of herbivory. A multivariate approach combining body mass and several dietary characters may identify a relationship not apparent in comparison with a single dietary measure.

In chapter four I proposed that performance trade-offs may influence the trajectory of functional evolution by driving major axes of morphological variation and divergence at short

timescales and leading to convergence at longer timescales. In the context of principal components analysis, the most common method for determining major axes of variation, such axes represent combinations of linearly correlated changes in multiple traits (or dimensions), sorted by the percent of variance explained and mutually uncorrelated. In the context of morphological integration and macroevolution, the principal components of variation have been referred to as "path[s] of least resistance" in response to evolution by selection (Goswami et al. 2014). When just a few axes explain most of the variation in a large, multidimensional set of traits it is reasonable to presume that some larger mechanism or process is acting to influence multiple traits simultaneously.

Some of the proposed mechanisms include genetic covariances (Futuyma, Keese & Scheffer 1993; Schluter 1996; Walker & Bell 2000; McKinnon & Rundle 2002), developmental constraints (Kaplan & Phillips 2006), or pleiotropy (Cheverud 1996). It seems that morphological integration itself does not explain such patterns but rather provides a framework in which to describe and quantify them. A difficulty in determining process is discerning which, among many potential processes, have acted to produce an ultimate pattern, including the possibility of multiple processes acting simultaneously. For example, although I have proposed in chapter four that performance trade-offs are sufficient to explain particular patterns of morphological covariance and trajectories of functional evolution, I cannot argue that they necessarily act in isolation of other mechanisms.

Given the frequent use of major axes of variation in the interpretation of morphological and functional diversity the unresolved question of what drives these axes seems fundamental. Future research to address this question will likely require a combination of approaches. First, a theoretical treatment of this question is needed to examine how multiple traits associated with a

performance trade-off would be expected to covary through evolution and how trade-offs might then influence the resulting major axes of variation. Second, more examples are needed of performance trade-offs at the organismal level and the particular morphological traits underlying the trade-off. Such examples can then be used to examine patterns of morphological variation across a clade and compare empirical major axes of variation with those expected based on a morphology-performance relationship. Lastly, it may be possible to use some expectation of the total "evolvable" forms in each case to eliminate the possibility that major axes of variation are simply the result of genetic or developmental constraints.

In chapters three and five I explore the use of mechanical advantage (MA), and its inverse, kinematic transmission (KT), in understanding patterns of morphological and functional diversification. MA has great appeal as a functional metric given that it is both easy to calculate from morphology and has biomechanical consequences for organismal performance. However, the interpretation of how differences in MA ultimately relate to differences in organismal performance presents a couple of challenges. First, MA reflects only the relative amplification of force or velocity through a system, not the absolute force or velocity (Arnold et al. 2011; McHenry and Summers 2011), and it is arguably absolute force or velocity that matters most for organismal performance. It has been shown that amplification of relative force or velocity may not necessarily translate into amplification of absolute relative force or velocity, respectively. For example, a lever with a low MA achieves a higher absolute output velocity when energy is lost primarily in the input (e.g. muscle input; McHenry 2012). However, when energy is lost primarily in the output (e.g. drag through a viscous medium) a lower MA results in lower absolute output velocity (McHenry et al. 2012). If selection were acting to increase absolute output velocity, selection would be expected to favor a lower MA in the former scenario and a

higher MA in the latter. By no means does this render MA uninformative as a functional metric (e.g. Anderson et al. 2014). But it does encourage caution in the interpretation of how the evolution of MA ultimately relates to the evolution organismal performance and behavior.

The second challenge to interpreting MA stems from the fact that MA may be confounded with differences in shape that have some functional basis other than relative force-velocity transmission. For example, the upper and lower beaks of pursuit diving, piscivorous birds (including waterfowl pursuit divers discussed in chapter five) are relatively shorter in height, narrower and more elongate. These shape differences translate into lower minimum MA values (given an output force at the tip of the beak) relative to other birds. One interpretation of these shape differences is that a lower MA increases the relative speed of the beak tip during jaw closing; that is, given the same input rotation to the beak, the beak tip will move over a greater distance (and thus relatively faster), potentially increasing the chance of a bird catching a prey item. However, an alternative interpretation is that a relatively longer beak simply increases the reach of the bird, enabling it to catch prey within a larger volume of water by simply rotating its head. The consequences of a longer beak underwater for absolute jaw closing velocity are unclear. If increasing the length of the jaw increases the area exposed to flow during closing then a longer jaw would be predicted to decrease absolute closing velocity by increasing drag on the jaw. Considering this, one could even argue that more elongate beaks evolve in pursuit divers to extend reach at the expense of reduced absolute closing velocity. Such an example serves to illustrate the potential challenge of drawing clear conclusions about the evolution of organismal function and performance from MA.

Computational frameworks for comparative functional morphology

This dissertation has sought to provide not only insights into broader scientific questions but also solutions to broader methodological challenges in the pursuit of those questions. The main methodological challenge encountered in this work was the lack of a free, open-source, and integrated workflow for three-dimensional biomechanical simulation using natural history specimens. In particular what was needed was: a free application enabling easy landmark and curve data collection from photographs, an algorithm for calibration of stereo cameras using checkerboard detection and the direct linear transformation (DLT) camera model, a free software platform for three-dimensional kinematic simulation, and a free three-dimensional interactive animation viewer for model visualization.

This dissertation contributes new, open-source solutions to each of these challenges as software packages in the R language (StereoMorph, linkR, and svgViewR; Appendices 1-3). Just as the process of science often evolves experimentation with novel uses of existing tools or methods, these packages experiment with what is possible on the R computing platform, particularly in the integration of R and the web browser. The digitizing application in StereoMorph goes further than any other current R package, except perhaps shiny (Chang et al. 2016), in integrating browser interactivity with the traditional R framework. And the svgViewR package is the only R package with the capacity to write standalone browser files (i.e. HTML) for the purposes of interactive, three-dimensional visualization. And the linkR package is the first R package created specifically for biomechanical simulation. Together, these three packages form a seamless and integrated workflow from data collection (StereoMorph) to biomechanical simulation and analysis (linkR), with the potential to interactively visualize both the morphometric data and simulation results (svgViewR).

Additionally, just as scientific discoveries can sometimes have unanticipated implications, the development of these R packages has already led to several unforeseen applications to other problems. Although there are a number of existing programs for manual digitization of video frames for kinematic analysis these programs are typically landmark-based: they enable manual or automated digitization of specific markers in order to extract general patterns of motion or rigid body motion. They have not focused on shape analysis at the level of the video frame. StereoMorph does not provide the automated tracking or processing speed to make it a high-throughput system for landmark-based kinematics. However, StereoMorph does provide an interface specifically designed for the digitization of shape, particularly the ability to quickly fit Bézier curves. This has enabled an exciting collaboration among my advisor, Mark Westneat, Brett Aiello (University of Chicago), and Melina Hale (University of Chicago) to quantify shape change in the pectoral fins of fishes during steady swimming. This is just the beginning of a promising future research program integrating shape analysis and kinematic analysis to better understand how morphology, material properties, and physics interrelate in organismal motion and performance.

A second unexpected application of the StereoMorph package has been its application to morphometric measurements of animals behaving in the wild. In the past year and a half I have begun an exciting collaboration with marine ecologist Caine Delacy to develop StereoMorph as an application for calibrating paired Go-Pros and taking three-dimensional measurements of swimming fish in the wild. Although there is commercial software for this application it has proven price prohibitive for some research groups and is limited in its capabilities. StereoMorph provides not only a free alternative but also an expanded set of tools such as enabling the collection of three-dimensional landmark data, rather than the customary practice of simple

lengths, when possible. StereoMorph has already been employed in the field (by C. Delacy) to take measurements of swimming ocean whitetip sharks in the Caribbean. Future improvements to StereoMorph for characterizing shape during animal motion has the potential to simultaneously benefit diverse fields and help bridge the gap between conservation studies and studies of organismal biomechanics.

An unforeseen application of the linkR package has been a fantastic collaboration with Beth Brainerd (Brown University) and Ariel Camp (England, at the moment) using linkage models to describe the *in vivo* kinematics of the operculum linkage (collected by A. Camp) in largemouth bass (*Micropterus salmoides*). The optimization routines in R have made it possible to fit parameters for two- and three-dimensional linkage models to the *in vivo* kinematics and in that way quantify the relative fit of different linkage models. One key advantage to using linkR, as opposed to multibody or linkage simulation programs, has been the flexibility of the linkR method in defining the linkage parameters. With linkR it has been possible to define input parameters using either the *in vivo* parameters directly or parameters to be optimized; for instance, defining a four-bar linkage but allowing a link's length to vary just as *in vivo*. This has then made it possible to evaluate how different simplifying assumptions (e.g. constant joint axes of rotation, constant link lengths) affect the overall accuracy of the linkage; his "breaks the mold" of the typical analyses performed using conventional linkage simulation programs. There is enormous potential in further extending linkR to build a more general and comprehensive application for fitting linkage models of diverse configurations to kinematic data, testing hypotheses on the motion constraints of functional systems, and identifying simplified parameterizations of complex movements.

The origins of geese and the evolution of feeding ecology in waterfowl

A third broader theme that extends throughout this work reflects back on an initial motivation of this work, that of reconstructing evolutionary transitions in the feeding ecology of waterfowl. Charles Darwin was perhaps the first to publish speculation on evolutionary transitions in waterfowl feeding (Darwin 1872). This speculation appears not in the first edition of The Origin of Species but in the sixth edition, in response to one of George Mivart's criticisms of natural selection. Mivart questioned how natural selection could produce extreme forms through gradual steps if each intermediate form had to be functional, noting as an example the transition from teeth to baleen in whales. In response, Darwin put forward the example of lamellae in waterfowl, speculating that the finer and more numerous lamellae of filter-feeding ducks had evolved from the coarser and less numerous lamellae of geese. The example is less extreme than the transformation of teeth to baleen, but the implication is that less extreme transformations over short timescales that could ultimately result in extreme transformations at longer timescales. Admittedly Darwin was simply using waterfowl as a demonstrative example, not presenting a thorough consideration of the polarity of transitions in waterfowl feeding. However, his speculation introduces the question of whether a filter-feeding duck-like form is derived from a grazing, more goose-like ancestor (goose-to-duck) or vice versa (duck-to-goose).

Even the earliest hypotheses on the phylogenetics within waterfowl, based solely on general and qualitative attributes of different species of waterfowl, recognized that neither geese nor ducks (as commonly defined) formed monophyletic groups (Delacour and Mayr 1945). Thus the group appeared to be characterized by repeated transitions along a continuum of primarily aquatic versus primarily terrestrial feeding modes. Some had proposed that waterfowl as a whole were nested within aquatic shorebirds (Delacour and Mayr 1945; Sibley et al. 1969), particularly

with the discovery of *Presbyornis* (Olson and Feduccia 1980), which possessed an undeniably duck-like skull but a wader-like postcranial skeleton. This would allow, among other parsimony considerations, a single origin for filter-feeding in birds and would favor a duck-to-goose transition. However, there had always been a strong case, based on morphology, for a sister relationship between waterfowl (Anseriformes) and the order Galliformes and this was later confirmed by studies based on molecular data (Sibley et al. 1988; Hackett et al. 2008). This implied that waterfowl had evolved from a fully terrestrial ancestor and renewed the prospect of a goose-to-duck transition.

It is over simplistic to assume the evolution of feeding ecology in waterfowl only followed a unidirectional transition along a single continuum. However, available evidence does support the hypothesis that a primarily filter-feeding, duck-like form represents the most likely ancestral form for the group while a more goose-like form or terrestrial grazing behavior represent convergent and derived states for the clade, thus resulting in a predominately duck-to-goose transition overall. Chapters two and four present evidence for a duck-to-goose transition using ancestral character estimations of diet and beak shape characters, respectively, across the waterfowl tree. The broad phylogenetic distribution among waterfowl of a less herbivorous diet and a more "duck-like" beak favors a more duck-like ancestral condition.

Moreover, these ancestral character estimates are consistent with at least three additional lines of evidence in support of the duck-to-goose hypothesis. The first is the presumed feeding ecology of the Eocene anseriform fossil *Presbyornis* (greater than 50 mya; Olson and Feduccia 1980). *Presbyornis* has been classified as the sister to Anatidae (Livezey 1997; Clarke et al. 2005) and chapter four showed that *Presbyornis* has a three-dimensional beak shape closely resembling that of extant filter-feeding ducks. Currently we have no way of knowing whether

Presbyornis possessed lamellae. However, the remarkable similarity in beak shape indicates filter-feeding as the most likely primary feeding behavior of both *Presbyornis* and, by current classification, the ancestor of the Anatidae family.

The second line of evidence in support of the duck-to-goose hypothesis is the near ubiquity of lamellae across waterfowl, the widespread capacity for filter-feeding among extant waterfowl, and the definitively duck-like beak shape of the Eocene anseriform fossil *Presbyornis*. Lamellae, keratinous comb-like ridges that line the upper and lower beak, are found in nearly all waterfowl. The only waterfowl lacking lamellae are the mergansers (*Mergus* and *Lophodytes*), which instead have keratinous, tooth-like serrations, and the screamers (*Anhima* and *Chauna*), which may in fact possess vestigial lamellae (Olson and Feduccia 1980). Lamellae are likely to have evolved for filter-feeding: the only other avian lineages possessing comparable structures, flamingos and prions, also filter-feed (Klages and Cooper 1992; Zweers et al. 1995).

Consistent with this widespread presence of lamellae, most waterfowl appear to be capable of filter-feeding. Using an online repository of bird behavior videos (ibc.lynxeds.com), with videos representing over 95% of waterfowl species, I have begun a preliminary survey of which waterfowl species exhibit dabbling behavior, the rapid and repetitive opening and closing of the beak in water that is characteristic of filter-feeding. I have found that dabbling behavior is widespread; even waterfowl that feed underwater have been observed using dabbling behavior to stir up and sieve suspended food particles from bottom sediments (Suter 1982; Tome and Wrubleski 1988). The widespread presence of lamellae and dabbling among waterfowl support filter-feeding as ancestral for the family Anatidae, which includes all waterfowl with the exception of Screamers.

The hypothesis of filter-feeding as ancestral for waterfowl implies not only grazing as a derived feeding behavior for waterfowl but also underwater browsing (i.e. the consumption of large underwater invertebrates such as urchins and mollusks) and pursuit diving (i.e. piscivory). Chapter five showed that each of these dietary and behavioral transitions was accompanied by a shift in beak shape, however the full scope of associated transformations to the feeding apparatus has yet to be fully explored. A recent investigation using contrast-enhanced computed tomography (CT) has revealed differences in the hyolingual morphology among three species representing grazing and dabbling waterfowl (Li and Clarke 2015). Yet it remains unknown how the jaw musculature differs among waterfowl with different feeding behaviors. Waterfowl present a particularly interesting group in which to investigate these differences because the biomechanical demands on the jaw apparatus vary dramatically among feeding behaviors. Dabbling involves rapid opening and closing of the beak in water (in some cases fully submerged), grazing involves repetitive opening and closing and biting or cropping at the beak tip, underwater browsing may emphasize underwater biting and grasping over filter-feeding, and pursuit diving requires the beak to open and close rapidly (but not repetitively) and exert a strong grasping force. A more through investigation of the anatomical specializations associated with each behavior will shed important insight on how musculoskeletal systems adapt to different biomechanical demands.

This dissertation has demonstrated the vital role of natural history collections in scientific inquiry. The questions inspired by the organisms represented in these collections have the potential to inform broader biological principles such as the evolutionary processes underlying functional evolution. The challenges faced in finding more efficient and accurate methods for extracting data from physical specimens lead to new solutions that have unforeseen applications

to other scientific fields and questions. Lastly, any insights gained in the study of these collections reflects back on the study system or clade of interest to paint a more comprehensive picture of the origins and transformations that have given rise to the diversity of life.

APPENDIX: STEREOMORPH: AN R PACKAGE FOR THE COLLECTION OF 3D LANDMARKS AND CURVES USING A STEREO CAMERA SETUP[1]

Abstract

Quantitative, three-dimensional measurements of anatomy in biology and paleontology are key to understanding the evolutionary processes underlying morphological, functional and ecological diversification. However, the collection of 3D morphometric data from a large number of samples or in the field is currently limited by methods that are either too costly, too time-consuming or lack portability. We present a new R package, StereoMorph, for the rapid and accurate collection of 3D landmarks and curves using two standard digital cameras. StereoMorph provides a complete set of tools for every step in the collection of 3D landmarks and curves using a stereo camera setup. This includes image processing and optimization functions for automated camera calibration using a checkerboard pattern, an easy-to-use application for digitizing landmarks and curves from photographs, and tools for reconstructing points and curves in 3D. The image processing tools and digitizing application are readily applicable to 2D morphometrics as well, enabling 2D landmarks and curves to be digitized and scaled automatically using a checkerboard pattern. We include five examples that demonstrate key functionalities of StereoMorph: automated detection of checkerboard corners, camera calibration, testing calibration accuracy, digitizing photographs and 3D curve reconstruction. With a setup costing less than $1500, we show that it is possible to achieve a mean reconstruction error of less than 30 microns. Once the cameras are assembled, specimens can be

[1]This chapter was originally published as: Olsen, A.M. and Westneat, M.W. 2015. StereoMorph: an R package for the collection of 3D landmarks and curves using a stereo camera setup. Methods in Ecology and Evolution 6:351–356.

photographed as quickly as with 2D morphometrics while digitizing takes two to three times as long as digitizing a single photograph. We conclude by presenting an accompanying tutorial which details all of the steps required to collect 3D landmarks and curves using StereoMorph. Additionally, we present a web blog that will provide a platform for updates and user questions and suggestions.

Introduction

Extensive morphometric surveys of diverse clades have the power to reveal large-scale patterns of morphological and ecological diversification (Clabaut et al. 2007; Angielczyk, Feldman & Miller 2011), informing questions ranging from how modularity shapes diversification (Drake & Klingenberg 2010) to how morphology relates to ecological function (Westneat et al. 2005). This is most often done by collection of 2D landmarks from single photographs. While this is sufficient in certain cases, many biological structures are inherently three-dimensional and lack clearly definable homologous landmarks, requiring the use of 3D landmarks and semilandmarks.

Several methods are available for characterizing 3D morphology (e.g. microscribe, CT, laser and optical scanning), but each poses a challenge to collecting data either from a large number of samples or in the field, principally in terms of cost, time and portability. Open-source methods have been developed for creating high resolution, 3D surface models from multiple camera images (Falkingham 2012). However, these methods typically require at least 20 images and several hours of computer processing time per specimen, making them less ideal for the collection of a small number of landmarks from hundreds of specimens.

An approach better suited to the collection of a few landmarks from many specimens is a simple, stereo camera setup. With this approach, two standard digital cameras are arranged in fixed positions such that their views overlap in a particular volume of space (Figure S.1).

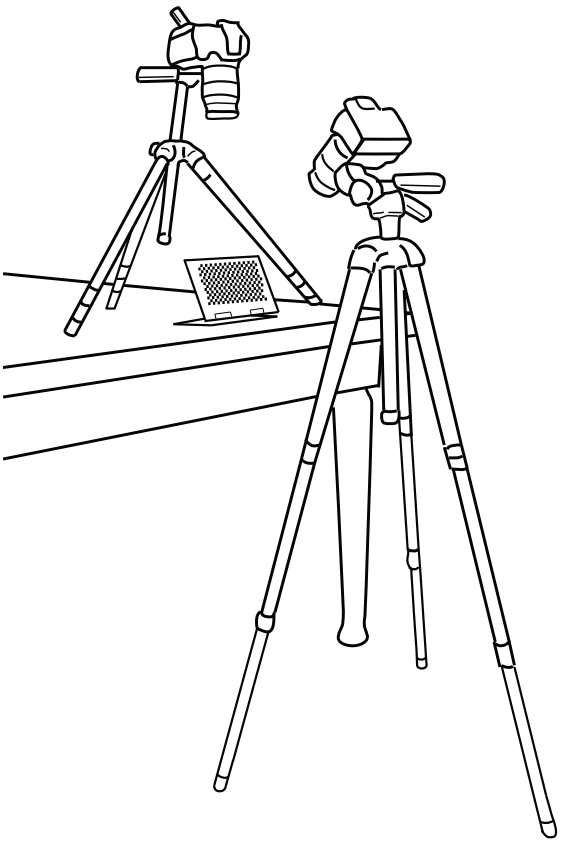

Figure S.1. The two-camera stereo setup used in the examples featured here, with a checkerboard positioned within the calibration volume.

Once the cameras are calibrated, any point visible in both camera views (such as landmarks on a specimen) can be reconstructed into 3D using the pixel coordinates of the point in both views and a set of calibration coefficients. In studies of 3D animal movements, where stereo camera camera reconstruction is used extensively (e.g. Hedrick 2008; Brainerd et al. 2010), these coefficients are often obtained using direct linear transformation (DLT). DLT uses reference points on a 3D calibration object digitized in both views to produce 11 calibration coefficients per camera view (Abdel-Aziz & Karara 1971).

Stereo camera reconstruction has several advantages over other existing morphometric methods. The cost of two digital cameras and tripods (less than $1500) is still less than half the cost of the cheapest scanning systems on the market that provide comparable accuracy. Moreover, those in the field of morphometrics likely already have access to at least one camera. Image acquisition is as simple as photographing the specimen. This allows a greater number of specimens to be imaged when specimen access is limited (e.g. museum visits) and enables imaging of live, mobile specimens. Lastly, compared to scanning devices, cameras are especially advantageous in the field being portable and capable of running on battery power and in low lighting.

Despite these advantages, several obstacles have prevented the widespread use of stereo camera reconstruction in 3D morphometrics. Stereo cameras are commonly calibrated using a precision-made, 3D calibration object that must be manually digitized (e.g. Chong & Stratford 2002). Testing the calibration accuracy is an equally laborious process, requiring a second, precision-made object, which must also be manually digitized (Chen, Armstrong & Raftopoulos 1994). While computational solutions to these obstacles exist in the field of computer vision (Bradski 2000), they have not been implemented as a self-contained package accessible to the average user.

In this paper, we describe StereoMorph, a new package written in the R language (R Core Team 2014) with tools for every step in the collection of 3D landmarks and curves using a stereo camera setup. We first present the major functions in StereoMorph. We then demonstrate the key functionalities of StereoMorph through five examples: automated detection of checkerboard corners, camera calibration, calibration accuracy assessment, use of the StereoMorph digitizing

Table S.1. Major functions of the StereoMorph package

Function name	Description
Checkerboard image processing	
drawCheckerboard	Creates a checkerboard pattern of a specified pixel size
findCheckerboardCorners	Automatically finds the internal corners of a checkerboard pattern in a photograph to subpixel precision
measureCheckerboardSize	Estimates square size of a checkerboard pattern to find square size in real-world units or automatically scale photographs for 2D morphometrics
resampleGridImagePoints	Fits a 12-parameter camera perspective model to imaged checkerboard corners and returns greater or fewer grid points
DLT calibration (Abdel-Aziz & Karara 1971; Abdel-Aziz 1974; Hedrick 2008)	
dltCalibrateCameras	Finds the optimized DLT coefficients for a stereo camera setup
dltTestCalibration	Tests the accuracy of a stereo camera calibration
Digitizing	
digitizeImage	Launches the StereoMorph Digitizing Application in the user's default web browser, enabling digitization of landmarks and curves
Reconstructing landmarks and curves in 3D	
dltReconstruct	Reconstructs the 3D position of 2D pixel coordinates in two or more camera views
dltMatchCurvePoints	Estimates corresponding curve points between two camera views using epipolar geometry (Yekutieli et al. 2007)
pointsAtEvenSpacing	Generates evenly spaced points from a point matrix (2D and 3D)
Landmark and curve operations	
unifyLandmarks	Returns the optimal alignment sequence of two or more point sets with overlapping points and a matrix of the aligned points (Rohlf 1990)
reflectMissingLandmarks	Reflects bilateral landmarks missing on one side across the plane of symmetry (Klingenberg, Barluenga & Meyer 2002)
alignLandmarksToMidline	Aligns a set of bilateral landmarks to the midline plane

application and curve reconstruction. We conclude by highlighting several resources for readers interested in using StereoMorph.

Description

All functions presented in this note are available in the R package StereoMorph (see Resources). StereoMorph imports or suggests several R packages, including shiny (RStudio and Inc. 2014), Rcpp (Eddelbuettel & Francois 2011), bezier (Olsen 2014), rjson (Couture-Beil 2014), jpeg (Urbanek 2014) and rgl (Adler & Murdoch 2014).

Examples

StereoMorph is a self-contained package, equipped with functions for image processing, DLT calibration, image digitization, and landmark and curve reconstruction (Table S.1). We present five examples that demonstrate key functionalities of StereoMorph. Readers can easily reproduce these examples by installing StereoMorph and downloading the 'Tutorial Files' zip folder from the StereoMorph github repository (see Resources). Lines preceded by '>' indicate R commands. To run the examples, load the StereoMorph package and change the current working directory in R to the unzipped 'Tutorial Files' folder.

```
> library(StereoMorph)
> setwd('[Add path here]/Tutorial Files')
```

Example 1: Finding checkerboard corners

A key function of StereoMorph is `findCheckerboardCorners`, which automatically detects the internal corners of a checkerboard pattern in a photograph to subpixel resolution (Bradski 2000). This function is used to calibrate stereo cameras, test the calibration accuracy and can also be used to automatically scale landmarks and curves for 2D morphometrics.

Begin by specifying an image with a checkerboard pattern; the first calibration image in the Tutorial Files folder will be used to demonstrate.

```
> image.file <- 'Calibration images/v1/DSC_0002.JPG'
```

Additional file paths can be specified such as where to save the corners or where to save a "verification image", in which the identified corners are drawn over the original image (Figure S.2).

```
> corner.file <- 'Calibration corners/v1/DSC_0002.txt'
> verify.file <- 'Calibration images verify/v1/DSC_0002.JPG'
```

Call `findCheckerboardCorners`, specifying the number of internal corners (intersections of black squares) along each dimension as `nx` and `ny`.

```
> corners <- findCheckerboardCorners(image.file, nx=21, ny=14,
  corner.file, verify.file)
```

The function takes 10-20 seconds per photograph on a Mac 2.9 GHz Intel Core i7 with 8 GB RAM, returning the corners and, if specified, saving a verification image to `verify.file` (Figure S.2).

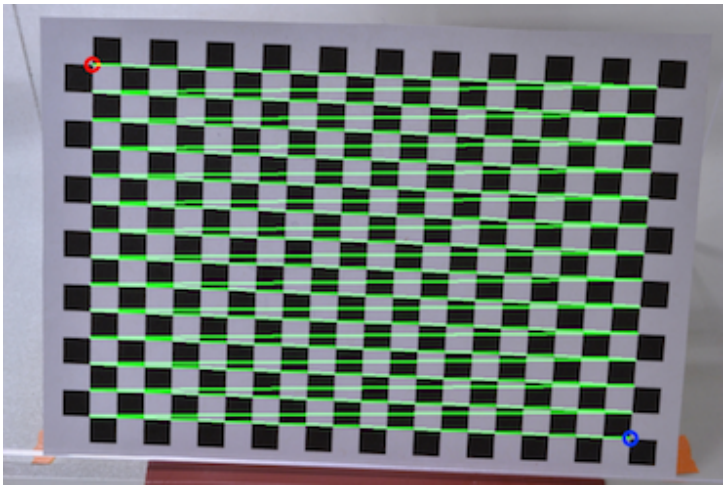

Figure S.2. A verification image created by `findCheckerboardCorners` showing the automatically detected, internal corners drawn over the original image. The first corner is indicated by a red circle, the last by a blue circle and all intervening points are joined by a green line.

Example 2: Calibrating stereo cameras

StereoMorph integrates the automated checkerboard detection with `nlminb` optimization from the R base package 'stats' (R Core Team 2014) to perform DLT camera calibration without the need to construct a 3D calibration object or manually digitize points. A checkerboard need only be photographed in four to eight different positions and orientations within the stereo camera volume (Figure S.1). The internal corners are detected and input to `dltCalibrateCameras`, which searches for the 3D positions of each checkerboard (as a set of translation and rotation parameters) that minimize the calibration error.

Assuming that the corners of a checkerboard photographed in different positions have been saved to individual text files, specify the names of each text file in the form of a two-column matrix.

```
> file <- cbind( paste0('Calibration corners/v1/', paste0('DSC_000',
  2:5, '.txt')), paste0('Calibration corners/v2/', paste0('DSC_000',
  2:5, '.txt')))
```

Here, the first and second columns correspond to the first and second camera views, respectively, and the four rows correspond to a checkerboard in four different positions. The function `readCheckerboardsToArray` reads these corners into an array, where `nx` and `ny` are the number of internal corners in the checkerboard. For this arrangement of cameras, the first camera viewed the checkerboard upside-down relative to the second camera (Figure S.1); this is corrected by reversing the corner order for the second view with `col.reverse` and `row.reverse`.

```
> coor.2d <- readCheckerboardsToArray(file, nx=21, ny=14,
  col.reverse=c(F, T), row.reverse=c(F, T))
```

Perform the calibration by calling `dltCalibrateCameras`, adding the size of the checkerboard squares in real-world units (here, mm) as `grid.size`.

```
> dlt_cal <- dltCalibrateCameras(coor.2d, nx=21, grid.size=6.348,
  print.progress=T)
```

With eight images total, `dltCalibrateCameras` runs in 20 s on the same hardware described earlier and outputs 11 calibration coefficients per camera view. These coefficients are sufficient to reconstruct any point in the calibrated volume, given its 2D coordinates in both camera views. Since these coefficients are specific to the zoom, focus and position of the cameras, it is essential that the cameras do not move once they are calibrated. However, once calibrated, an unlimited number of specimens can be cycled through the calibration volume and photographed.

Example 3: Testing calibration accuracy

StereoMorph allows users to easily assess the accuracy of a calibration using a checkerboard, ideally of a different square size to test for proper scaling. As in the calibration step, this checkerboard is photographed in several different positions and the corners are automatically detected. Begin by loading a set of these corners from the tutorial files.

```
> file <- cbind(paste0('Test corners/v1/', paste0('DSC_00', 11:20,
  '.txt')), paste0('Test corners/v2/', paste0('DSC_00', 11:20, '.txt')))
> test_corners <- readCheckerboardsToArray(file, nx=21, ny=14,
  col.reverse=c(F, T), row.reverse=c(F, T))
```

Read in the calibration coefficients.

```
> cal.coeff <- as.matrix(read.table("cal_coeffs.txt"))
```

Call `dltTestCalibration`, including the square size of the second checkerboard pattern.

```
> dlt_test <- dltTestCalibration(cal.coeff=cal.coeff, coor.2d=
  test_corners, nx=21, grid.size=4.233)
```

Several different accuracy assessments can be viewed using the `summary` function. One useful assessment is the inter-point distance error (IPD error). This is the difference in distance between randomly selected, reconstructed pairs of points on the checkerboard and their true distance, determined by the grid dimensions. IPD error can be plotted as a histogram.

```
> hist(dlt_test$ipd.error, breaks=20)
```

For this calibration, the mean IPD error is less than 25 microns (Figure S.3).

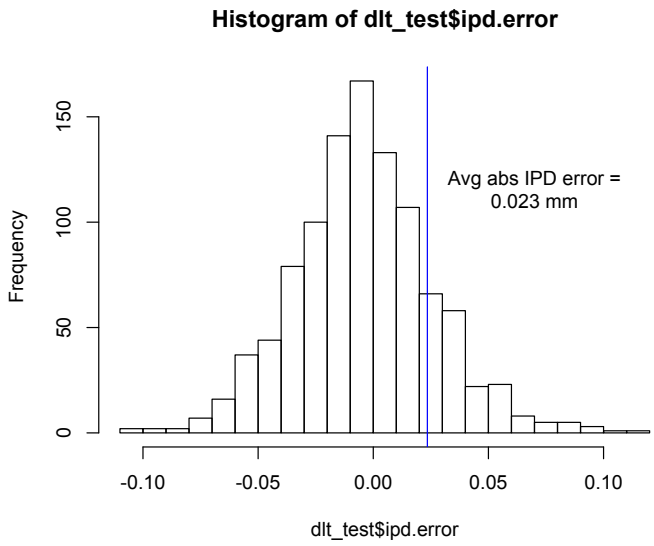

Figure S.3. A histogram of the inter-point distance error for reconstructed points on a checkerboard (N=1029), one of several measures for assessing calibration accuracy.

Example 4: Digitizing photographs

StereoMorph features an easy-to-use, browser-based digitizing application for the collection of landmarks and Bézier curves from photographs, applicable to both 2D and 3D morphometrics (Figure S.4). The app is launched from R by calling the function `digitizeImage` with several

possible input parameters, including: the image(s) to be digitized (`image.file`), where to save the landmarks and curves (`landmarks.file`, `curve.points.file`), and the names of the landmarks and curves to be digitized (`landmarks.ref`, `curves.ref`).

```
> digitizeImage(image.file = 'Object Images', landmarks.file =
  'Landmarks 2D', control.points.file = 'Control points 2D',
  curve.points.file = 'Curve points 2D', landmarks.ref =
  'landmarks_ref.txt', curves.ref = 'curves_ref.txt')
```

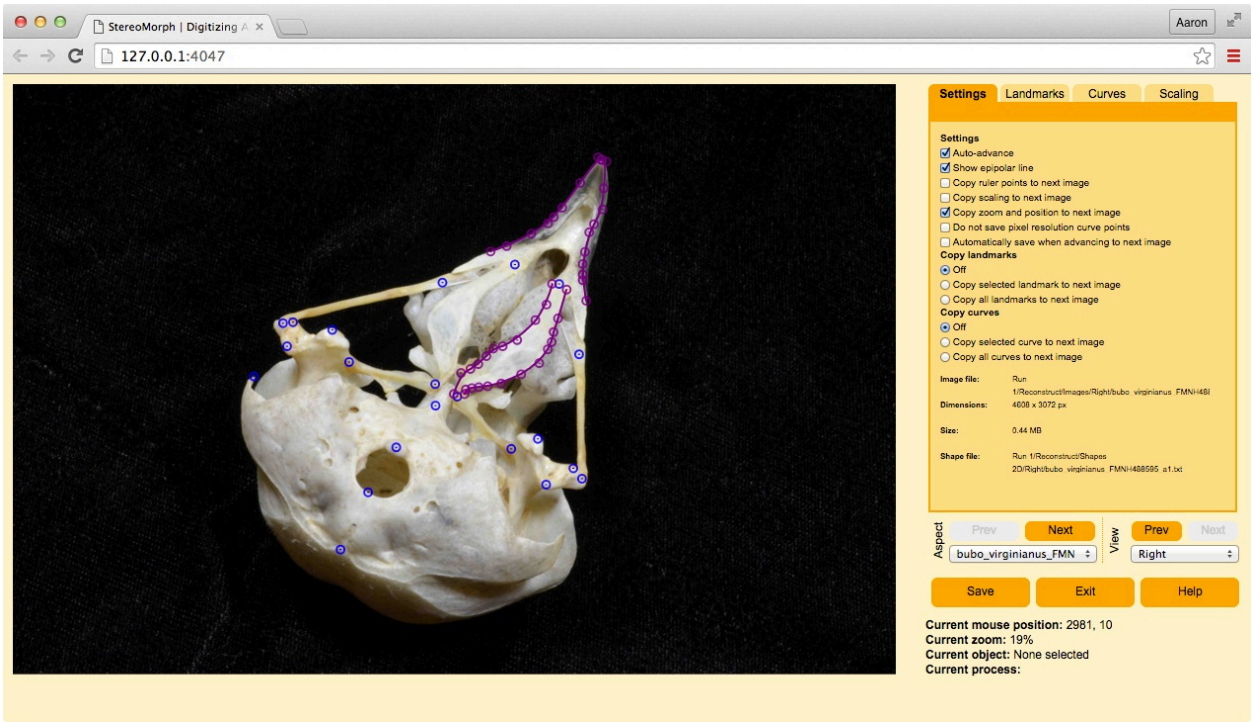

Figure S.4. The StereoMorph digitizing application, showing landmarks and curves digitized in one camera view of a Great Horned Owl skull.

The digitizing app opens in the user's default web browser (the user does not need to be connected to the internet to use the app). The user can perform most operations using a mouse or trackpad, such as navigating around the image, zooming in and out, and adding or moving landmarks or Bézier curve control points.

Example 5: Curve reconstruction

Once landmarks and curves have been digitized in both camera views, they can be reconstructed in 3D using the DLT calibration coefficients (surface reconstructions are not currently possible). For reconstruction, the digitized 2D points must correspond to the same point in 3D space. This poses a challenge for curve reconstruction since points at the same relative position along curves in two views will not necessarily represent the same 3D point. StereoMorph uses the DLT coefficients and epipolar geometry to identify corresponding points between the two views (Yekutieli et al. 2007) and then reconstructs these matching points. Begin by loading digitized 2D curve points from two views and the calibration coefficients.

```
> curve.points <- readLandmarksToList(paste0("Curve points 2D/obj_a1_v",
  1:2, ".txt"), row.names=1)
> cal.coeff <- as.matrix(read.table("cal_coeffs.txt"))
```

Call `dltMatchCurvePoints` to find the corresponding curve points between the two views.

```
> dlt_mcp <- dltMatchCurvePoints(curve.points, cal.coeff)
```

Now that corresponding curve points in each view have been identified, they can be reconstructed.

```
> dlt_recon <- dltReconstruct(cal.coeff, dlt_mcp$match.lm.list)
> lm.list <- landmarkMatrixToList(dlt_recon$coor.3d)
```

Since there are several hundred curve points, call `pointsAtEvenSpacing` to reduce the number of points for each curve.

```
> lm.list$pterygoid_crest_R <-
  pointsAtEvenSpacing(lm.list$pterygoid_crest_R, n=10)
> lm.list$tomium_R <- pointsAtEvenSpacing(lm.list$tomium_R, n=50)
```

This reconstruction process is repeated for landmarks and curves from three different aspects of the same specimen, producing point sets with overlapping points but in different orientations. Read these three point sets into an array and unify them into a single point set using `unifyLandmarks`.

```
> lm.array <- readLandmarksToArray(paste0("Landmarks and curves
3D/obj_a", 1:3, ".txt"), row.names=1)
> unify_lm <- unifyLandmarks(lm.array, min.common=5)
```

For specimens with bilateral symmetry, landmarks missing from one side can be reflected across the midline.

```
> reflect <- reflectMissingLandmarks(unify_lm$lm.matrix)$lm.matrix
```

Lastly, use the `plot3d` function from the rgl package to visualize the 3D landmarks and curve points (Figure S.5).

```
> library(rgl)
> is_curve <- grepl('[0-9]+$', rownames(reflect))
> r <- apply(reflect, 2, 'max') - apply(reflect, 2, 'min')
> plot3d(reflect[!is_curve, ], aspect=c(r/r[3]), size=3)
> plot3d(reflect[is_curve, ], col='red', size=3, add=TRUE)
```

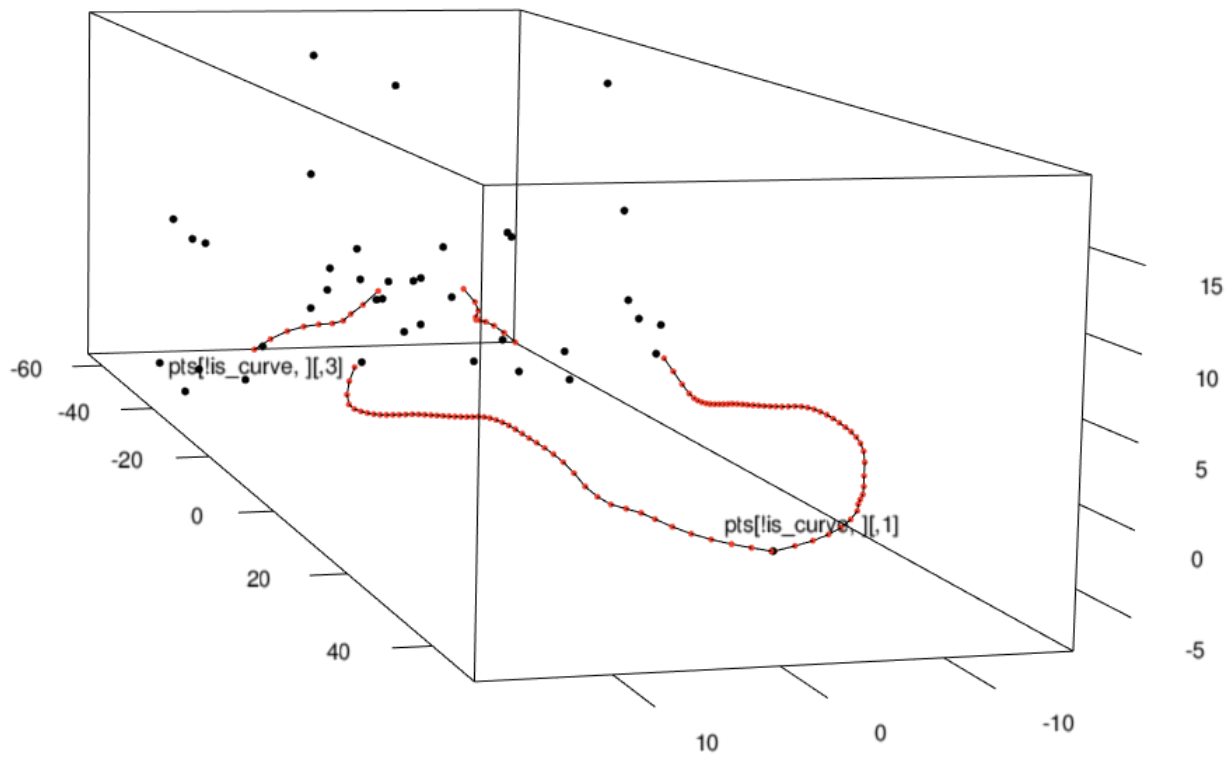

Figure S.5. Landmarks (black) and curve points (red) after unification of three different aspects and reflection of missing bilateral landmarks.

Resources

StereoMorph is freely available for download at http://cran.r-project.org/. This article is accompanied by a PDF tutorial detailing all of the steps required to collect 2D and 3D landmarks and curves using StereoMorph. Due to advances in computer vision and imaging technologies we anticipate continual updates to the package and welcome user suggestions and contributions. The site stereomorph.blogspot.com will provide a platform to introduce updates and a space for users to ask questions and contribute comments and suggestions. Detailed descriptions and examples for specific functions can be found in the StereoMorph reference manual at http://cran.r-project.org/web/packages/StereoMorph.

LITERATURE CITED

Abdel-Aziz, Y. I. 1974. Photogrammetric potential of non metric cameras.

Abdel-Aziz, Y. I., and H. M. Karara. 1971. Direct linear transformation into object space coordinates in close-range photogrammetry. In *ASP Symposium on Close Range Photogrammetry*:1-18. American Society of Photogrammetry, Falls, Church.

Abzhanov, A., M. Protas, B. R. Grant, P. R. Grant, and C. J. Tabin. 2004. *Bmp4* and morphological variation of beaks in Darwin's finches. Science (Wash. D. C.). 305:1462-1465.

Abzhanov, A., W. P. Kuo, C. Hartmann, B. R. Grant, P. R. Grant, and C. J. Tabin. 2006. The calmodulin pathway and evolution of elongated beak morphology in Darwin's finches. Nature (Lond.). 442:563-567.

Adams, D. C. 2014. A generalized K statistic for estimating phylogenetic signal from shape and other high-dimensional multivariate data. Syst. Biol. 63:685-697.

Adams, D. C. 2016. Evaluating modularity in morphometric data: challenges with the RV coefficient and a new test measure. Methods Ecol. Evol.

Adams, D. C., and E. Otárola-Castillo. 2013. geomorph: an R package for the collection and analysis of geometric morphometric shape data. Methods Ecol. Evol. 4:393-399.

Adams, D. C., and R. N. Felice. 2014. Assessing trait covariation and morphological integration on phylogenies using evolutionary covariance matrices. PLoS One. 9:e94335.

Adler, D., and D. Murdoch. 2014. rgl: 3D visualization device system (OpenGL). URL http://CRAN.R-project.org/package=rgl.

Aerts, P. 1991. Hyoid morphology and movements relative to abducting forces during feeding in *Astatotilapia elegans* (Teleostei: Cichlidae). J. Morphol. 208:323-345.

Agüero, M. L., P. G. Borboroglu, and D. Esler. 2014. Trophic Ecology of Breeding White-Headed Steamer-Duck (*Tachyeres leucocephalus*). Waterbirds. 37:88-93.

Albertson, R. C., J. T. Streelman, and T. D. Kocher. 2003. Directional selection has shaped the oral jaws of Lake Malawi cichlid fishes. Proc. Natl. Acad. Sci. 100:5252-5257.

Alfaro, M. E., D. I. Bolnick, and P. C. Wainwright. 2005. Evolutionary consequences of many-to-one mapping of jaw morphology to mechanics in labrid fishes. Am. Nat. 165:E140-E154.

Anderson, P. S. L. 2010. Using linkage models to explore skull kinematic diversity and functional convergence in arthrodire placoderms. J. Morphol. 271:990-1005.

Anderson, P. S. L., T. Claverie, and S. N. Patek. 2014. Lever and linkages: mechanical trade-offs in a power-amplified system. Evolution. 68:1919-1933.

Anderson, P. S. L., and M. W. Westneat. 2009. A biomechanical model of feeding kinematics for *Dunkleosteus terrelli* (Arthrodira, Placodermi). Paleobiology. 35:251-269.

Anderson, P., and S. N. Patek. 2015. Mechanical sensitivity reveals evolutionary dynamics of mechanical systems. Proc. R. Soc. Lond. B Biol. Sci. 282:20143088.

Angielczyk, K. D., C. R. Feldman, and G. R. Miller. 2011. Adaptive evolution of plastron shape in emydine turtles. Evolution. 65:377-394.

Anker, G. 1974. Morphology and kinetics of the head of the stickleback, *Gasterosteus aculeatus*. Trans. Zool. Soc. Lond. 32:311-416.

Arbour, J. H., and H. López-Fernández. 2013. Ecological variation in South American geophagine cichlids arose during an early burst of adaptive morphological and functional evolution. Proc. R. Soc. Lond. B Biol. Sci. 280:20130849.

Arnold, A. S., C. T. Richards, I. G. Ros, and A. A. Biewener. 2011. There is always a trade-off between speed and force in a lever system: comment on McHenry (2010). Biol. Lett. 7:878-879.

Arnold, S. J. 1983. Morphology, performance and fitness. Am. Zool. 23:347-361.

Arnold, S. J. 1992. Constraints on phenotypic evolution. Am. Nat. 140:S85-S107.

Bailey, M., S. A. Petrie, and S. S. Badzinski. 2008. Diet of mute swans in lower Great Lakes coastal marshes. J. Wildl. Manag. 72:726-732.

Barbosa, A. 1996. Relationship between bill morphology and preening behaviour in waders. Ethol. Ecol. Evol. 8:291-296.

Barbosa, A., and E. Moreno. 1999. Evolution of foraging strategies in shorebirds: an ecomorphological approach. Auk. 116:712-725.

Bardwell, E., C. W. Benkman, and W. R. Gould. 2001. Adaptive geographic variation in western scrub-jays. Ecology. 82:2617-2627.

Barnes, G. G., and V. G. Thomas. 1987. Digestive organ morphology, diet, and guild structure of North American Anatidae. Can. J. Zool. 65:1812-1817.

Benkman, C. W. 2003. Divergent selection drives the adaptive radiation of crossbills. Evolution. 57:1176-1181.

Benkman, C. W., and A. K. Lindholm. 1991. The advantages and evolution of a morphological novelty. Nature (Lond.). 349:519-520.

Bergert B. A., and P. C. Wainwright. 1997. Morphology and kinematics of prey capture in the syngnathid fishes Hippocampus erectus and Syngnathus floridae. Mar. Biol. 127:563–570.

Bertram, J. E. A., and A. A. Biewener. 1988. Bone curvature: sacrificing strength for load predictability? J. Theor. Biol. 131:75-92.

Bjorndal, K. A. 1980. Nutrition and grazing behavior of the green turtle *Chelonia mydas*. Mar. Biol. (Berl.). 56:147-154.

Blomberg, S. P., T. Garland, and A. R. Ives. 2003. Testing for phylogenetic signal in comparative data: behavioral traits are more labile. Evolution. 57:717-745.

Blomberg, S. P., T. Garland, and A. R. Ives. 2003. Testing for phylogenetic signal in comparative data: behavioral traits are more labile. Evolution. 57:717-745.

Boag, P. T., and P. R. Grant. 1984. The classical case of character release: Darwin's finches (Geospiza) on Isla Daphne Major, Galápagos. Biol. J. Linn. Soc. 22:243-287.

Bock, W. J. 1964. Kinetics of the avian skull. J. Morphol. 114:1-41.

Bookstein, F. L. 1989. "Size and shape": a comment on semantics. Syst. Biol. 38:173-180.

Bout, R. G., and G. A. Zweers. 2001. The role of cranial kinesis in birds. Comp. Biochem. Physiol. Part A Mol. Integr. Physiol. 131:197-205.

Bout, R. G., and J. L. Dubbeldam. 1991. Functional morphological interpretation of the distribution of muscle spindles in the jaw muscles of the mallard (*Anas platyrhynchos*). J. Morphol. 210:215-226.

Bradski, G. 2000. The opencv library. Doctor Dobbs Journal. 25:120-126.

Brainerd, E. L., D. B. Baier, S. M. Gatesy, T. L. Hedrick, K. A. Metzger, S. L. Gilbert, and J. J. Crisco. 2010. X-ray reconstruction of moving morphology (XROMM): precision, accuracy and applications in comparative biomechanics research. J. Exp. Zool. Part A. 313:262-279.

Bright, J. A., J. Marugán-Lobón, S. N. Cobb, and E. J. Rayfield. 2016. The shapes of bird beaks are highly controlled by nondietary factors. Early Edition.

Brodsky, L. M., and P. J. Weatherhead. 1985. Time and energy constraints on courtship in wintering American black ducks. Condor. 87:33-36.

Brusca, R. C., and G. J. Brusca. 1990. Invertebrates, 1st edition. Sinauer Associates, Inc Sunderland, Massachusetts.

Bucher, E. H., D. Tamburini, A. Abril, and P. Torres. 2003. Folivory in the white-tipped plantcutter *Phytotoma rutila*: seasonal variations in diet composition and quality. J. Avian Biol. 34:211-216.

Burleigh, J. G., R. T. Kimball, and E. L. Braun. 2015. Building the avian tree of life using a large-scale, sparse supermatrix. Mol. Phylogenet. Evol. 84:53-63.

Burleigh, J. G., R. T. Kimball, and E. L. Braun. 2015. Building the avian tree of life using a large-scale, sparse supermatrix. Mol. Phylogenet. Evol. 84:53-63.

Butler, M. A., and A. A. King. 2004. Phylogenetic comparative analysis: a modeling approach for adaptive evolution. Am. Nat. 164:683-695.

Bühler, P. 1981. Functional anatomy of the avian jaw apparatus. Pp. 439-468 *in* King, A. S., and J. McLellard, eds. Form and function in birds. Vol. 2. Academic Press, New York.

Camp, A. L., and E. L. Brainerd. 2014. Role of axial muscles in powering mouth expansion during suction feeding in largemouth bass (*Micropterus salmoides*). J. Exp. Biol. 217:1333-1345.

Chang, W., J. Cheng, J. J. Allaire, Y. Xie, and J. McPherson. 2016. shiny: Web Application Framework for R. URL https://CRAN.R-project.org/package=shiny.

Chen, L., C. W. Armstrong, and D. D. Raftopoulos. 1994. An investigation on the accuracy of three-dimensional space reconstruction using the direct linear transformation technique. J. Biomech. 27:493-500.

Cheverud, J. M. 1996. Developmental integration and the evolution of pleiotropy. Am. Zool. 36:44-50.

Choat, J. H., and K. D. Clements. 1998. Vertebrate herbivores in marine and terrestrial environments: a nutritional ecology perspective. Annu. Rev. Ecol. Syst. 29:375-403.

Chong, A. K., and P. Stratford. 2002. Underwater digital stereo-observation technique for red hydrocoral study. Photogrammetric engineering and remote sensing. 68:745-752.

Clabaut, C., P. M. E. Bunje, W. Salzburger, and A. Meyer. 2007. Geometric morphometric analyses provide evidence for the adaptive character of the Tanganyikan cichlid fish radiations. Evolution. 61:560-578.

Claessens, L. P. 2009. The skeletal kinematics of lung ventilation in three basal bird taxa (emu, tinamou, and guinea fowl). J. Exp. Zool. Part A. 311:586-599.

Clarke, J. A., C. P. Tambussi, J. I. Noriega, G. M. Erickson, and R. A. Ketcham. 2005. Definitive fossil evidence for the extant avian radiation in the Cretaceous. Nature (Lond.). 433:305-308.

Clarke, S. J., G. H. Miller, M. L. Fogel, A. R. Chivas, and C. V. Murray-Wallace. 2006. The amino acid and stable isotope biogeochemistry of elephant bird (*Aepyornis*) eggshells from southern Madagascar. Quat. Sci. Rev. 25:2343-2356.

Clauss, M., A. Schwarm, S. Ortmann, W. J. Streich, and J. Hummel. 2007. A case of non-scaling in mammalian physiology? Body size, digestive capacity, food intake, and ingesta passage in mammalian herbivores. Comp. Biochem. Physiol. Part A Mol. Integr. Physiol. 148:249-265.

Clauss, M., P. Steuer, D. W. H. Müller, D. Codron, and J. Hummel. 2013. Herbivory and body size: allometries of diet quality and gastrointestinal physiology, and implications for herbivore ecology and dinosaur gigantism. PLoS One. 8:e68714.

Clauss, M., W. J. Streich, C. L. Nunn, S. Ortmann, G. Hohmann, A. Schwarm, and J. Hummel. 2008. The influence of natural diet composition, food intake level, and body size on ingesta passage in primates. Comp. Biochem. Physiol. Part A Mol. Integr. Physiol. 150:274-281.

Clayton, D. H., B. R. Moyer, S. E. Bush, T. G. Jones, D. W. Gardiner, B. B. Rhodes, and F. Goller. 2005. Adaptive significance of avian beak morphology for ectoparasite control. Proc. R. Soc. Lond. B Biol. Sci. 272:811-817.

Clayton, D. H., and P. Cotgreave. 1994. Relationship of bill morphology to grooming behaviour in birds. Anim. Behav. 47:195-201.

Clements, J. F., T. S. Schulenberg, M. J. Iliff, D. Roberson, T. A. Fredericks, B. L. Sullivan, and C. L. Wood. 2014. The eBird/Clements checklist of birds of the world: Version 6.9. URL http://www.birds.cornell.edu/clementschecklist/download/.

Cook, C., B. J. Gut, E. M. Rix, J. Schneller, and M. Seitz. 1974. Water Plants of the World: A Manual for the Identification of the Genera of Freshwater Macrophytes, 1st edition. Dr. W. Junk b.v. Pub Hague.

Cooper, W. E., and L. J. Vitt. 2002. Distribution, extent, and evolution of plant consumption by lizards. J. Zool. (Lond.). 257:487-517.

Cooper, W. J., K. Parsons, A. McIntyre, B. Kern, A. McGee-Moore, and R. C. Albertson. 2010. Bentho-pelagic divergence of cichlid feeding architecture was prodigious and consistent during multiple adaptive radiations within African rift-lakes. PLoS One. 5:e9551.

Cooper, W. J., and M. W. Westneat. 2009. Form and function of damselfish skulls: rapid and repeated evolution into a limited number of trophic niches. BMC Evol. Biol. 9:24.

Cork, S. J. 1996. Optimal digestive strategies for arboreal herbivorous mammals in contrasting forest types: why koalas and colobines are different. Aust. J. Ecol. 21:10-20.

Couture-Beil, A. 2014. rjson: JSON for R. URL http://CRAN.R-project.org/package=rjson.

Cummings, M. E. 2007. Sensory trade-offs predict signal divergence in surfperch. Evolution. 61:530-545.

Darwin, C. 1872. The origin of species by means of natural selection: or, the preservation of favored races in the struggle for life, 6th Edition. John Murray Albemarle Street, London.

Davies, S. 1978. The food of emus. Aust. J. Ecol. 3:411-422.

Dawson, M. M., K. A. Metzger, D. B. Baier, and E. L. Brainerd. 2011. Kinematics of the quadrate bone during feeding in mallard ducks. J. Exp. Biol. 214:2036-2046.

De Visser, J., and C. Barel. 1998. The expansion apparatus in fish heads, a 3-D kinetic deduction. Neth. J. Zool. 48:361-395.

Delacour, J., and E. Mayr. 1945. The family Anatidae. Wilson Bull. 57:3-55.

Demment, M. W., and P. J. Van Soest. 1985. A nutritional explanation for body-size patterns of ruminant and nonruminant herbivores. Am. Nat. 125:641-672.

Derryberry, E. P., N. Seddon, S. Claramunt, J. A. Tobias, A. Baker, A. Aleixo, and R. T. Brumfield. 2012. Correlated evolution of beak morphology and song in the neotropical woodcreeper radiation. Evolution. 66:2784-2797.

Dial, K. P. 2003. Evolution of avian locomotion: correlates of flight style, locomotor modules, nesting biology, body size, development, and the origin of flapping flight. Auk. 120:941-952.

Donne-Goussé, C., V. Laudet, and C. Hänni. 2002. A molecular phylogeny of Anseriformes based on mitochondrial DNA analysis. Mol. Phylogenet. Evol. 23:339-356.

Donne-Goussé, C., V. Laudet, and C. Hänni. 2002. A molecular phylogeny of Anseriformes based on mitochondrial DNA analysis. Mol. Phylogenet. Evol. 23:339-356.

Drake, A. G., and C. P. Klingenberg. 2010. Large-scale diversification of skull shape in domestic dogs: disparity and modularity. Am. Nat. 175:289-301.

Druzinsky, R. E. 1993. The time allometry of mammalian chewing movements: chewing frequency scales with body mass in mammals. J. Theor. Biol. 160:427-440.

Dudley, R., and G. J. Vermeij. 1992. Do the power requirements of flapping flight constrain folivory in flying animals? Funct. Ecol. 6:101-104.

Dunning, J. B, Jr. 2008. CRC handbook of avian body masses. CRC press Boca Raton, FL.

Ebbinge, B., K. Canters, and R. Drent. 1975. Foraging routines and estimated daily food intake in Barnacle Geese wintering in the northern Netherlands. Wildfowl. 26:5-19.

Eddelbuettel, D., and R. Francois. 2011. Rcpp: Seamless R and C++ integration. J. Statist. Soft. 40:1-18.

Ellerby, D. J., and S. P. Gerry. 2011. Sympatric divergence and performance trade-offs of bluegill ecomorphs. Evol. Biol. (N. Y.). 38:422-433.

Endler, J. A. 1980. Natural selection on color patterns in *Poecilia reticulata*. Evolution. 34:76-91.

Endler, J. A. 1982. Convergent and divergent effects of natural selection on color patterns in two fish faunas. Evolution. 36:178-188.

Falkingham, P. L. 2012. Acquisition of high resolution three-dimensional models using free, open-source, photogrammetric software. Palaeontol. Electron. 15:15pp.

Felsenstein, J. 1973. Maximum-likelihood estimation of evolutionary trees from continuous characters. Am. J. Hum. Genet. 25:471.

Felsenstein, J. 1985. Phylogenies and the comparative method. Am. Nat. 125:1-15.

Foster, D. J., J. Podos, and A. P. Hendry. 2008. A geometric morphometric appraisal of beak shape in Darwin's finches. J. Evol. Biol. 21:263-275.

Franz, R., J. Hummel, D. W. H. Müller, M. Bauert, J. Hatt, and M. Clauss. 2011. Herbivorous reptiles and body mass: effects on food intake, digesta retention, digestibility and gut capacity, and a comparison with mammals. Comp. Biochem. Physiol. Part A Mol. Integr. Physiol. 158:94-101.

Estrella S. M., J. A. Masero. 2007. The use of distal rhynchokinesis by birds feeding in water. J. Exp. Biol. 210:3757–3762.

Frazzetta, T. H. 1962. A functional consideration of cranial kinesis in lizards. J. Morphol. 111:287-319.

Freckleton, R. P., P. H. Harvey, and M. Pagel. 2002. Phylogenetic analysis and comparative data: a test and review of evidence. Am. Nat. 160:712-726.

Frei, S., S. Ortmann, C. Reutlinger, M. Kreuzer, J. Hatt, and M. Clauss. 2014. Comparative digesta retention patterns in ratites. Auk: Ornithol. Adv. 132:119-131.

Fritz, J., S. Hammer, C. Hebel, A. Arif, B. Michalke, M. T. Dittmann, D. W. H. Müller, and M. Clauss. 2012. Retention of solutes and different-sized particles in the digestive tract of the ostrich (*Struthio camelus massaicus*), and a comparison with mammals and reptiles. Comp. Biochem. Physiol. Part A Mol. Integr. Physiol. 163:56-65.

Fuentes, C., M. I. Sánchez, N. Selva, and A. J. Green. 2004. The diet of the marbled Teal *Marmoreneta angustirostris* in southern Alicante, Eastern spain. Rev. Écol. 59:475-490.

Fulton, T. L., B. Letts, and B. Shapiro. 2012. Multiple losses of flight and recent speciation in steamer ducks. Proc. R. Soc. Lond. B Biol. Sci. 279:2339-2346.

Futuyma, D. J., M. C. Keese, and S. J. Scheffer. 1993. Genetic constraints and the phylogeny of insect-plant associations: responses of Ophraella communa (Coleoptera: Chrysomelidae) to host plants of its congeners. Evolution. 47:888-905.

Garland, T. Garland, T, Jr., and A. R. Ives. 2000. Using the past to predict the present: confidence intervals for regression equations in phylogenetic comparative methods. Am. Nat. 155:346-364.

Garland, T., P. H. Harvey, and A. R. Ives. 1992. Procedures for the analysis of comparative data using phylogenetically independent contrasts. Syst. Biol. 41:18-32.

Gasaway, W. C. 1976. Volatile fatty acids and metabolizable energy derived from cecal fermentation in the willow ptarmigan. Comp. Biochem. Physiol. Part A Mol. Integr. Physiol. 53:115-121.

Gaston, K. J., and T. M. Blackburn. 1995. Birds, body size and the threat of extinction. Philos. Trans. R. Soc. Lond. B Biol. Sci. 347:205-212.

Geist, V. 1974. On the relationship of social evolution and ecology in ungulates. Am. Zool. 14:205-220.

Ghalambor, C. K., D. N. Reznick, and J. A. Walker. 2004. Constraints on adaptive evolution: the functional trade-off between reproduction and fast-start swimming performance in the Trinidadian guppy (*Poecilia reticulata*). Am. Nat. 164:38-50.

González, J., H. Düttmann, and M. Wink. 2009. Phylogenetic relationships based on two mitochondrial genes and hybridization patterns in Anatidae. J. Zool. (Lond.). 279:310-318.

Goodall, C. 1991. Procrustes methods in the statistical analysis of shape. J. R. Statist. Soc. B. 53:285-339.

Gosler, A. G. 1987. Pattern and process in the bill morphology of the Great Tit Parus major. Ibis. 129:451-476.

Goswami, A., J. B. Smaers, C. Soligo, and P. D. Polly. 2014. The macroevolutionary consequences of phenotypic integration: from development to deep time. Philos. Trans. R. Soc. Lond. B Biol. Sci. 369:20130254.

Grajal, A., S. D. Strahl, R. Parra, M. G. Dominguez, and A. Neher. 1989. Foregut fermentation in the hoatzin, a neotropical leaf-eating bird. Science (Wash. D. C.). 245:1236-1238.

Grant, B. R., and P. R. Grant. 1982. Niche shifts and competition in Darwin's finches: *Geospiza conirostris* and congeners. Evolution:637-657.

Grant, P. R. 1981. The feeding of Darwin's finches on *Tribulus cistoides* (L.) seeds. Anim. Behav. 29:785-793.

Grant, P. R., B. R. Grant, J. N. Smith, I. J. Abbott, and L. K. Abbott. 1976. Darwin's finches: population variation and natural selection. Proc. Natl. Acad. Sci. 73:257-261.

Grant, P. R., and B. R. Grant. 2006. Evolution of character displacement in Darwin's finches. Science (Wash. D. C.). 313:224-226.

Greenberg, R., V. Cadena, R. M. Danner, and G. Tattersall. 2012. Heat loss may explain bill size differences between birds occupying different habitats. PLoS One. 7:e40933.

Grubich, J. R., and M. W. Westneat. 2006. Four-bar linkage modelling in teleost pharyngeal jaws: computer simulations of bite kinetics. J. Anat. 209:79-92.

Guillemain, M., G. R. Martin, and H. Fritz. 2002. Feeding methods, visual fields and vigilance in dabbling ducks (Anatidae). Funct. Ecol. 16:522-529.

Guillemette, M. 1994. Digestive-rate constraint in wintering common eiders (*Somateria mollissima*): implications for flying capabilities. Auk. 111:900-909.

Gurd, B. D. 2006. Filter-feeding dabbling ducks (*Anas* spp.) can actively select particles by size. Zoology (Jena). 109:120-126.

Gurd, D. B. 2007. Predicting resource partitioning and community organization of filter-feeding dabbling ducks from functional morphology. Am. Nat. 169:334-343.

Gurd, D. B. 2008. Mechanistic analysis of interspecific competition using foraging trade-offs: implications for duck assemblages. Ecology. 89:495-505.

Gussekloo, S. W., M. G. Vosselman, and R. G. Bout. 2001. Three-dimensional kinematics of skeletal elements in avian prokinetic and rhynchokinetic skulls determined by Roentgen stereophotogrammetry. J. Exp. Biol. 204:1735-1744.

Hackett, S. J., R. T. Kimball, S. Reddy, R. C. K. Bowie, E. L. Braun, M. J. Braun, J. L. Chojnowski, W. A. Cox, K. Han, J. Harshman, C. J. Huddleston, B. D. Marks, K. J. Miglia, W. S. Moore, F. H. Sheldon, D. W. Steadman, C. C. Witt, and T. Yuri. 2008. A phylogenomic study of birds reveals their evolutionary history. Science (Wash. D. C.). 320:1763-1768.

Hagan, A. A., and J. E. Heath. 1980. Regulation of heat loss in the duck by vasomotion in the bill. J. Therm. Biol. 5:95-101.

Hall, M. I., and C. F. Ross. 2007. Eye shape and activity pattern in birds. J. Zool. (Lond.). 271:437-444.

Harmon, L. J., J. T. Weir, C. D. Brock, R. E. Glor, and W. Challenger. 2008. GEIGER: investigating evolutionary radiations. Bioinformatics (Oxf.). 24:129-131.

Hartenberg, R. S., and J. Denavit. 1964. Kinematic synthesis of linkages. McGraw-Hill.

Havera, S. P. 1998. Waterfowl of Illinois: status and management. Phoenix Publishing Urbana, IL.

Hedrick, T. L. 2008. Software techniques for two-and three-dimensional kinematic measurements of biological and biomimetic systems. Bioinsp. & Biomim. 3:034001.

Herrel, A., J. Podos, B. Vanhooydonck, and A. P. Hendry. 2009. Force-velocity trade-off in Darwin's finch jaw function: a biomechanical basis for ecological speciation? Funct. Ecol. 23:119-125.

Herrel, A., J. Podos, S. K. Huber, and A. P. Hendry. 2005. Bite performance and morphology in a population of Darwin's finches: implications for the evolution of beak shape. Funct. Ecol. 19:43-48.

Herrel, A., J. Podos, S. K. Huber, and A. P. Hendry. 2005a. Bite performance and morphology in a population of Darwin's finches: implications for the evolution of beak shape. Funct. Ecol. 19:43-48.

Herrel, A., J. Podos, S. K. Huber, and A. P. Hendry. 2005b. Bite performance and morphology in a population of Darwin's finches: implications for the evolution of beak shape. Funct. Ecol. 19:43-48.

Hiiemae, K. M. 2000. Feeding in mammals. Pp. 411-448 *in* Schwenk, K., ed. Feeding: form, function and evolution in tetrapod vertebrates. Academic Press, San Diego, CA.

Hoese, W. J., J. Podos, N. C. Boetticher, and S. Nowicki. 2000. Vocal tract function in birdsong production: experimental manipulation of beak movements. J. Exp. Biol. 203:1845-1855.

Hoese, W. J., and M. W. Westneat. 1996. Biomechanics of cranial kinesis in birds: Testing linkage models in the white-throated sparrow (*Zonotrichia albicollis*). J. Morphol. 227:305-320.

Holzman, R., D. C. Collar, R. S. Mehta, and P. C. Wainwright. 2011. Functional complexity can mitigate performance trade-offs. Am. Nat. 177:E69-E83.

Huber, S. K., and J. Podos. 2006. Beak morphology and song features covary in a population of Darwin's finches (*Geospiza fortis*). Biol. J. Linn. Soc. 88:489-498.

Hulsey, C. D., and P. C. Wainwright. 2002. Projecting mechanics into morphospace: disparity in the feeding system of labrid fishes. Proc. R. Soc. Lond. B Biol. Sci. 269:317-326.

Hérrisant, M. 1748. Sur les mouvemens du bec des oiseaux et particuliérement du canard. Hist. Acad. R. Sci. 1748:345-386.

Irschick, D. J., J. J. Meyers, J. F. Husak, and J. Le Galliard. 2008. How does selection operate on whole-organism functional performance capacities? A review and synthesis. Evol. Ecol. Res. 10:177-196.

Irschick, D. J., L. J. Vitt, P. A. Zani, and J. B. Losos. 1997. A comparison of evolutionary radiations in mainland and Caribbean Anolis lizards. Ecology. 78:2191-2203.

Iwaniuk, A. N., and J. E. Nelson. 2001. A comparative analysis of relative brain size in waterfowl (Anseriformes). Brain Behav. Evol. 57:87-97.

Jaekel, M., and D. B. Wake. 2007. Developmental processes underlying the evolution of a derived foot morphology in salamanders. Proc. Natl. Acad. Sci. 104:20437-20442.

James, H. F., and D. A. Burney. 1997. The diet and ecology of Hawaii's extinct flightless waterfowl: evidence from coprolites. Biol. J. Linn. Soc. 62:279-297.

Janis, C. M. 2000. Patterns in the evolution of herbivory in large terrestrial mammals: the Paleogene of North America. Pp. 168-222 *in* Sues, H., ed. Evolution of Herbivory in Terrestrial Vertebrates. Cambridge University Press, Cambridge, UK.

Johnsgard, P. A., ed. 1978. Ducks, geese, and swans of the world. University of Nebraska Press Lincoln, NE.

Johnson, K. P., and M. D. Sorenson. 1998. Comparing molecular evolution in two mitochondrial protein coding genes (cytochrome *b* and ND2) in the dabbling ducks (Tribe: Anatini). Mol. Phylogenet. Evol. 10:82-94.

Kaplan, R. H., and P. C. Phillips. 2006. Ecological and developmental context of natural selection: maternal effects and thermally induced plasticity in the frog *Bombina orientalis*. Evolution. 60:142-156.

Karasov, W. H. 1990. Digestion in birds: chemical and physiological determinants and ecological implications. Stud. Avian Biol. 13:l-4.

Kear, J., ed. 2005. Bird families of the world: ducks, geese and swans. Oxford University Press Oxford, UK.

Kingsford, R. T. 1989. Food of the Maned Duck *Chenonetta jubata* during the breeding season. Emu. 89:119-124.

Kingsolver, J. G., H. E. Hoekstra, J. M. Hoekstra, D. Berrigan, S. N. Vignieri, C. E. Hill, A. Hoang, P. Gibert, and P. Beerli. 2001. The strength of phenotypic selection in natural populations. Am. Nat. 157:245-261.

Klages, N. T. W., and J. Cooper. 1992. Bill morphology and diet of a filter-feeding seabird: the broad-billed prion *Pachyptila vittata* at South Atlantic Gough Island. J. Zool. (Lond.). 227:385-396.

Klasing, K. C. 1998. Comparative avian nutrition. CAB International Wallingford, UK.

Klingenberg, C. P. 2008. Morphological integration and developmental modularity. Annu. Rev. Ecol. Evol. Syst.:115-132.

Klingenberg, C. P., M. Barluenga, and A. Meyer. 2002. Shape analysis of symmetric structures: quantifying variation among individuals and asymmetry. Evolution. 56:1909-1920.

Klingenberg, C. P., and J. Marugán-Lobón. 2013. Evolutionary covariation in geometric morphometric data: analyzing integration, modularity, and allometry in a phylogenetic context. Syst. Biol. 62:591-610.

Konow N., A. L. Camp, and C. P. J. Sanford. 2008. Congruence between muscle activity and kinematics in a convergently derived prey-processing behavior. Integr. Comp. Biol. 48:246–260.

Konow, N., and C. P. J. Sanford. 2008. Biomechanics of a convergently derived prey-processing mechanism in fishes: evidence from comparative tongue bite apparatus morphology and raking kinematics. J. Exp. Biol. 211:3378-3391.

Konuma, J., and S. Chiba. 2007. Trade-Offs between Force and Fit: Extreme Morphologies Associated with Feeding Behavior in Carabid Beetles. Am. Nat. 170:90-100.

Kooloos, J., A. R. Kraaijeveld, G. Langenbach, and G. A. Zweers. 1989. Comparative mechanics of filter feeding in *Anas platyrhynchos*, *Anas clypeata* and *Aythya fuligula* (Aves, Anseriformes). Zoomorphology (Berl.). 108:269-290.

Kooloos, J., and G. A. Zweers. 1989. Mechanics of drinking in the mallard (*Anas platyrhynchos*, Anatidae). J. Morphol. 199:327-347.

Korschgen, C. E., L. S. George, and W. L. Green. 1988. Feeding ecology of canvasbacks staging on Pool 7 of the Upper Mississippi River. Pp. 237-249 *in* Weller, M. W., ed. Waterfowl in winter. University of Minnesota Press, Minneapolis, MN.

Kulemeyer, C., K. Asbahr, P. Gunz, S. Frahnert, and F. Bairlein. 2009. Functional morphology and integration of corvid skulls-a 3D geometric morphometric approach. Front. Zool. 6:2-2.

Landers, J. L., T. T. Fendley, and A. S. Johnson. 1977. Feeding ecology of wood ducks in South Carolina. J. Wildl. Manag. 41:118-127.

Larson, G. L. 1976. Social behavior and feeding ability of two phenotypes of *Gasterosteus aculeatus* in relation to their spatial and trophic segregation in a temperate lake. Can. J. Zool. 54:107-121.

Lauder, G. V. 1982. Patterns of evolution in the feeding mechanism of actinopterygian fishes. Am. Zool. 22:275-285.

Lavery, H. J. 1971. Studies of waterfowl (Anatidae) in north Queensland. 6. Feeding methods and foods. Qld. J. Agric. Anim. Sci. 28:255-273.

Lavin, S. R., W. H. Karasov, A. R. Ives, K. M. Middleton, and T. Garland, Jr. 2008. Morphometrics of the avian small intestine compared with that of nonflying mammals: a phylogenetic approach. Physiol. Biochem. Zool. 81:526-550.

Law, T., and R. Blake. 1996. Comparison of the fast-start performances of closely related, morphologically distinct threespine sticklebacks (*Gasterosteus* spp.). J. Exp. Biol. 199:2595-2604.

Legendre, P. 2014. lmodel2: Model II Regression. URL http://CRAN.R-project.org/package=lmodel2.

Leopold, A. S. 1953. Intestinal morphology of gallinaceous birds in relation to food habits. J. Wildl. Manag. 17:197-203.

Li, Z., and J. A. Clarke. 2015. The craniolingual morphology of waterfowl (Aves, anseriformes) and its relationship with feeding mode revealed through contrast-enhanced X-ray computed tomography and 2D morphometrics. Evol. Biol. (N. Y.). 43:12-25.

Liu, X., and J. Wang. 2014. Parallel Kinematics: Type, Kinematics, and Optimal Design. Springer.

Livezey, B. C. 1986. A phylogenetic analysis of recent anseriform genera using morphological characters. Auk. 103:737-754.

Livezey, B. C. 1997. A phylogenetic analysis of basal Anseriformes, the fossil *Presbyornis*, and the interordinal relationships of waterfowl. Zool. J. Linn. Soc. 121:361-428.

Lohmann, G. P., and P. N. Schweitzer. 1990. On eigenshape analysis. Pp. 166- *in* Proceedings of the Michigan morphometrics workshop. Vol. 145.

Losos, J. B. 2011. Convergence, adaptation, and constraint. Evolution. 65:1827-1840.

MacLeod, N. 2009. Part 18 - Form & Shape Models. Palaeontol. Newsl.

Marchant, S., and P. J. Higgins, eds. 1990. Handbook of Australian, New Zealand and Antarctic birds. Oxford University Press Oxford, UK.

Marks, C. O., and M. J. Lechowicz. 2006. Alternative designs and the evolution of functional diversity. Am. Nat. 167:55-66.

Marquiss, M., and R. Rae. 2002. Ecological differentiation in relation to bill size amongst sympatric, genetically undifferentiated crossbills *Loxia* spp. Ibis. 144:494-508.

Martins, E. P., and T. F. Hansen. 1997. Phylogenies and the comparative method: a general approach to incorporating phylogenetic information into the analysis of interspecific data. Am. Nat. 149:646-667.

Marugán-Lobón, J., and A. D. Buscalioni. 2009. New insight on the anatomy and architecture of the avian neurocranium. Anat. Rec. 292:364-370.

Masman, D., and M. Klaassen. 1987. Energy expenditure during free flight in trained and free-living Eurasian kestrels (*Falco tinnunculus*). Auk. 104:603-616.

Mayhew, P. W., and D. C. Houston. 1993. Food throughput time in European wigeon *Anas penelope* and other grazing waterfowl. Wildfowl. 44:174-177.

McBee, R. H., and G. C. West. 1969. Cecal fermentation in the willow ptarmigan. Condor. 71:54-58.

McCarthy, J. M. 2006. Geometric design of linkages. Vol. 11 Springer-Verlag New York.

McCracken, K. G., C. P. Barger, M. Bulgarella, K. P. Johnson, M. K. Kuhner, A. V. Moore, J. L. Peters, J. Trucco, T. H. Valqui, K. Winker, and R. E. Wilson. 2009. Signatures of High-Altitude Adaptation in the Major Hemoglobin of Five Species of Andean Dabbling Ducks. Am. Nat. 174:631-650.

McCracken, K. G., J. Harshman, D. A. McClellan, and A. D. Afton. 1999. Data set incongruence and correlated character evolution: an example of functional convergence in the hind-limbs of stifftail diving ducks. Syst. Biol. 48:683-714.

McHenry, M. J. 2012. When skeletons are geared for speed: the morphology, biomechanics, and energetics of rapid animal motion. Integr. Comp. Biol. 52:588-596.

McHenry, M. J., T. Claverie, M. V. Rosario, and S. N. Patek. 2012. Gearing for speed slows the predatory strike of a mantis shrimp. J. Exp. Biol. 215:1231-1245.

McHenry, M. J., and A. P. Summers. 2011. A force-speed trade-off is not absolute. Biol. Lett. 7:880-881.

McKinnon, J. S., and H. D. Rundle. 2002. Speciation in nature: the threespine stickleback model systems. Trends Ecol. Evol. 17:480-488.

McNab, B. K. 1994. Energy conservation and the evolution of flightlessness in birds. Am. Nat. 144:628-642.

Metzger, K. 2002. Cranial Kinesis in Lepidosaurs: Skulls in Motion. Pp. 15-46 *in* Aerts, P., K. D'Août, A. Herrel, and R. Van Damme, eds. Topics in Functional and Ecological Vertebrate Morphology. Shaker Publishing, Maastricht.

Meyer, A. 1989. Cost of morphological specialization: feeding performance of the two morphs in the trophically polymorphic cichlid fish, *Cichlasoma citrinellum*. Oecologia. 80:431-436.

Middleton, B. A., and A. G. van der Valk. 1987. The food habits of greylag and barheaded geese in the Keoladeo National Park, India. Wildfowl. 38:94-102.

Mills, J. A., and A. F. Mark. 1977. Food preferences of takahe in Fiordland National Park, New Zealand, and the effect of competition from introduced red deer. J. Anim. Ecol. 46:939-958.

Milton, S. J., W. R. J. Dean, and W. R. Siegfried. 1994. Food selection by ostrich in southern Africa. J. Wildl. Manag. 58:234-248.

Mitchell, K. J., B. Llamas, J. Soubrier, N. J. Rawlence, T. H. Worthy, J. Wood, M. S. Y. Lee, and A. Cooper. 2014. Ancient DNA reveals elephant birds and kiwi are sister taxa and clarifies ratite bird evolution. Science (Wash. D. C.). 344:898-900.

Morton, E. S. 1978. Avian arboreal folivores: why not? In *The Ecology of arboreal folivores*:123-30. Conservation and Research Center, National Zoological Park, Smithsonian Institution, Washington, DC.

Mosa, S. G. 1993. Fall and winter diet and habitat preferences of the Andean Tinamou (*Nothura pentlandii*) in the Northwest Argentina. Stud. Neotrop. Fauna Environ. 28:123-128.

Moyer, B. R., A. T. Peterson, and D. H. Clayton. 2002. Influence of bill shape on ectoparasite load in Western Scrub-Jays. Condor. 104:675-678.

Muller, M. 1989. A quantitative theory of expected volume changes of the mouth during feeding in teleost fishes. J. Zool. (Lond.). 217:639-661.

Munson, E. S., and W. D. Robinson. 1992. Extensive folivory by Thick-billed Saltators (*Saltator maxillosus*) in southern Brazil. Auk. 109:917-919.

Müller, D. W. H., D. Codron, C. Meloro, A. Munn, A. Schwarm, J. Hummel, and M. Clauss. 2013. Assessing the Jarman-Bell principle: scaling of intake, digestibility, retention time and gut fill with body mass in mammalian herbivores. Comp. Biochem. Physiol. Part A Mol. Integr. Physiol. 164:129-140.

Nabavizadeh, A. 2016. Evolutionary trends in the jaw adductor mechanics of ornithischian dinosaurs. Anat. Rec. 299:271-294.

Naranjo, L. G. 1986. Aspects of the biology of the horned screamer in southwestern Colombia. Wilson Bull. 98:243-256.

Nudds, T. D., and J. N. Bowlby. 1984. Predator-prey size relationships in North American dabbling ducks. Can. J. Zool. 62:2002-2008.

O'Brien, H. D., and J. Bourke. 2015. Physical and computational fluid dynamics models for the hemodynamics of the artiodactyl carotid rete. J. Theor. Biol. 386:122-131.

O'Connor, P. M. 2004. Pulmonary pneumaticity in the postcranial skeleton of extant Aves: a case study examining Anseriformes. J. Morphol. 261:141-161.

O'Steen, S., A. J. Cullum, and A. F. Bennett. 2002. Rapid evolution of escape ability in Trinidadian guppies (Poecilia reticulata). Evolution. 56:776-784.

Olsen, A. M. 2014. bezier: Bezier Curve and Spline Toolkit. URL http://cran.r-project.org/package=bezier.

Olsen, A. M. 2015. Exceptional avian herbivores: multiple transitions toward herbivory in the bird order Anseriformes and its correlation with body mass. Ecol. Evol. 5:5016-5032.

Olsen A. M. 2016a. linkR: 3D Lever and Linkage Mechanism Modeling. URL http://cran.r-project.org/package=linkR.

Olsen A. M. 2016b. svgViewR: 3D Animated Interactive Visualizations using SVG. URL http://cran.r-project.org/package=svgViewR.

Olsen, A. M. In prep. Congruence of a performance trade-off, a major axis of shape variation, and morphological convergence in the evolution of the waterfowl feeding system (Aves: Anseriformes).

Olsen, A. M., and M. W. Westneat. 2015. StereoMorph: an R package for the collection of 3D landmarks and curves using a stereo camera set-up. Methods Ecol. Evol. 6:351-356.

Olsen, A. M., and M. W. Westneat. In review. Linkage Mechanisms in the Vertebrate Skull: Structure and Function of Three-Dimensional, Multi-loop, Force Transmission Systems.

Olson, E. C., and R. L. Miller. 1958. Morphological integration. University of Chicago Press.

Olson, S. L., and A. Feduccia. 1980. *Presbyornis* and the origin of the Anseriformes. Smithson. Contrib. Zool. 323:1-24.

Olson, S. L., and H. F. James. 1991. Descriptions of thirty-two new species of birds from the Hawaiian Islands: Part I. Non-Passeriformes. Ornithol. Monogr. 45:1-88.

Orme, D., R. Freckleton, G. Thomas, T. Petzoldt, S. Fritz, N. Isaac, and W. Pearse. 2013. caper: Comparative Analyses of Phylogenetics and Evolution in R. URL https://CRAN.R-project.org/package=caper.

Oufiero, C. E., R. A. Holzman, F. A. Young, and P. C. Wainwright. 2012. New insights from serranid fishes on the role of trade-offs in suction-feeding diversification. J. Exp. Biol. 215:3845-3855.

Owen, M. 1972. Some factors affecting food intake and selection in white-fronted geese. J. Anim. Ecol. 41:79-92.

Pagel, M. 1999. Inferring the historical patterns of biological evolution. Nature (Lond.). 401:877-884.

Paradis, E., J. Claude, and J. Strimmer. 2004. Ape: analyses of phylogenetics and evolution in R language. Bioinformatics (Oxf.). 20:289-290.

Parchman, T. L., and C. W. Benkman. 2002. Diversifying coevolution between crossbills and black spruce on Newfoundland. Evolution. 56:1663-1672.

Patek, S. N., B. N. Nowroozi, J. E. Baio, R. L. Caldwell, and A. P. Summers. 2007. Linkage mechanics and power amplification of the mantis shrimp's strike. J. Exp. Biol. 210:3677-3688.

Paulus, S. L. 1984. Activity budgets of nonbreeding gadwalls in Louisiana. J. Wildl. Manag. 48:371-380.

Paulus, S. L. 1988. Time-activity budgets of nonbreeding Anatidae: A review. Pp. 135-152 *in* Waterfowl in winter. University of Minnesota Press, Minneapolis.

Perry, M. C., and F. M. Uhler. 1988. Food habits and distribution of wintering canvasbacks, *Aythya valisineria*, on Chesapeake Bay. Estuaries. 11:57-67.

Pinheiro, J., D. Bates, S. DebRoy, D. Sarkar, and R. C. Team. 2016. {nlme}: Linear and Nonlinear Mixed Effects Models. URL http://CRAN.R-project.org/package=nlme.

Podos, J. 2001. Correlated evolution of morphology and vocal signal structure in Darwin's finches. Nature (Lond.). 409:185-188.

Poole, A., ed. 2005. The Birds of North America Online. Cornell Laboratory of Ornithology Ithaca, NY URL http://bna.birds.cornell.edu/BNA/.

Pough, F. H. 1973. Lizard energetics and diet. Ecology. 54:837-844.

Price, S. A., and S. S. B. Hopkins. 2015. The macroevolutionary relationship between diet and body mass across mammals. Biol. J. Linn. Soc. 115:173-184.

Price, T. 1991. Morphology and ecology of breeding warblers along an altitudinal gradient in Kashmir, India. J. Anim. Ecol. 60:643-664.

Price, T. D., P. R. Grant, H. L. Gibbs, and P. T. Boag. 1984. Recurrent patterns of natural selection in a population of Darwin's finches. Nature (Lond.). 309:787-789.

Projecto-Garcia, J., C. Natarajan, H. Moriyama, R. E. Weber, A. Fago, Z. A. Cheviron, R. Dudley, J. A. McGuire, C. C. Witt, and J. F. Storz. 2013. Repeated elevational transitions in hemoglobin function during the evolution of Andean hummingbirds. Proc. Natl. Acad. Sci. 110:20669-20674.

Prop, J., and T. Vulink. 1992. Digestion by barnacle geese in the annual cycle: the interplay between retention time and food quality. Funct. Ecol. 6:180-189.

Prum, R. O., J. S. Berv, A. Dornburg, D. J. Field, J. P. Townsend, E. M. Lemmon, and A. R. Lemmon. 2015. A comprehensive phylogeny of birds (Aves) using targeted next-generation DNA sequencing. Nature (Lond.). 526:569-573.

R Core Team. 2015. *R: A Language and Environment for Statistical Computing*. R Foundation for Statistical Computing, Vienna, Austria. URL http://www.R-project.org/.

R Core Team. 2016. *R: A Language and Environment for Statistical Computing*. R Foundation for Statistical Computing, Vienna, Austria. URL http://www.R-project.org/.

RStudio, and Inc. 2014. shiny: Web Application Framework for R. URL http://CRAN.R-project.org/package=shiny.

Revell, L. J. 2009. Size-correction and principal components for interspecific comparative studies. Evolution. 63:3258-3268.

Revell, L. J. 2010. Phylogenetic signal and linear regression on species data. Methods Ecol. Evol. 1:319-329.

Revell, L. J. 2012. phytools: an R package for phylogenetic comparative biology (and other things). Methods Ecol. Evol. 3:217-223.

Reznick, D. N., M. J. Butler IV, F. H. Rodd, and P. Ross. 1996. Life-history evolution in guppies (*Poecilia reticulata*) 6. Differential mortality as a mechanism for natural selection. Evolution. 50:1651-1660.

Reznick, D., and J. A. Endler. 1982. The impact of predation on life history evolution in Trinidadian guppies (*Poecilia reticulata*). Evolution. 36:160-177.

Roberts, C. M. 1987. Experimental analysis of resource sharing between herbivorous damselfish and blennies on the Great Barrier Reef. J. Exp. Mar. Biol. Ecol. 111:61-75.

Robinson, B. W. 2000. Trade offs in habitat-specific foraging efficiency and the nascent adaptive divergence of sticklebacks in lakes. Behaviour. 137:865-888.

Robinson, B. W., D. S. Wilson, and G. O. Shea. 1996. Trade-offs of ecological specialization: an intraspecific comparison of pumpkinseed sunfish phenotypes. Ecology. 77:170-178.

Rohlf, F. J. 1990. Morphometrics. Annu. Rev. Ecol. Syst. 21:299-316.

Rohlf, F. J., and D. Slice. 1990. Extensions of the Procrustes method for the optimal superimposition of landmarks. Syst. Biol. 39:40-59.

Schluter, D. 1984. Body size, prey size and herbivory in the Galápagos lava lizard, *Tropidurus*. Oikos. 43:291-300.

Schluter, D. 1993. Adaptive radiation in sticklebacks: size, shape, and habitat use efficiency. Ecology. 74:699-709.

Schluter, D. 1995. Adaptive radiation in sticklebacks: trade-offs in feeding performance and growth. Ecology. 96:82-90.

Schluter, D. 1996. Adaptive radiation along genetic lines of least resistance. Evolution. 50:1766-1774.

Schluter, D., T. Price, A. O. Mooers, and D. Ludwig. 1997. Likelihood of ancestor states in adaptive radiation. Evolution. 51:1699-1711.

Schluter, D., and J. D. McPhail. 1992. Ecological character displacement and speciation in sticklebacks. Am. Nat. 140:85-108.

Schondube, J. E., and C. M. del Rio. 2003. The flowerpiercers' hook: an experimental test of an evolutionary trade-off. Proc. R. Soc. Lond. B Biol. Sci. 270:195-198.

Sedinger, J. S. 1997. Adaptations to and consequences of an herbivorous diet in grouse and waterfowl. Condor. 99:314-326.

Sibley, C. G., J. E. Ahlquist, and B. L. Monroe, Jr. 1988. A classification of the living birds of the world based on DNA-DNA hybridization studies. Auk. 105:409-423.

Sibley, C. G., K. W. Corbin, and J. H. Haavie. 1969. The relationships of the flamingos as indicated by the egg-white proteins and hemoglobins. Condor. 71:155-179.

Sidlauskas, B. 2008. Continuous and arrested morphological diversification in sister clades of characiform fishes: a phylomorphospace approach. Evolution. 62:3135-3156.

Smith, N. D. 2012. Body mass and foraging ecology predict evolutionary patterns of skeletal pneumaticity in the diverse "waterbird" clade. Evolution. 66:1059-1078.

Smith, T. B. 1987. Bill size polymorphism and intraspecific niche utilization in an African finch. Nature (Lond.). 329:717-719.

Smith, T. B. 1990. Resource use by bill morphs of an African finch: evidence for intraspecific competition. Ecology. 71:1246-1257.

Smith, T. B. 1993. Disruptive selection and the genetic basis of bill size polymorphism in the African finch *Pyrenestes*. Nature (Lond.). 363:618-620.

Sokal, R. R., and F. J. Rohlf. 2012. Biometry (4th edn). WH Freeman and Company New York.

Sorenson, M. D., A. Cooper, E. E. Paxinos, T. W. Quinn, H. F. James, S. L. Olson, and R. C. Fleischer. 1999. Relationships of the extinct moa-nalos, flightless Hawaiian waterfowl, based on ancient DNA. Proc. R. Soc. Lond. B Biol. Sci. 266:2187-2193.

Squires, J. R., and S. H. Anderson. 1995. Trumpeter swan (*Cygnus buccinator*) food habits in the Greater Yellowstone Ecosystem. Am. Midl. Nat. 133:274-282.

Sraml, M., L. Christidis, S. Easteal, P. Horn, and C. Collet. 1996. Molecular relationships within Australasian waterfowl (Anseriformes). Aust. J. Zool. 44:47-58.

Stayton, C. T. 2006. Testing hypotheses of convergence with multivariate data: morphological and functional convergence among herbivorous lizards. Evolution. 60:824-841.

Stayton, C. T. 2015. The definition, recognition, and interpretation of convergent evolution, and two new measures for quantifying and assessing the significance of convergence. Evolution. 69:2140-2153.

Stearns, S. C. 1989. Trade-offs in life-history evolution. Funct. Ecol. 3:259-268.

Steuer, P., K. Südekum, D. W. H. Müller, R. Franz, J. Kaandorp, M. Clauss, and J. Hummel. 2011. Is there an influence of body mass on digesta mean retention time in herbivores? A comparative study on ungulates. Comp. Biochem. Physiol. Part A Mol. Integr. Physiol. 160:355-364.

Steuer, P., K. Südekum, T. Tütken, D. W. H. Müller, J. Kaandorp, M. Bucher, M. Clauss, and J. Hummel. 2014. Does body mass convey a digestive advantage for large herbivores? Funct. Ecol. 28:1127-1134.

Strahl, S. D. 1988. The social organization and behaviour of the Hoatzin *Opisthocomus hoazin* in central Venezuela. Ibis. 130:483-502.

Suhonen, J., R. V. Alatalo, and L. Gustafsson. 1994. Evolution of foraging ecology in Fennoscandian tits (*Parus* spp.). Proc. R. Soc. Lond. B Biol. Sci. 258:127-131.

Sustaita, D., and F. Hertel. 2010. In vivo bite and grip forces, morphology and prey-killing behavior of North American accipiters (Accipitridae) and falcons (Falconidae). J. Exp. Biol. 213:2617-2628.

Suter, W. 1982. Vergleichende Nahrungsökologie von überwinternden Tauchenten (*Bucephala*, *Aythya*) und Bläßhuhn (*Fulica atra*) am Untersee-Ende/Hochrhein (Bodensee). Ornithol. Beob. 79:225-254.

Svanbäck, R., and P. Eklöv. 2003. Morphology dependent foraging efficiency in perch: a trade-off for ecological specialization? Oikos. 102:273-284.

Swanson, G. A., M. I. Meyer, and J. R. Serie. 1974. Feeding ecology of breeding blue-winged teals. J. Wildl. Manag. 38:396-407.

Swanson, G. A., and J. C. Bartonek. 1970. Bias associated with food analysis in gizzards of blue-winged teal. J. Wildl. Manag. 43:739-746.

Tattersall, G. J., D. V. Andrade, and A. S. Abe. 2009. Heat exchange from the toucan bill reveals a controllable vascular thermal radiator. Science (Wash. D. C.). 325:468-470.

Temeles, E. J., and W. J. Kress. 2003. Adaptation in a plant-hummingbird association. Science (Wash. D. C.). 300:630-633.

Tome, M. W., and D. A. Wrubleski. 1988. Underwater foraging behavior of canvasbacks, lesser scaups, and ruddy ducks. Condor. 90:168-172.

Trewick, S. 1996. The diet of kakapo (*Strigops habroptilus*), takahe (*Porphyrio mantelli*) and pukeko (*P. porphyrio melanotus*) studied by faecal analysis. Notornis. 43:79-112.

Urbanek, S. 2014. jpeg: Read and write JPEG images. URL http://CRAN.R-project.org/package=jpeg.

Uyeda, J. C., D. S. Caetano, and M. W. Pennell. 2015. Comparative analysis of principal components can be misleading. Syst. Biol. 64:677-689.

Van Gennip, E., and H. Berkhoudt. 1992. Skull mechanics in the pigeon, *Columba livia*, a three-dimensional kinematic model. J. Morphol. 213:197-224.

Vanhooydonck, B., R. S. James, J. Tallis, P. Aerts, Z. Tadic, K. A. Tolley, G. J. Measey, and A. Herrel. 2014. Is the whole more than the sum of its parts? Evolutionary trade-offs between burst and sustained locomotion in lacertid lizards. Proc. R. Soc. Lond. B Biol. Sci. 281:20132677.

Veltman, C. J., K. J. Collier, I. M. Henderson, and L. Newton. 1995. Foraging ecology of blue ducks *Hymenolaimus malacorhynchos* on a New Zealand river: Implications for conservation. Biol. Conserv. 74:187-194.

Wainwright, P. C. 1996. Ecological explanation through functional morphology: the feeding biology of sunfishes. Ecology. 77:1336-1343.

Wake, D. B. 1991. Homoplasy: the result of natural selection, or evidence of design limitations? Am. Nat. 138:543-567.

Walker, J. A., and M. A. Bell. 2000. Net evolutionary trajectories of body shape evolution within a microgeographic radiation of threespine sticklebacks (*Gasterosteus aculeatus*). J. Zool. (Lond.). 252:293-302.

Warton, D. I., and F. K. C. Hui. 2011. The arcsine is asinine: the analysis of proportions in ecology. Ecology. 92:3-10.

Weller, M. W. 1972. Ecological studies of Falkland Islands' waterfowl. Wildfowl. 23:25-44.

Westneat, M. W. 1990. Feeding mechanics of teleost fishes (Labridae; Perciformes): A test of four-bar linkage models. J. Morphol. 205:269-295.

Westneat, M. W. 1991. Linkage biomechanics and evolution of the jaw protrusion mechanism of the sling-jaw wrasse, *Epibulus insidiator*. J. Exp. Biol. 159:165-184.

Westneat, M. W. 1994. Transmission of force and velocity in the feeding mechanisms of labrid fishes (Teleostei, Perciformes). Zoomorphology (Berl.). 114:103-118.

Westneat, M. W. 1995. Feeding, function, and phylogeny: analysis of historical biomechanics in labrid fishes using comparative methods. Syst. Biol. 44:361-383.

Westneat, M. W. 2003. A biomechanical model for analysis of muscle force, power output and lower jaw motion in fishes. J. Theor. Biol. 223:269-281.

Westneat, M. W., J. H. Long, W. Hoese, and S. Nowicki. 1993. Kinematics of birdsong: functional correlation of cranial movements and acoustic features in sparrows. J. Exp. Biol. 182:147-171.

Westneat, M. W., M. E. Alfaro, P. C. Wainwright, D. R. Bellwood, J. R. Grubich, J. L. Fessler, K. D. Clements, and L. L. Smith. 2005. Local phylogenetic divergence and global evolutionary convergence of skull function in reef fishes of the family Labridae. Proc. R. Soc. Biol. Sci. Ser. B. 272:993-1000.

Winterbottom, R., and D. A. McLennan. 1993. Cladogram Versality: Evolution and Biogeography of Acanthuroid Fishes. Evolution. 47:1557-1571.

Wishart, R. A. 1983. The behavioral ecology of the American Wigeon (*Anas americana*) over its annual cycle. Ph.D. Thesis. Univ. of Manitoba, Winnipeg, MB.

Wood, J. R., N. J. Rawlence, G. M. Rogers, J. J. Austin, T. H. Worthy, and A. Cooper. 2008. Coprolite deposits reveal the diet and ecology of the extinct New Zealand megaherbivore moa (Aves, Dinornithiformes). Quat. Sci. Rev. 27:2593-2602.

Wu, P., T. Jiang, J. Shen, R. B. Widelitz, and C. Chuong. 2006. Morphoregulation of avian beaks: comparative mapping of growth zone activities and morphological evolution. Dev. Dyn. 235:1400-1412.

Wu, P., T. Jiang, S. Suksaweang, R. B. Widelitz, and C. Chuong. 2004. Molecular shaping of the beak. Science (Wash. D. C.). 305:1465-1466.

Yanega, G. M., and M. A. Rubega. 2004. Feeding mechanisms: Hummingbird jaw bends to aid insect capture. Nature (Lond.). 428:615-615.

Yekutieli, Y., R. Mitelman, B. Hochner, and T. Flash. 2007. Analyzing octopus movements using three-dimensional reconstruction. J. Neurophysiol. 98:1775-1790.

Zelditch, M. L., D. L. Swiderski, and H. D. Sheets. 2004. Geometric morphometrics for biologists: a primer, 1st edition. Elsevier Academic Press.

Zusi, R. L. 1984. A functional and evolutionary analysis of rhynchokinesis in birds. Smithson. Contrib. Zool. 395:1-40.

Zweers, G. A. 1974. Structure, movement, and myography of the feeding apparatus of the mallard (*Anas platyrhynchos* L.) A study in functional anatomy. Neth. J. Zool. 24:323-467.

Zweers, G., F. De Jong, H. Berkhoudt, and J. V. Berge. 1995. Filter feeding in flamingos (*Phoenicopterus ruber*). Condor. 97:297-324.

van Gils, J. A., J. H. Beekman, P. Coehoorn, E. Corporaal, T. Dekkers, M. Klaassen, R. Van Kraaij, R. De Leeuw, and P. P. De Vries. 2008. Longer guts and higher food quality increase energy intake in migratory swans. J. Anim. Ecol. 77:1234-1241.

van der Leeuw, A. H. J., K. Kurk, P. C. Snelderwaard, R. G. Bout, and H. Berkhoudt. 2003. Conflicting demands on the trophic system of Anseriformes and their evolutionary implications. Anim. Biol. 53:259-302.

van der Meij, M. A. A., and R. G. Bout. 2008. The relationship between shape of the skull and bite force in finches. J. Exp. Biol. 211:1668-1680.